NTNU

Norwegian University of
Science and Technology

Analysis of Self-Excited Induction Generator for use in Rural Area with Electronic Load Controller and Additional Compensation Methods

Aurora Andersson
Eirin Bye

Master of Energy and Environmental Engineering
Submission date: June 2016
Supervisor: Trond Toftevaag, ELKRAFT

Norwegian University of Science and Technology
Department of Electric Power Engineering

Abstract

The objective of this thesis is to provide a throughout analysis of the possible use of an induction generator in isolated operation in rural area, using the principles of electronic load control to maintain stable operation. The requirements given are based on local conditions, where the SEIG is intended to operate to provide basic electricity supply for people living far away from a centralized grid connection.

A theoretical description of the challenges related to operation of an induction generator in isolated mode is given, providing knowledge about what a control system for this purpose have to take into consideration. The main challenge is all the mutually dependant parameters, and the difficulty to determine their relations when no parameter can be assumed 100 % constant. The relations of highest importance in the investigations presented in this thesis is the dependency between voltage level, reactive power balance and frequency.

Possible options for load controller design and alternatives for reactive power compensation are studied, and presented in view of given system requirements. Since it is the request from Remote Hydrolight to investigate the possibility of using their existing triac controlled technology with SEIG, it is used as a reference case when both a simulation model and a laboratory set-up is built based on knowledge gained in the literature study. The main drawback to the triac solution is its consumption of reactive power, which results in a voltage drop. Based on the theory, this voltage drop was expected to be severe. Simulation and laboratory results is however more promising, and the triac solution might be used without compensation for the case of controlling only resistive loads. A second option for ELC, the uncontrolled rectifier using chopper controlled dump load, is also implemented in a simulation model. The latter showed the best voltage regulation, but the triac solution had better voltage waveforms and less THDs [%] measured.

When simulating different ratings of load size it was discovered that the SEIG system seems to be more vulnerable for changes in reactive power if the total load is small compared to the rating of the generator. A shortage of reactive power might be a more

sensitive issue at this operation point, which is something to take into consideration when designing the ratings of the power system.

The connection of an induction motor as a load is the most likely "worst case"-scenario of load connection in a system like the one studied, and this is used as a scenario for testing possible reactive compensation methods in both lab and simulations. In all cases the connection results in a severe voltage drop caused by the inrush current and reactive power consumption. A too high ratio of motor size versus generator results in total voltage collapse. Some type of compensation will be necessary in order to maintain system voltage during connection of a motor.

Of the reactive compensation options studied, the switched capacitor has the most potential. The quality of the voltage regulation provided by this unit depends on the amount of capacitors connected. This is again affecting on the total costs. As the inductive load in the system is most likely an IM, a small number of capacitors can be used dimensioned to match typical IM sizes. If this solution does not provide desired voltage levels, a slight increase or reduction in frequency can be used to further adjust the voltage level. Increased frequency was used as a method to provide rated voltage at loading conditions with increased reactive power consumption. It was found possible to maintain the voltage measured at the village load within given limits even when the IM was connected, and at the same time keeping the frequency within given limits as well.

As a final recommendation to Remote Hydrolight, it is stated that the triac ELC can most likely be used without compensation given only resistive load. For the case of sudden connection of inductive loads like an IM, a combination of switched capacitor and small adjustments in frequency is suggested.

Sammendrag

Maalet med denne oppgaven er aa gi en grundig analyse av mulig bruk av en induksjonsgenerator i isolert drift i utviklingsland, ved hjelp av prinsippene for elektronisk lastkontroll for aa opprettholde stabil drift. Kravene er gitt basert paa lokale forhold, hvor induksjonsgeneratoren skal gi grunnleggende stroemforsyning til folk uten tilgang til vanlig nettilknytning.

En teoretisk beskrivelse av utfordringene knyttet til drift av en induksjonsgenerator i isolert modus er gitt, og gir kunnskap om hva et reguleringssystem for dette formaalet maa ta hensyn til. Den stoerste utfordringen er alle gjensidig avhengige parametere, og det er vanskelig aa fastslaa deres forhold naar ingen parameter kan antas 100 % konstant. Forholdet av hoeyeste viktighet i undersoekelsene som presenteres i denne avhandlingen er avhengigheten mellom spenningsnivaa, reaktiv effektbalanse og frekvens.

Mulige alternativer for lastkontrollerens utforming og alternativer for reaktiv effektkompensasjon er studert, og presenteres i lys av gitte systemkrav. Siden det er en forespoersel fra Remote Hydrolight aa undersoeke muligheten for aa bruke deres eksisterende triackontrollerte ELC-teknologi med SEIG, er det brukt som en referanse baade naar en simuleringsmodell og et laboratoriumoppsett er bygget basert paa kunnskapen fra litteraturstudiet. Den stoerste ulempen til triac loesning er dens forbruk av reaktiv effekt, noe som resulterer i et spenningsfall. Basert paa teorien er dette spenningsfallet forventet aa vaere kraftig. Simuleringer og laboratorieresultater er imidlertid mer lovende, og triacloesningen kan bli brukt uten kompensasjon for aa kontrollere bare resistive laster. Et annet alternativ for ELC, ukontrollert likeretter med IGBT-kontrollert dumplast, er ogsaa implementert i en simuleringsmodell. Sistnevnte viste den beste spenningsreguleringen, men triacloesningen hadde bedre spenningskurver og mindre THDs [%] maalt.

Naar ulike stoerrelser paa total tilknyttet last ble simulert, ble det oppdaget at SEIG systemet ser ut til aa vaere mer saarbart for endringer i reaktiv effekt hvis den totale belastningen er liten i forhold til generatoren. Mangel paa reaktiv effekt tilfoert kan vre et mer kritisk paa dette operasjonspunktet, som er noe aa ta hensyn til ved utforming av et slikt system.

Tilkoblingen av en induksjonsmotor (IM) som en last er det mest sannsynlige "worst case"-scenarioet av mulige lasttilkoblinger i et system slikt som det aktuelle studert i denne oppgaven, og dette blir brukt som et scenario for aa teste eventuelle reaktive kompensasjonsmetoder baade i laboratoriet og i simuleringer. I alle tilfeller resulterer tilkoblingen i et kraftig spenningsfall foraarsaket av startstroemmen og dens reaktive effektforbruk. En altfor stor motorstoerrelse versus generatorstoerrelse resulterer i total spenningskollaps. En form for kompensasjon vil vaere noedvendig for aa opprettholde systemspenning under tilkobling av en motor.

Av de reaktive kompenseringsmulighetene som er undersoekt har svitsjet kondensator stoerst potensial. Kvaliteten paa spenningsreguleringen gitt av denne enheten er avhengig av antall kondensatorer som kan tilkobles. Dette vil igjen paavirke de totale kostnadene, saa det blir et optimaliseringsproblem. Den induktive lasten i systemet som er mest sannsynlig at tilkobles er en IM, og for disse kan man dimensjonere et lite antall kondensatorer som matcher typiske IM stoerrelser. Hvis denne loesningen ikke gir oensket spenningsnivaa, kan en liten oekning eller reduksjon i frekvens brukes til aa justere spenningsnivaaet ytterligere. Oekt frekvens ble brukt som en metode for aa gi oekt spenning under tilkoblinger av laster med hoeyt reaktivt effektforbruk i laboratorietestene. Det ble funnet mulig aa opprettholde spenningen innenfor gitte grenser selv nar IM er tilkoblet, og paa samme tid holde frekvensen innenfor gitte grenser.

Som en siste anbefaling til Remote Hydrolight, gis det at triac ELC-loesningen kan mest sannsynlig brukes uten kompensasjon gitt ren resistiv last. For plutselige tilkoblinger av induktiv last som for eksempel en IM, er en kombinasjon av svitsjet kondensator og smaa justeringer i frekvens foreslaatt.

Acknowledgements

We would like to express our gratitude for the helpful and interesting discussion with our project supervisor, Trond Toftevaag. He has an outstanding knowledge and curiosity about electrical machines, which he has shared with us.

In addition we would like to thank Anders Austegard, not only for helping us understand the problem and given helpful insight in the field of study, but also for his engagement with Remote HydroLight. We are grateful for the opportunity to contribute in this area, provided by Austegard and Engineers Without Borders.

For the useful discussions and help with the understanding of the theory, and for help with building and understanding the simulation model, we would like to thank Professor Roy Nilsen, Phd candidate Atle Rygg and postdoctoral researcher Raymondo Torres from NTNU and Kjell Ljoekelsy, Olve Moe and Salvatore D'Arco from Sintef Energy.

For their help with everything practical in relation to the laboratory test, we would like to express our gratitude towards Aksel Hanssen, Baard Almaas, Vladimir Klubicka and Svein Erling Norum from the service department at NTNU Department of Electric Power Engineering.

A special thank goes to a fellow student, Eirik Haustveit. He has an incredible interest and knowledge for the relevant field of study, and has through several conversations enlightened us with his knowledge.

Finally, we would like to thank each other for the good cooperation and good company. Not only for the work related to this thesis, but also for the previous years as colleagues at NTNU.

Contents

List of Figures

List of Tables

Abbreviations

AC	**A**lternating **C**urrent
DC	**D**irect **Current**
dl	**d**ump **l**oad
ELC	**E**lectronic **L**oad **C**ontrol
FC-TCR	**F**ixed **C**apacitor- **T**hyristor **C**ontrolled **R**eactor
IGBT	**I**nsulated-**G**ate **B**ipolar **T**ransistor
IM	**I**nduction **M**otor
KCL	**K**irchhoffs **C**urrent **L**aw
PD	**P**hase **D**elay
PF	**P**ower **F**actor
PLL	**P**hase **L**ocked **L**oop
pu	**p**er **u**nit
PWM	**P**ulse **W**idth **M**odulation
RF	**R**ipple **F**actor
RMS	**R**oot **M**ean **S**quare
SEIG	**S**elf **E**xcited **I**nduction **G**enerator
SSR	**S**ub**S**ynchronous **R**esonance
SVC	**S**tatic **V**ar **C**ompensation
THD	**T**otal **H**armonic **D**istortion
vl	resistive **v**illage **l**oad
VSI	**V**oltage **Source I**nverter
Y	Star connection
Δ	Delta connection

Symbols

a	distance	m
B	magnetic force	T
C	capacitance	F
E	induced voltage	V
f	frequency	Hz
I	RMS line current	A
J	inertia	$\frac{Kgm^2}{s}$
P	power	W (Js^{-1})
Q	reactive power	Var
R	resistance	Ω
S	apparent power	VA
s	slip	%
V	RMS line voltage	V

ω	angular frequency	$rads^{-1}$
α	firng angle	^{o}
τ	Torque	Nm
n	rotational speed	rpm

Chapter 1

Introduction

This thesis is a continuation of a specialization project, conducted during the fall of 2015 as a result of the course TET4525 at the Department of Electric Power Engineering at NTNU. This is later referred to as the project thesis [1].

1.1 Motivation

Power generation from renewable energy has become essential to provide electricity at low cost in decentralized areas of developing countries. Grid connection is often not accessible, so small systems for stand-alone operation is developed to meet this need. As engineers, one of the best tings we can do in order to aid the development is to provide simple and robust technology for self-operation in the local communities. This project is written in collaboration with the ideal organization Engineers Without Boarders for a company called Remote Hydrolight, introduced in the following section.

1.2 Background

Remote Hydrolight is a small company involved in training, manufacturing and installation of micro hydro power plants in Afghanistan. Their mission statement is "To assist those desiring to utilize available water resources to generate electric power at a reasonable cost". They have developed a system for controllable pico hydro power generation in isolated operation. All the equipment is produced locally, with long-time support provided by trained Afghan equipment manufacturers.

Remote Hydrolight have developed a solution for automatic control of a stand-alone power generation system using a synchronous generator. This is called an Electronic

Load Controller (ELC). The controller is relatively simple, robust and cheap to manufacture and maintain in operation. It is designed for a run-of-river pico hydro system, using a synchronous generator. The water is running a turbine connected to a generator, supplying a village load in a small isolated grid. Remote Hydrolight wishes to extend their operation to India, and the request has been to examine the possible extension of the principles used in their ELC-system to be used with an induction generator there.

The synchronous generator has traditionally been used for power generation in stand-alone operations. The induction generator is an alternative, and is increasingly being used because of several advantages. Some of these are a brush less system, lower cost, robustness, less need of maintenance and operational simplicity. In addition, the induction generator provides self protection against short circuits and overcurrents and it can generate power at different rotational speeds. The disadvantages however, are reactive power consumption and poor voltage and frequency regulation. When connected to a grid, the grid controls the frequency and voltage, so the regulation is not an issue. In remote areas, where the induction generator is operated in isolated mode, there is no main grid to provide this regulation. Hence the regulation of voltage and frequency are of great importance.

Given that the operation behavior of the induction generator is quite different from the synchronous generator, it may be necessary to redevelop the excising control system or make a new design for the system using an induction generator. The request from Remote Hydrolight is to provide a thorough examination on this topic.

1.3 Objective

The objective is to provide a throughout analysis of the possible use of an induction generator in isolated operation using the principles of electronic load control to maintain stable operation. The requirements given are based on local conditions in rural areas, where the SEIG is intended to operate to provide basic electricity supply for people living far away from a centralized grid connection.

A theoretical description of the challenges related to operation of an induction generator in isolated mode is given, providing knowledge about what a control system for this purpose have to take into consideration. Possible options for load controller design and alternatives for reactive power compensation are studied, and presented in view of the given requirements.

Both a simulation model and a laboratory set-up is built based on knowledge gained in the literature study, and a throughout description is given of the steps necessary in

that process. Results from simulation and laboratory work are presented and compared, giving a practical understanding of the behaviour of the SEIG + ELC system. Different loads are connected, and the necessity of, and/or possible use of, compensation methods is analyzed.

1.4 Scope of Work

- Further study of existing ELC solution, other ELC options and compensation methods presented in the project report (autumn 2015), and extended literature survey. Selection of suitable alternative(s).
- Introductory mapping of technical demands and limitations for the system in view of: - Power quality (voltage and frequency range) - Degree of simplicity - Price
- Modeling and simulation of selected ELC alternative(s) and reactive power compensation.
- Testing the SEIG in a laboratory set-up: - testing with resistive and inductive load - testing with ELC at different operation conditions - testing of different compensation methods
- Validation of the simulation model based on the laboratory results (if time permits)

1.5 Limitations

The studied system is limited to include only 3 phase generators feeding 3 phase loads, and these loads are assumed symmetric at all times.

Both simulations and laboratory tests has been run using constant speed input to the generator. With a well-functioning ELC this is a justified simplification. In reality it is the input torque of the hydro power turbine that is almost constant, depending on water inflow. Modeling with constant torque instead of constant speed will be left for future work.

Regulation is not included in the simulation or laboratory tests. The triac controlled ELC is tested using fixed firing angles and tuned resistance values.

Transmission lines is not included in simulations or laboratory set up, so the real power quality is difficult to state. All results are related to the given limits of voltage and quality given by Remote Hydrolight, measured at the terminals of the generator.

Starting the induction generator without any residual magnetizing current is not included in the investigations.

Cost is an important parameter in the evaluations made in this thesis, but since actual values is hard to obtain these evaluations is made on the basis of qualified assumptions.

1.6 Software

- Report written in LaTeX environment.
- Simulations in Matlab/SimPowerSystem
- Laboratory results analyzed with FlukeView Power Quality Analyzer

1.7 Instrumentation

The instruments used in the laboratory work is given in appendix A

1.8 Structure of Report

Chapter 2 contains a system description, providing an overview for understanding of components and parameters discussed throughout the thesis. Specific requirements for isolated operation in rural areas are given.

Chapter 3 contains the theoretical background used to explain choices and assumptions covering power quality and costs.

Chapter 4 covers important relations for the use of an induction generator in isolated operation, with specific attention to the effects of load connections.

Chapter 5 covers the theoretical background for possible reactive compensation methods that might be an alternative to use in combination with and ELC.

Chapter 6 contains an overview of the literature study covering existing alternatives for ELC technology used in combination with an SEIG, and a discussion providing the two alternatives most suited for further investigation.

Chapter 7 covers the steps necessary to build a simulation model from scratch, with the intention of testing the chosen ELC solution with an SEIG.

Chapter 8 contains the simulation results.

Chapter 9 covers the steps necessary to build a laboratory set-up to be able to test the existing ELC circuit board developed byt Remote Hydrolight with an SEIG and reactive compensation alternatives.

Chapter 10 contains the laboratory results.

Chapter 11 contains the conclusions made from the findings in this thesis.

Chapter 12 provides suggestions for further work.

Chapter 2

System Description

This chapter is dedicated to give the reader a basic understanding of the system to be evaluated, and the specific boundaries applied to a system developed for use in rural area.

2.1 Overview

The system is given in figure 2.1, and consists of an isolated induction generator driven by a turbine in a run-of-river hydropower station.

The capacitor bank is a necessary extra component when an induction generator is used. It will provide the reactive power needed for self-excitation and operation at rated voltage, that normally would be provided by a grid if the system was connected to one. The system is defined as pico hydro, meaning the rated power of the unit is between 1 - 10 kW. In larger hydro power applications the use of a speed governor is common for regulation. This is expensive, and not beneficial for smaller systems.

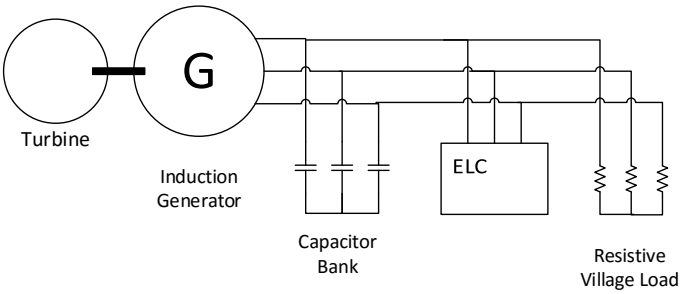

FIGURE 2.1: System overview

Instead, an electronic load controller (ELC) is used for the same purpose. When the system sensors register a change in the attached load, a control function will dissipate correspondingly less or more to an attached system of dump loads. This is done in order to maintain a constant electrical load P_e seen from the generator, and hence keeping the stability given by the motor torque balance equations (2.1) and (2.2).

$$J\frac{d\omega}{dt} = \tau_m - \tau_e \tag{2.1}$$

$$J\omega\frac{d\omega}{dt} = P_m - P_e \tag{2.2}$$

The dump load is normally used as a water heater, which is a low quality application for utilization of the excess power. There is no use of water storage in run-of-river plants. The produced energy is hence seen as an immediate renewable source like for instance wind or solar power, but it is more efficient and has a lower cost per kWh than the alternatives.

The village load consist mainly of resistive load used for lightening bulbs, and maybe some small inductive loads and an induction motor to for instance run a fan or a pump. The allowed frequency and voltage tolerances are adapted to use in rural areas. These conditions are discussed further in the coming sections.

2.2 Simplicity, Reliability and Cost

The most important objective used throughout the evaluations and the development of this system is to keep the cost as low as possible within given limits. An basis for further evaluations is given in 3.2.

The system to be evaluated and tested in laboratory in this thesis is the existing solution developed by Remote Hydrolight for use in rural areas of Afghanistan. Their assumptions are used as foundation for the research presented, and it is assumed that the requirements are universal for areas defined as rural.

The developed system must be as simple as possible to make, install and operate, but still function well. Reliability is important, but no system can be 100 % reliable. A very reliable system will be too costly for the consumers, and this is therefore not the parameter of highest importance. The operating limits are given in 2.3.1 and discussed in 3.1.

The software developed for the solution are given with the option of free downloading, and the idea for the hardware system is that it should be manufactured locally with available cost-efficient materials. The cost of the RH-developed ELC is 35 times lower compared to other similar ELCs [2]. One of the reasons for this is that some normally implemented components are excluded from the design. According to Remote Hydrolights experiences, the local personnel will not correct any errors until the system is completely broken, and it is seen as better suited to change the whole unit rather than components if any damage should occur. For instance, a relay for over-voltage is not included, but instead the installation is set-up with two identical circuit boards. In case of severe failure, the second board is used. On the other hand, security margins for voltage and current components are however high, ensuring necessary robustness to go with the minimalistic design.

2.3 Requirements

In order to give an advice for which technology is preferred to be used with induction generator, the specific system requirements for the combination of an SEIG and an ELC in rural application are presented in the following section.

2.3.1 Frequency and Voltage Tolerances

For Remote Hydrolight, the voltage variation is seen as the parameter of highest importance. The stability of the voltage will be prioritized over a fast response rate of the control system used [2]. A limit is given with the interval 220-240 V, corresponding to a $\pm$ 4.35 % deviation from nominal voltage. For a system with star connected generator, the deviation in line-to-line voltage corresponds to $\pm$ 17.4 V. The limits for that system will be 383 - 417 V.

The frequency is not as critical, as none of the load connected will be strictly depending on frequency level. Operating frequency is set to 50 Hz, and the tolerance limit is first given to be between 40 and 70 Hz. This might be a problem for speed dependant loads as fans or pumps, but in general a 10 % increase in frequency is acceptable and used as limit for further evaluation. The technical aspects of changes and disturbances in frequency and voltage level will be discussed further in 3.1

As of disturbances in the quality of the voltage delivered, the parameter Total Harmonic Distortion (THD) is used. No specific limit is given, but it is a goal to keep this at a minimum level. Experience says that the harmonic content in the voltage produced

by Remote Hydrolights ELC is high, but it has not been a priority to mitigate these disturbances. Special attention has been given to this parameter in this thesis, and it is described further in section 3.1.1.

.

2.3.2 Type of Load

As explained briefly in the introduction, the village load consist mainly of resistive load used for lightening bulbs. The existing ELC design made by Remote Hydrolight has this as a limiting condition. It can however occur connection of some small inductive loads, and specifically it is interesting to evaluate the possible connection of an induction motor to run for instance a fan or a pump. As will be discussed in Chapter 4, the stability of the induction motor is very sensitive to changes in both active and reactive power balance.

In this pico hydro system, the intended generator rated value will be approximately 4-6 kW. For an active load close to the machines rated value, the connected reactive consumption is also high, which is directly related to the magnetizing current. A too high magnetizing current will result in high losses. The dimensioning of the system should therefore be in the scale where the total power load does not exceed 0.8 pu of output from the machine [3]. A litmit is set allowing the loads to have rated value between 1.5 and 2.5 the size of the generator, corresponding to pu values between 0.4 and 0.67.

In the simulations given in Chapter 8, a 4 kW induction machine is used as a base. The attached load is set to 2.67 kW, which is the higher of the limits given. In the laboratory work presented in Chapter 10, a 1.5 kW induction machine is used. Correspondingly, the load is set to 1.5 the generator size, calculated to be 1 kW.

To give a perspective of the scope of this project, a reference is made to a case study from 2002. It covers all steps necessary for the installation of a pico hydro power station in Kenya [4]. There, a 1.5 kW induction generator is estimated to cover a total load of 60 households. With this, each house receives enough power to supply one or two light bulbs and one radio.

2.4 Summary

An appropriate ELC solution for this purpose should have the right balance between cost, reliability, robustness and simplicity. The positive effect of adjusting the system to provide an improved balance has to be seen in relation to the possible extra disturbances, complications and costs the additional components will result in.

As limiting parameters for further analysis, frequency and voltage tolerances is given at respectively $\pm$ 10 % and $\pm$ 4.35 %. The attached load has a possible range between 0.4 and 0.67 pu the size of the rated power of the generator.

Chapter 3

Basis of Comparison

This chapter is intended to provide the reader with an understanding of the parameters used to compare different technical solutions in the following chapters of the report.

3.1 Power Quality

As a single power producer in a micro grid, the whole value chain from production to delivery at the end user has to be considered in the design of the power system. The quality of the electrical power delivered to the end user by a power system can be described in several terms, and this section is dedicated to cover fundamental insight about continuity of service, transients and harmonic distortion.

Continuity of service means the systems ability to stay within given threshold levels of voltage and frequency on a longer time perspective. In the Norwegian power grid, the frequency has to be kept within 50 Hz $\pm$ 2 % for areas with temporary loss of connection to the main grid [5]. The limits for rural electrification was given at $\pm$ 10 %, justified with the assumption that there are little to no frequency dependant loads in that case.

The voltage variation limits given by Remote Hydrolight for this thesis was at $\pm$ 4.35 %. The given slow variations interval of voltage level in Norway is given at $\pm$ 10 % measured at the consumer. A limitation for the laboratory set-up will be the lack of long power lines that can contribute to even further voltage loss, so the stricter limits is kept for considering the quality of the voltage produced by and measured at the terminals of the SEIG + ELC system.

Transients is used to describe variations in waveform that are resulting in over- or undervoltage conditions during short time periods. Common sources of overvoltage are

lightning strokes, switching of devices or loose connections. A typical cause of under-voltage transients is connection of motors to the system. In earlier days, the equipment used was designed to handle magnitudes of several times the normal peak voltage and current for short time intervals. This has become more complex as more of the loads used are electronically controlled, and hence has a lower withstand capability. The equipment used in rural areas today are however not as sensitive, and robustness of equipment is one of the requirements given by Remote Hydrolight for their design. [6]

It is chosen to look specifically into the harmonics distortion in the next subsection, as key findings from this theoretical basis is central in further results.

3.1.1 Harmonic Distortions

Most of the relevant ELC design solutions are using power electronic equipment, which in practice are nonlinear loads. Being nonlinear means that they draw currents that are not smooth sinusoidal at the system fundamental frequency. The waveform of this current can be decomposed into several sinusoidal waves with frequencies at multiples of the fundamental frequency. The harmonics distortions are steady-state distortions as they repeat every period.

If a waveform deviates from the sinusoidal shape, it can be represented by using Fourier analysis. This representation can be done for both voltage and current waveform. The total waveform i_s, is the sum of its Fourier components, as shown in equation (3.1). The dominant part of a distorted current waveform is the fundamental component, denoted as i_{s1}. This is at the fundamental frequency f_1, which here will be the line frequency. The i_{sh} component is at the h harmonic, with the frequency $f_h = hf_1$.

$$i_s(t) = i_{s1}(t) + \sum_{h \neq 1} i_{sh}(t) \tag{3.1}$$

The total harmonic distortion (THD) is a value used to measure all the distortions. As given in equation (3.2) It is defined as the ratio of the sum of the harmonic components divided to the fundamental component. [7]

$$THD(\%) = \sqrt{\sum_{h \neq 1} (\frac{I_{sh}}{I_{s1}})^2} \tag{3.2}$$

Harmonics in voltage are caused by harmonics in current. In Norway, the allowed level of voltage harmonics in the grid is 5 or 8 %, measured as an average over accordingly 1 week or 10 minutes [5].

The current components at harmonic frequencies are not contributing to the real power, but it is disturbing the power factor. The displacement power factor (DPF) is the same as the "normal" power factor if this system consisted of linear loads, defined as the cosine of the angle between current and voltage. The power factor (PF) for the nonsinusoidal waveform can be calculated from equation (3.3).

$$PF = \frac{I_{s1}}{I_s} DPF = \frac{1}{\sqrt{1 + THD^2}} DPF \tag{3.3}$$

where I_{s1} and I_s denotes the rms value of the fundamental harmonic component and the current waveform, respectively [7].

As can be seen form the equation, an increase in THD results in a decrease in PF of the system. An ELC solution that creates too high levels of harmonics will make the reactive power balance more complex.

The harmonic components of higher order can flow in different parts of the isolated system. Where it flows depends on the impedance they represent at the different harmonic frequencies [8], given in equations (3.4) and (3.5).

$$X_C = \frac{1}{2\pi f C} \tag{3.4}$$

$$X_L = 2\pi f L \tag{3.5}$$

The equivalent circuit of an induction motor will be presented in figure 4.1. As can be seen in that figure, an induction motor can be represented as a set of resistors and inductors. In the case of the core windings of the generator, the internal losses are highly dependant of amount of disturbance from harmonic components. Hysteresis losses are proportional to frequency, and eddy current losses vary as the square of the frequency. Hence, voltage components of higher frequencies will produce additional losses in the core, that again will result in increasing the operating temperature of the core. [9]

The capacitive elements in a power system will experience the highest amount of reactive disturbance of higher order harmonics. This is given by equation (3.4), as its reactance is inversely proportional to the frequency. A capacitor bank will basically act like a sink, attracting most of the harmonic currents and hence it might become overloaded [9].

Harmonics, with special focus on 3rd and 3rd multiples, can also be produced if the 3 phase system is unbalanced. Given that a complete balanced system is an assumptions defined in the limitations of the thesis, this is not considered further. It is however kept in mind if the simulation or lab results should produce high levels of these types of harmonics.

3.2 Cost and Size

As given in the introduction, the common thread in this thesis is a focus on cost-benefit evaluations when it comes to different technical alternatives. Given that direct cost comparisons are difficult, the objective of this section is to provide a basis of understanding of the cost relations in the key components used in the coming chapters.

Resistors The dump load used is of pure resistive value, like for instance a water heater. The size of the resistance depends on the desired max dissipated voltage in the ELC. The price of resistors are not seen as an vital factor, but it is mentioned to keep in mind that a high resistive value results in a large component.

Capacitors A capacitor bank has to be attached to the system for providing the self-excitation of the induction generator. The size of this will, as proven later in this thesis, depend on the generators rating and the load connection. Additionally, it might be chosen as an alternative for reactive compensation in the system, presented in Chapter 5.

Approximations on capacitance price is found in [10] and [11], assuming a ratio of 2 US$/KVAr. It does however not reveal the type of capacitor used, and is not used as a base. Instead, an approximation stating that the cost of a capacitor will increase with the C-value in Farad is used.

Inductors: The inductor price depends fundamentally on the inductance value, on the root mean square current, and on the power level [12].

Sensors and Other Additional Equipment: As a common-sense approach, it is used as a basis that the adding of additional equipment like for instance a current sensor is costly. The existing solution from Remote Hydrolight uses voltage sensors to adjust the dissipation to the dump load, and this is seen as the minimum requirement. Any

addition of similar components has to be evaluated in relation to the given improvements they represent.

Generator Size: One big motivation for using induction generator instead of a synchronous generator is the reduction in price, especially for the case of generators with low power ratings [3]. As a basis, it is stated that an increased power rating will result in increased price.

Chapter 4

Self-Excited Induction Generator (SEIG)

This chapter gives a short explanation of the basic principles of the induction machine, followed by the relevant theory for an induction generator in isolated mode, referred to as a Self-Excited Induction Machine (SEIG). The SEIG is a challenge to regulate because of its complex relation between its system parameters. There is a mutual influence between the voltage, frequency and power, and when a generator is not connected to the grid some of the previously fixed values will be variable. The challenges related to different loads and the objectives the controller needs to fulfill is given. This chapter is based on the theory given in the preliminary project [1].

4.1 Basic Operation of the Induction Machine

The induction machine can be operated as both a generator and a motor, and connected in both star and delta configuration. The neutral is only available when the machine is connected in star. When the machine is operating as a motor, voltage is applied to the stator and current is flowing in the stator windings. This produces a magnetic field, $\mathbf{B_s}$ which rotates at speed n_s. The field passes over the rotor bars and induces a voltage in the rotor. It is the relative motion between the rotor and the stator that makes this possible. The induced voltage results in a current flowing in the rotor windings which lags behind the voltage. The current produces a magnetic field, $\mathbf{B_r}$, which rotates at the same speed as the stator field. The rotor rotates at a different speed, n_r. The induced torque resulting from the magnetic fields is given in equation (4.1)

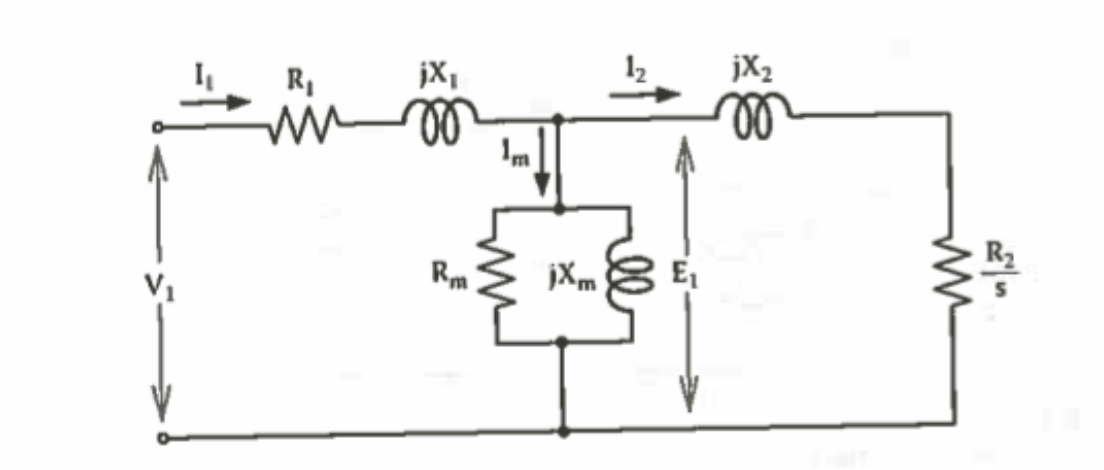

FIGURE 4.1: Per phase equivalent circuit for the induction machine

Source: [13] p. 24

$$\tau_{ind} = k\mathbf{B_r}x\mathbf{B_s} \tag{4.1}$$

The equivalent circuit of an induction machine is given in figure 4.1. Where E_1 is the induced rotor voltage referred to the stator. R_1 and X_1 represents the stator resistance and leakage reactance, respectively, R_m and X_m are the core loss resistance and the magnetizing reactance, and R_2 and X_2 are the rotor resistance and reactance values referred to the stator. The slip of the machine, s, is given in equation (4.2). The slip is given by the relation between the the speed of the magnetic rotating field, n_s and the mechanical rotor speed, n_r.

$$s = \frac{n_s - n_r}{n_s} \tag{4.2}$$

The rotor frequency is related to the electric frequency and the slip, as given in equation (4.3).

$$f_r = sf_s \tag{4.3}$$

The Torque-speed curve for an induction machine is given in figure 4.2, and shows the relation between the induced torque and the rotor speed, referred to a constant speed of the magnetic fields, denoted as n_{sync}. If the machine is working as a motor, n_r is lower than n_s, and the slip is positive. The motor region is the left part of the curve. If it is working as a generator, n_r is higher than n_s, and hence the slip is negative. The generator region is the right part of the curve. This figure shows the variation in

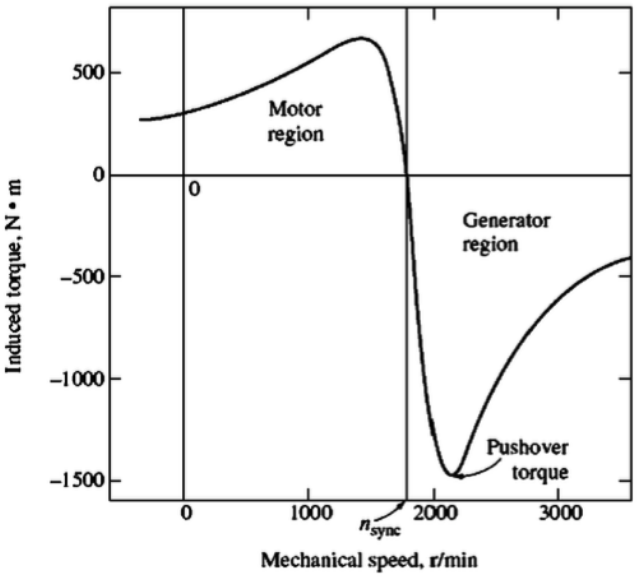

FIGURE 4.2: Torque-speed curve for an induction machine

Source: [14] p. 461

mechanical speed of the rotor n_r with a fixed electrical frequency of 50 Hz. When the SEIG is not connected to the grid to maintain this frequency it gets more complicated.

[13], [14], [15]

4.2 Basic Operation of SEIG

The induction machine consumes reactive power, and this is the main challenge for the use of this machine as generator in isolated operation. A grid connected system will supply the reactive power needed automatically, and provide a fixed frequency and voltage level. In stand alone systems it is necessary to have an external source of reactive power permanently connected to the terminals to enable self-excitation and further voltage build-up. A fixed capacitor bank is connected to the generator terminals for the reactive power supply.

When starting an induction generator in isolated operation, a process called self-excitation is necessary for voltage build-up. The capacitors connected to the terminals and the residual magnetism in the generator enables this. In the exception of completely loss of residual magnetism, some techniques for recovering magnetism are given by Bjrnstedt, J. in [13]. When the generator is starting and reaches a certain speed, the residual magnetism induces a voltage in the stator, which generates a current flowing through the capacitors. The generator is now operating like a synchronous generator, with n_r

equal to n_s. At some point a transition to asynchronous operation takes place, and this leads to the self-excitation. The current in the terminals generates a magnetic field in the rotor, in the same direction as the residual magnetism. This leads to a higher induced voltage in the stator, and hence higher stator current. This will again reinforce the magnetic field. This process goes on until the generator is saturated.

The size of the capacitor bank depends on the no-load characteristics of the generator and the load connected. The capacitance value that will provide enough reactive power for rated voltage at no load is calculated from the machines magnetizing curve in subsection 4.3. When loads are connected to the generator, the need for reactive power changes and additional reactive supply will be necessary. This, as well as other impact from load changes, are covered in subsection 4.4. In addition to adding the capacitor bank, an external controller will be necessary to maintain voltage and frequency within given limits. This is the main task of an electronic load controller (ELC), and the following sections provides background information about SEIG operation that a controller with this purpose have to take into consideration.

[13], [15], [16].

4.3 Magnetizing Curve and Calculation of C

The magnetizing curve, also known as the excitation curve, shows the relation between the terminal voltage and the magnetizing current required by the machine. The terminal voltage is given as a function of the magnetizing current at no load at a given frequency. The curve is related to the machine properties, and can vary from machine to machine, but the general shape is the same. The curve can be found from operating the induction machine as motor at no load and measuring the current I_m in figure 4.1 at different voltage levels V_1. It is important that this is done at a constant frequency, as the characteristics of the curve changes with frequency.

Figure 4.3 shows a typical magnetizing curve given together with straight lines for capacitors. In the left part, the magnetizing curve is given together with different lines for capacitors, corresponding to different values of C. In the right part the curve is shown for different frequencies, where $\omega_3 > \omega_2 > \omega_1$. The curves in the figure starts in the origin. Due to the residual magnetism which produces a small voltage, the curve does not start in the origin in reality, so this is a simplification. The straight part in the beginning of the curve is the self-excitation line.

From the magnetizing curve, we find the intersection point between the curve and the desired output voltage. This intersection point is used to find the slope of the needed

capacitance that will provide enough reactive power to obtain that operation point. The slope is equal to the reactance of the capacitor, which in turn gives the needed value of C. This is given in equation (4.4).

$$X_c = \frac{V_t}{I_m} = \frac{1}{wC} \tag{4.4}$$

This capacitance is connected to the terminals of the generator, and normally referred to as a capacitor bank. The reactive power produced by the capacitor bank is given by equation (4.5).

$$Q = VI = \frac{V^2}{X_c} = wCV^2 \tag{4.5}$$

It is important that the current corresponding to the value of C chosen does not exceed the rated current, so the current is the limiting parameter for finding a maximum value of C. The minimum value for C will be the value that gives a straight line parallel to the excitation line. This can be seen in the left part of figure 4.3, denoted as *Small C*. This is the minimum value for the self-excitation process to take place.

The way of finding the needed value of the capacitor bank through no-load test is generally an underestimation of the capacitance required at no-load. However, it is seen as a quite good approximation for machines with ratings lower than 5 kW [3].

If the capacitance line is close to the excitation line of the generator, there may not always be excitation when the generator is started. The excitation process is also dependent on the speed that rotates the generator. Choosing a high enough value of capacitance and providing sufficient build-up speed will increase the probability of achieving excitation [18], [19].

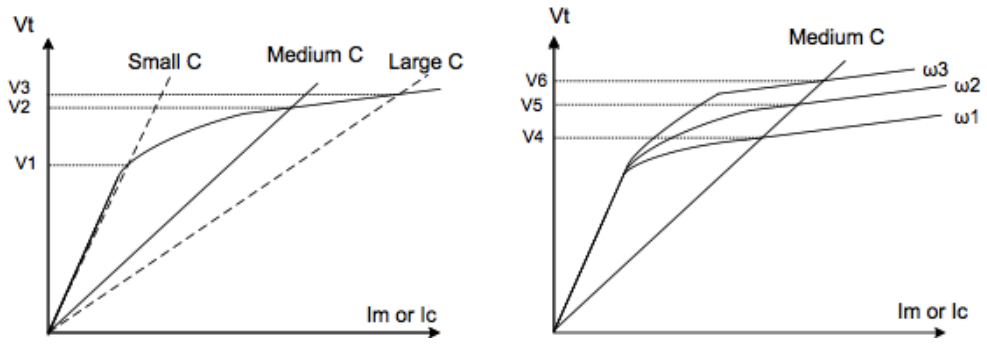

FIGURE 4.3: Magnetizing curve and capacitor lines

Source: [17] p. 15

The magnetizing curve is dependent on the frequency. An increase in frequency given an increase in voltage levels corresponding to the same current. If the frequency is decreased, the voltage will also decrease. This is shown in figure 4.3. If the frequency is decreased, the current corresponding to rated voltage may be higher than the rated current. A too high current results in an increases saturation in the generators windings, which will result in decreased efficiency caused by power dissipation. This can also potentially damage the machine. If the operation point for rated voltage corresponds to a too high current, the solution can be to increase the frequency. As the voltage is dependent on the frequency, it is interesting to investigate how this relation is. If a small increase in frequency results in a rather large voltage increase, and frequency change may be used as voltage regulation. This will be further looked into in the laboratory tests, given in chapter 10.

[3], [13], [17], [20],

4.4 SEIG with Loads

In the following explanation of how the induction generator is influenced by different loads connected, a constant induced torque is assumed. The loads considered in this section is resistive and inductive loads.

The terminal voltage and the frequency varies with changes in loads connected to the generator. Equation (4.5) shows that the reactive power produced by the capacitor bank is proportional to the applied voltage squared, and therefore how the reactive power is very sensitive to the changes in voltage and vice versa. Loads connected can cause variation in voltage, which again can affect the active and reactive power drawn by and delivered to the generator. A more detailed explanation on how the induction generator is affected by different loads is given in this section.

4.4.1 Resistive Load

Changes in the size of the active load connected to the generator will cause changes in the voltage level. This is due to both active power balance and reactive power balance in the system. First, the reactive power related to changes in active power is explained, and the resulting effect on the voltage level. Then the active power balance is related to voltage and frequency changes. It is important to be aware that these are not to separate explanations, but that both active and reactive unbalance will happen simultaneously, and both will cause changes in voltage.

An increased active load upon the generator leads to higher reactive power consumption in the generator. An approximate relation is given in figure 4.4. This is given for an induction generator connected to a grid, but the relation will be similar for isolated operation. P_N and Q_N is the rated active and reactive power for the machine. Q_0 is the reactive power needed by the generator at no-load. [21]

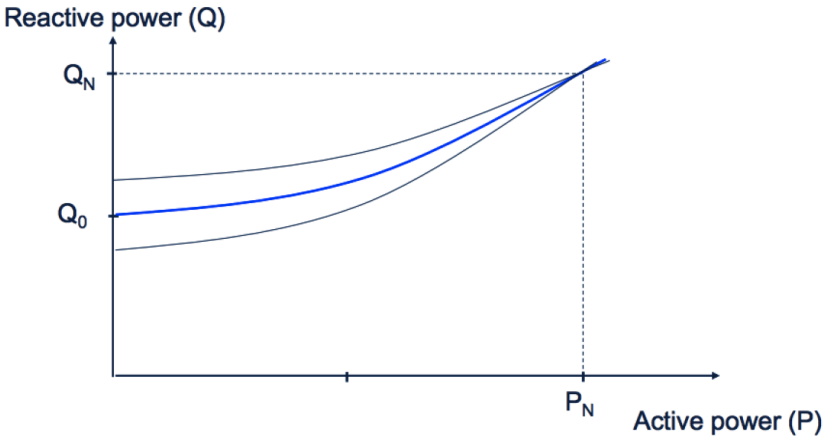

FIGURE 4.4: Reactive power consumption as a function of active power load

Source: [21] p. 25

When the load increases, the generator requires a higher amount of reactive power to maintain the voltage level. If there is no increase in reactive power supply, the magnetizing current provided by the capacitor bank will be lower than the current needed to maintain rated terminal voltage. The result will be a reduction in voltage, as can be seen from the magnetizing curve given in figure 4.3. Figure 4.5 shows the terminal voltage variation with resistive loads for an induction generator operating at constant speed.

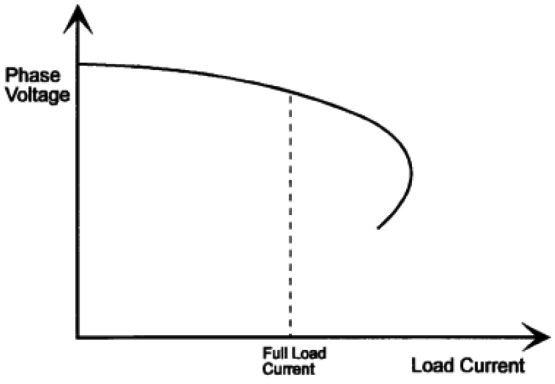

FIGURE 4.5: Typical terminal voltage and load current relation for an induction generator with fixed capacitor bank operating at constant speed

Source: [3] p. 36

Figure 4.5 does however not take into account the speed variations that will occur in a micro-hydro system. The frequency will vary due to the power-speed characteristics for a turbine. The curve for an impulse turbine is given in figure 4.6, where the turbine operates at constant flow. Thus, the speed variation in the turbine is entirely caused by the changes in load. When operating in generator mode, the turbine is operating in the area to the right of the maximum of the curve.

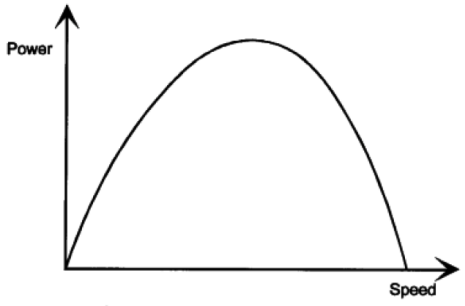

FIGURE 4.6: Power speed characteristics for a turbine in a micro hydro scheme

Source: [3] p. 37

If the electrical torque and the mechanical torque delivered to the generator is not constant, the speed of the rotor will change, as presented in equations (2.1) and (2.2). From equation (4.3) it is given that the frequency varies with the slip and the speed of the rotor. The slip increases with total active power drawn by the load. The frequency variation is usually limited to 5 %, due to the steep characteristics of the torque-speed curve given in figure 4.2.

[13], [15], [22]

If the generator is operating at an equilibrium, with mechanical torque equal to the electrical torque, the rotor speed will be constant. If the electrical power is decreased, the speed of the rotor will increase, resulting in an increased frequency. As explained in the previous section with reference to the magnetizing curve, this will give a higher voltage level. The speed will increase until the voltage reaches a value where power balance is obtained again. If on the other hand the electrical power in the system is increased, the rotor speed will decrease. This will give a reduction in voltage. The new operation point will be at a frequency that corresponds to a lower voltage resulting in a balance in the power in the system. If the load increases to a level where the voltage drops too low, the reactive power produced falls and it can result in de-magnetizing of the system and total voltage collapse.

[3], [13], [22]

4.4.2 Inductive Loads

If inductive loads are connected to the generator, they will consume reactive power. This means that some of the current from the capacitors will go to the load instead of the generator. This will reduce the reactive power supply to the generator, and the generator voltage will drop. An inductive load is influencing the total capacitance by decreasing the effective value. This is shown in the equation (4.6), where the parallel connection of the capacitor bank and the inductive load is represented as a new and reduced actual capacitance value.

$$C_{eff} = C - \frac{L}{R_l^2 + (\omega_{nL})^2} \tag{4.6}$$

R_l is the resistance corresponding to the resistive loads. If the inductance L is small, it will not have much influence on the capacitance value. If the value of L is high, it will have a greater effect. A considerable reduction in C_{eff} effects the previously described slope of the capacitor line expressed in equation (4.4). A reduction of C_{eff} will result in the reduction of the induction generators terminal voltage. If the resulting C_{eff} becomes smaller than the defined C_{min} for the system, the voltage will collapse. [13].

The voltage drop caused by the inductive loads will cause an increase in speed. This is because a reduction in voltage causes a reduction in the active power consumed by the loads. Hence, the power balance is disturbed, and the speed increases. The increase in speed will increase the voltage, and the speed will increase until a level where power balance between the power consumed by the loads and the power delivered by the turbine is reached again. Hence, the inductive loads will influence the frequency in the system.

4.4.2.1 Induction Motor as Load

The induction motors as a load represents a challenge to the system, especially during start up. The starting current, or inrush current, is the most critical parameter. This can be as high as 6 times the rated current [23], depending on the supplier and type of motor. As well, the reactive power consumption is higher during start-up than steady state operation of the motor. The current transient will cause a voltage dip in the power supply system. Hence, across-the-line starting of induction motors may not be possible without any adjustments [15].

4.4.2.2 Combination of Resistive and Inductive Loads

A lower power factor is equivalent to a higher share of inductive loads. Figure 4.7 shows the relation between the terminal voltage and the power output from a generator for different power factors of the total load connected. Figure 4.8 shows the frequency variations for the same scenarios. [13]

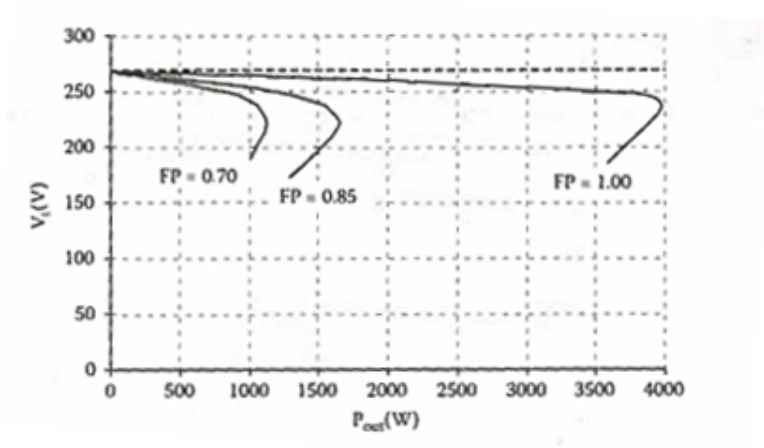

FIGURE 4.7: Terminal voltage variation for different load power factors as a function of active power output

Source: [13] p. 102

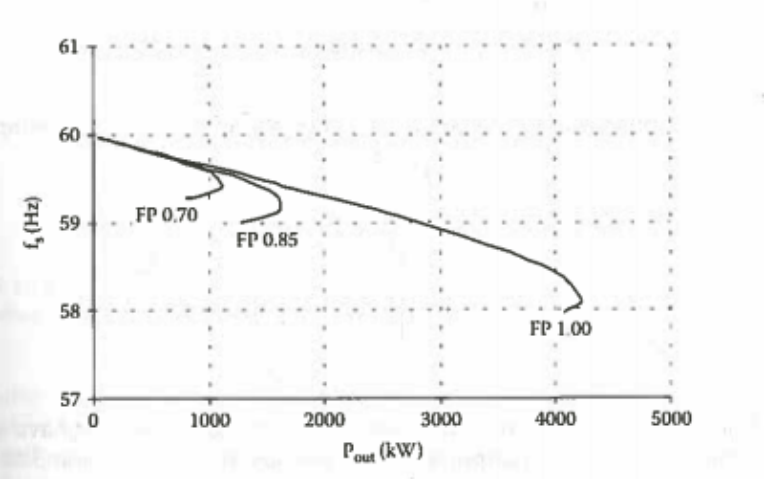

FIGURE 4.8: Frequency variation for different load power factors as a function of active power output

Source: [13] p. 103

From these figures, it can be seen that the voltage and frequency collapse occurs at lower voltage levels for lower power factor. A higher share of inductive loads thus gives a smaller range of operation before collapse.

4.4.3 Discussion

As explained in this chapter, the different loads connected to the isolated generator influences both voltage and frequency. To be able to control these variables, both active and reactive power should be balanced.

The reactive power consumption increases with the active power loads. If the active load is constant, so will also the generators reactive consumption be. If the active load is balanced by for instance an ELC, there will not be changes in the voltage and frequency caused by variable active power, and the problem is reduced to balancing the reactive consumption of the inductive loads. In this, the inductive load will include the inductance from the ELC itself.

Inductive loads effect both voltage and frequency when connected to an induction generator. In the previous system with an synchronous generator, the ELC has been used for frequency regulation. Working with the induction generator however, this may not be sufficient for maintaining the voltage. An increased share of inductive loads will result in voltage and frequency collapse at lower levels of power output from the generator, and will require more from the control system.

To sum up, the control of the induction generator is challenging, as it requires a combined speed and voltage control with mutually dependent parameters.

Chapter 5

Methods for Reactive Compensation Combined with an ELC

As concluded in the project thesis [1], a SEIG + ELC system with a fixed capacitor bank as the only source of reactive compensation will probably result in poor voltage regulation. If there is unbalance in the reactive power in the system, it will affect the voltage level: If there is too much reactive power, the voltage will be too high. If there is a lack of reactive power, the voltage will decrease below rated value, and may even lead to total voltage collapse. Additional reactive compensation might be necessary to improve the voltage regulation when the generator is operating at different loading conditions.

As stated in section 2.3.2, the power factor of the village load will mainly be close to unity, so the reactive compensation will mostly be needed if the ELC solution consumes reactive power. It is also of interest to consider the case where an induction motor is connected as a load to the system. This load will draw reactive power, and has a very high share of inductive consumption during its start-up.

Considering the scope of the project, only the simplest and cheapest possibilities for reactive compensation are considered. Based on the previous evaluations presented in the project, and extended literature study on this field, it is chosen to further evaluate three options for reactive compensation: Fixed and switched capacitors, Series capacitors and SVC.

5.1 Switched Capacitors

The switched capacitor scheme is viewed at the most relevant compensation method to use with the SEIG + ELC system. The working principle is simple, easy to understand and easy to implement in a simulation model and a laboratory set-up.

One or more switched capacitors can be connected in parallel with the existing capacitor bank, used to provide the varying need for reactive power at different loading conditions. With this solution, the shunt capacitance value can be dimensioned for full resistive load, and the system can be designed to switch in one or several capacitors when the voltage level decreases below a certain value due to shortage of reactive supply in the system. This provides voltage regulation in discrete steps, given that the capacitor can only be switched logically on or off. Hence, this method may not be able to provide the correct amount of reactive power and hence voltage level at varying input and loading conditions [24].

This option requires an additional sensor, which reads the voltage and accordingly switches in the optimal combination of the available capacitors to improve the power factor in the system by trying to archive reactive balance in the system. [24].

If the amount of capacitors needed in the system is high, this is an expensive solution for reactive compensation. Addition of an extra capacitor also includes an extra switch, which is costly and that might provide disturbing transients. If the allowed operating voltage range is wide, a discrete voltage regulation may be sufficient and it will not be necessary with many capacitors to provide the compensation. Sources suggest it for use in rural electrification, which is the topic of interest [25].

5.2 Series Compensation

Series compensation is a less complex solution compared to switched capacitor or controlled inductors, without a control circuit design and does not have the operational problems associated with harmonics and switching transients [26].

Series capacitors are always seen in a combination with a parallel connected capacitor bank, as it cannot provide reactive power for the self-magnetization process alone.

The combination of series and shunt capacitance can be done either by short shunt or long shunt connection. Short shunt means connection of the series capacitors at the load side of the shunt capacitance, and long shunt means connection at the generator. The short shunt solution requires lower capacitance values which will be less expensive [26].

The short shunt option gives a better voltage regulation compared to the long shunt configuration and thus have better performance [24], [26]. It is found to be the better solution, as it can easily deliver power up to rated power with the smallest reduction in voltage [27].

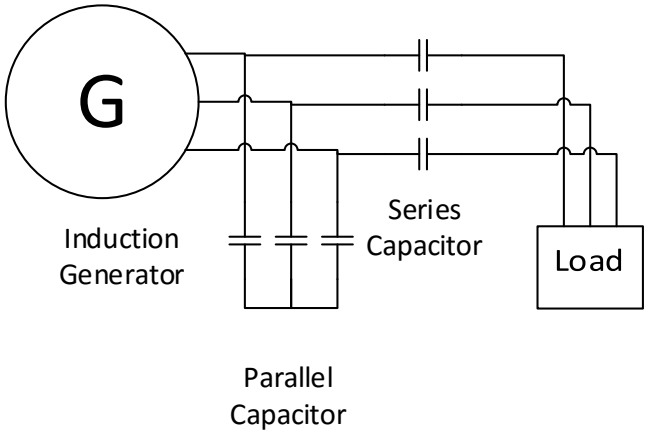

FIGURE 5.1: Series compensation with short shunt connection

While the reactive power produced by a parallel capacitor is determined by the voltage, the reactive power supplied by a series capacitor is determined by the current.The reactive power supplied is given by equation (5.1).

$$Q = \frac{V^2}{X} = I^2 X \tag{5.1}$$

If an increase in current is equivalent with an increase in reactive power demand, this might be a suitable solution. As discussed in the project thesis [1], the main advantage of a series capacitor is the fact that the reactive power production will be proportional with the load increase, and hence the reactive power demand. For the ELC however, it is not necessarily the case. If there is an ELC in the system, the active power will be constant. It needs to be investigated how this solution will work with a constant active current and a varying reactive current, if this compensation is to be used in combination with an ELC.

With a correct combination of the capacitors in the short-shunt configuration, it is supposed to be possible to have an almost flat load characteristics and the need for additional reactive compensation will be eliminated [26]. When choosing the size of the

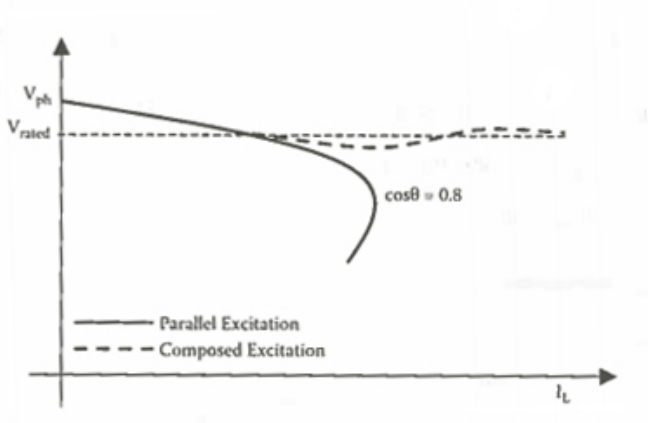

FIGURE 5.2: Influence of the series capacitance on relationship between terminal voltage and load

Source: [13] p. 83

shunt and the series capacitance, the shunt is first determined, and used as a base of choosing the series capacitance. The shunt capacitance is set to the no-load value or increased slightly from this. Chan, T.F. [28] describes a factor k, defined as the ratio of series capacitive reactance to shunt capacitive reactance. Experimental tests are done for a 4-pole, 50 Hz, 380 V, 5.4 A, 2 kW, star-connected squirrel cage induction generator, the best compensation is obtained for k = 0.40. Other articles suggest different ratios between the shunt and series capacitor, where the factor k is between 1 and 0.4 [26], [27], [29], [30]

The main disadvantage of this solution is the possible occurance of subsynchrounous resonance (SSR) in the system while supplying inductive loads and dynamic loads [24]. SSR is is oscillations in the voltage and current at lower frequencies than the fundamental. A series capacitor with a SEIG feeding an induction motor may cause SSR, which leads to excessive voltage and current, as well as oscillations in the speed of the motor. Also the developed torque will oscillate, and this will restrict the speed of the motor. The frequency of the oscillation depends on the value of the series capacitor and the impedance of the load, and the SEIG is sensitive to subharmonics distortions. SSR can however be avoided, given an optimum combination of the shunt at series capacitance. [29]

Also, the possibility of disconnection of one or more of the capacitors will cause unbalance in the system, as it will imply loosing one of the three phases. Unbalanced systems are not taken into consideration in this thesis for limiting purposes.

Given that it will be easy to implement in both a simulation model and in a laboratory set-up, it is interesting to investigate the possible use of series compensation in combination with a SEIG + ELC system. This is the cheapest and simplest of the evaluated

compensation methods, and if it is found to be working within the given boundaries for voltage and frequency it might be a very interesting option.

5.3 Static Var Compensator: Fixed Capacitor Thyristor Controlled Reactor

A Static Var Compensator (SVC) is by definition a shunt connected static var generator and/or absorber whose output is varied to control specific parameters (e.g. voltage, frequency) of the electric power system. SVCs are used for its advantages of having a fast response and continuous control of reactive power, immediately implying that it will have some advantages compared to both series and switched capacitors.

The output from a thyristor can be controlled by its firing angle. Connected in anti-parallel in series with an impedance, a variable reactive consumption can be controlled. Figure 5.3 shows the basic operation principle. Connecting this in parallel with a fixed capacitor, the actual reactive power generation Q_C is adjusted by the variable reactive power absorption Q_L. [24], [31], [32]

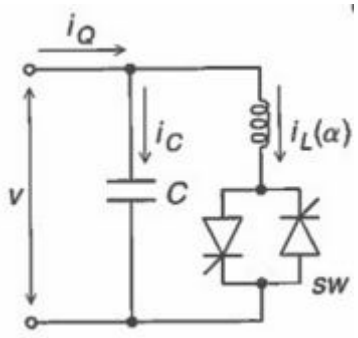

FIGURE 5.3: Basic FC-TCR static var generator

Source: [31] p. 155

The relationship of controlling the final amount of C given a parallel connection of C and an adjustable L was presented in equation (4.6) in section 4.4.2. It is not crucial to obtain perfect values for C and L, as long as it is possible to control the resulting L value with the thyristor. The connected system will then always experience the correct C_{eff}.

For a ELC control system with a high influence of changes in reactive power, a reactive power compensation unit with controllable output might be necessary.

A paradox worth mentioning is the fact that reactive power consumed by an inductor, Q_L is inversely proportional with the value of inductance L. Hence, for consuming a

small amount of reactive power at a given voltage level, a large value of L is needed. Depending on type of inductor, the physical size will also be increasing with the value, possibly resulting in extreme sizes of the components needed.

The addition of the controllable thyristor complicates the scheme, which directly results in an increase in costs. If something fails in the control of the inductor, the resulting reactive power delivered by the capacitor might lead to too high levels of voltage.

5.4 Discussion

The choice of compensation method depends on the needed quality of the reactive compensaion delivered. If it is important to obtain the exact VAr value, the FC-TCR method is recommended. If a descrete-step regulation of the voltage is accepted by the system limits, this will be an easier and most likely a less expensive solution. It is assumed that the fixed capacitor solution will be sufficient for the system evaluated in this thesis, but the conclusion is left til after the actual functionality is investigated further.

The series capacitor is seen as an interesting outsider. It is not mentioned in the litterature as a regular compensation method for the case of having already an ELC maintaining constant power, but it represents the simplest and less expensive option for compensation, so some introductory investigations in simulation and laboratory environment is interesting also for this.

Chapter 6

ELC Design Options

In the Project work [1], four possible options for controller design was presented. As listed in Chapter 2, the technologies has to be evaluated in terms of reliability but also robustness, complexity and cost. The options are again evaluated and presented with additional information in the following chapter.

6.1 Triac Controlled Dump Load

This is the existing solution in the ELC developed by Remote Hydrolight for use with a synchronous generator. It consists of a triac, which is adjusting the amount of power dissipated to the dump load by varying its firing angle. A triac works like a bidirectional thyristor, conducting current in both directions and hence in both half periods of the current waveform.

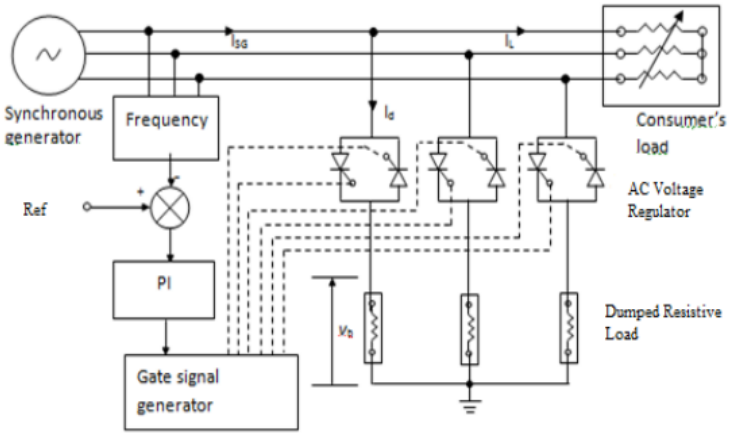

FIGURE 6.1: Basic principle of triac controlled ELC

Source [33]

Figure 6.1 shows the basic working principle for this solution. The voltage is used as the input to a controller, which is using a PI regulator to sense if the frequency of the voltage is higher or lower than the reference case of 50 Hz. By doing this, it is measuring if the attached load voltage has increased or decreased in relation to the point of equilibrium. From this, the gate signal controlling the firing angle of the triacs are adjusted to maintain the load balance explained in section 2.1.

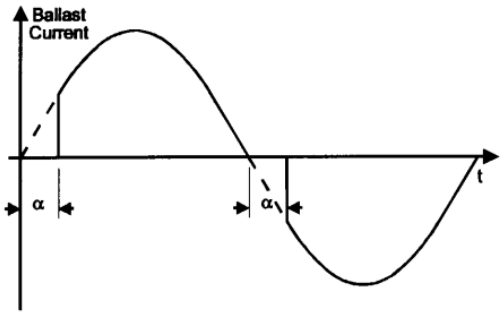

FIGURE 6.2: Waveform of dump load current in a trac controlled ELC

Source [3] p. 48

The firing angle is delaying the ballast load current in relation to the voltage, resulting in an internal consumption of reactive power. The current waveform to the ballast load is given in figure 6.2, where α is the firing angle. The worst distortion of the current waveform is when the firing angle is set to 90 ^{o}. This distortions is causing harmonics as explained in 3.1.1, which is also worst at 90 ^{o} as the chopping of the waveform is at its most dramatic in this point. As concluded in [1], this is the main drawbacks for using thyristor solution with an induction generator, and it is anticipated to need an additional reactive compensator in order to work sufficiently.

Using an ELC with thyristor controlled dump load is generally seen as an old and little efficient method to use compared to other available power electronics solutions. For rural electrification applications however, other parameters as robustness will be of higher value. The thyristors has a high thermal capacity, and a good protection against overvoltage and overcurrent situations.

In Remote Hydrolights 15 years of experience, the thyristor controlled solution used with a synchronous generator has been working well when the village load is purely resistive. A report published in 2015 [34] presents this solution as a suited option for implementation also with an SEIG, this time loacted in a rural area of Brazil. The load connection is varying its power factor, and it is stated that some sort of reactive compensation is needed. A static var compensator (SVC) similar to the one presented in 5.3 is added to the configuration. The option of including the compensation in the same closed loop as the voltage control is chosen over two separate control loops to keep

the system simple. The field test reports satisfactory results, where the systems was tested for several different situations of change in main load.

The request from Remote Hydrolight is to evaluate the viability of this solution used with an induction generator. If it is possible, it will be very easy to use the same components and manufacturers as previously, enabling a faster implementation of the next stages of their project.

[7], [34]

6.2 Binary Logic-Switched Dump Load

By switching in and out a combination of fixed resistors with binary weighted values, the binary logic controller will produce a variable resistive dump load to balance the total power output according to changes in consumer load. With this method, one can optimise the possible load steps with using a minimized number of resistors and switches. As a response to changes in consumer load, the controller will calculate and switch in the optimal combination of the dump loads.

Since the only controlled device are logical on/off switches, the problem of harmonic distortion that are influencing the other ELC options are of less importance. The binary logic method will normally use solid-state switching relays which include a zero-voltage switching circuit. This will reduce the THD associated with the transient switching.

Using this method in a three-phase system is a complex and costly operation as it requires a relatively high number of ballast loads to work sufficiently. Each load will need a switching device, and since the output only can be varied in fixed steps the voltage regulation will not be of high quality. For the specific use of providing electricity in rural areas where the voltage quality restrictions is not too high, this is a possible option.

This solutions provides no additional reactive power compensation, and is previously been used in systems using a synchronous generator feeding only resistive loads. One research paper published in 2015 [35] suggests this method in combination with an induction generator, with the frequency as a control parameter. The results verify that the THD is low, but that the voltage regulation is poor. It is suggested to implement a voltage control loop instead of the frequency. This is because, as discussed in section 3.1, the limitations of voltage always will be of higher importance than the frequency.

[1], [3], [36], [35]

6.3 Uncontrolled Rectifier with Chopper Controlled Dump Load

An "uncontrolled rectifier"-ELC consists of a diode bridge rectifier, and a single chopper that controls the dissipation to the connected dump load. A chopper is a self-commutating switching device, such as for instance an insulated-gate bipolar transistor (IGBT). This solution is mentioned by several sources, including [3], to be the best working options of the available cost-friendly ELC solutions. The one-phase configuration is shown in figure 6.3.

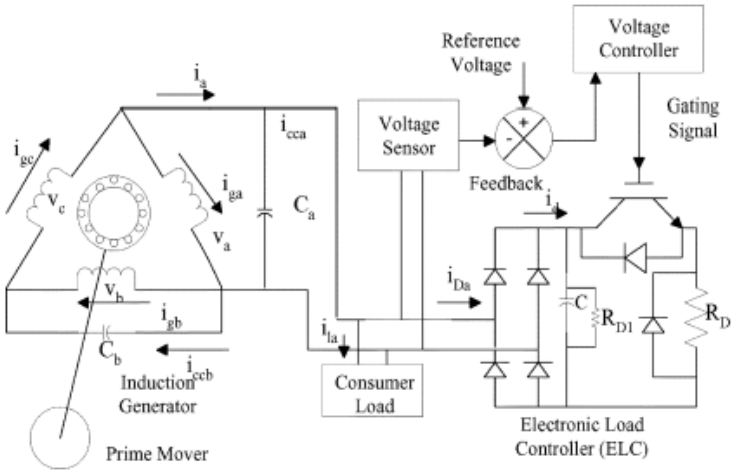

FIGURE 6.3: Basic principle of uncontrolled rectifier with chopper type ELC

Source [37]

Rectifying the dump load voltage has its main advantage in the fact that the control is reduced down to one semiconductor device. It is therefore cost-effective, user friendly, almost maintenance free and also easy to construct in rural areas where it has been tested by several developers. For the chopper operation a pulse width modulation (PWM) can be used where the duty cycle of this pulse output is being controlled. There is examples of the chopper having a duty cycle from 0 to 100 %, but also where it is reduced to 5 to 95 % to avoid damage. [25], [38], [37], [39]

The configuration is connected with a capacitor bank in parallel, as is needed for any controller type to ensure self excitation of the SEIG. In tests including inductive load in the village, the use of additional reactive compensation like series capacitors or switching of additional shunt capacitors are suggested. [38], [25]

The least expensive way to convert AC to DC is through uncontrolled diodes, giving that the power flow can only go in this direction. The DC voltage on the output of the rectifier should have as little ripples as possible, and therefore it is often seen in combination with

a parallel connected filtering capacitor. Because the current flow though the rectifier is not of continuous flow, this device draws a highly distorted current. This might not be allowed in some cases according to harmonic standards. In a comparing test with the thyristor-controlled ELC described in section 6.1, it is shown that the level of harmonics produced by the uncontrolled rectifier at the worst case is twice the amount of the thyristor-controlled ELCs worst case level of harmonics [37]. For the uncontrolled rectifier, the amount of THD increases with increased power consumed by the dump load. [7], [40]

With costs in mind, this solution will demand similar resources as the triac controlled solution. A PI controller will use the registered voltage to calculate the duty cycle of the chopper that will maintain power balance, but controlling only one chopper instead of three triacs. The capacitor bank will be of the same size for the same ratings.

6.4 Controlled Rectifier with Chopper Controlled Dump Load

The controlled rectifier has a similar configuration as the one uncontrolled solution presented in the previous subsection, but the key difference is the use of controllable thyristors instead of diodes in the AC-DC rectification. It makes this configuration capable to decouple the control of the real and the reactive power, and no additional reactive compensation will be needed.

In this solution, the task of controlling the impedance is changed from controlling voltage directly to controlling current. Assuming that the voltage and frequency is control is achieved, this means that the generator current i_G has to be constant. Since the voltage and the size of the capacitor bank is constant, so is the capacitor current i_C. In order to maintain this, the parameter to keep constant as to maintain frequency and voltage level is the generator-capacitor current.

The use of thyristors in the bridge instead of diodes makes it possible to also control reactive power. By using a bigger capacitor bank than the other mentioned ELC options, which is dimensioned for the maximum consumption of reactive power in both the generator and the load, the phase angle of the thyristors in the bridge can be controlled to consume the variable excess reactive power delivered by the capacitor bank. Increasing the capacitor bank and including more sensors and equipment will however, as commented in 3.2 be more expensive.

In order to keep the current controlled, the changes in load current i_L caused by load differences has to be compensated by a controller current i_{ct}. The control algorithm

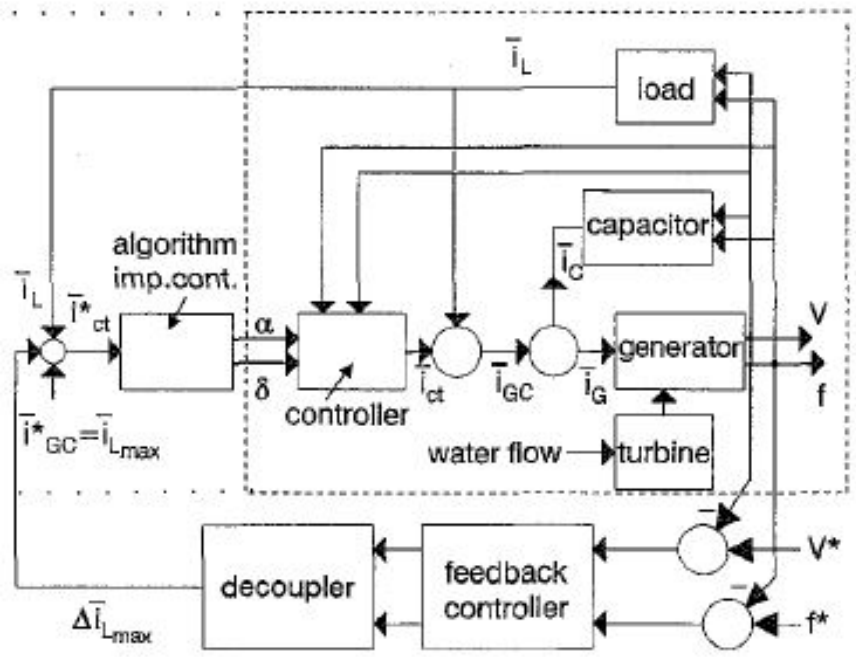

FIGURE 6.4: Structure of Controlled Rectifier + Chopper algorithm

Source [41]

computes the thyristor angle α and the pulse width to maintain i_{ct} constant. The structure is shown in the figure 6.4. [41]

As for the uncontrolled rectifier, the THD is highest at no consumer load. [42] suggest three design strategies for reducing this value: Decreasing R_{DC} to increase operating range, or shifting the control area of the thyristor bridge by including switching capacitors or an SVC for reactive power control internal in the system. The latter solution showed less total THD.

An important argument for an uncontrolled rectifier-solution is that only one power electronic component needs to be controlled. In this scheme the thyristor bridge is also controlled which increases the complexity. However, excluding the need for an additional reactive compensating unit in case of inductive loading is a powerful argument, but it looses its strength if the resulting THD production is so high that a compensating unit for this is necessary.

6.5 Voltage Source Inverter (VSI) with Dump Load

This configuration of this ELC is similar to the two previously mentioned rectifier bridge solutions, but both the complexity and hence the control possibilities are taken one step further. The semiconductor device used in the VSI is of a bidirectional type, like for instance transistors.

A big advantage for this solution is that the VSI operates constantly at 50 Hz and is able to maintain the electrical frequency of the SEIG constant under normal operation. The balancing is then reduced to only concern balancing for voltage control.

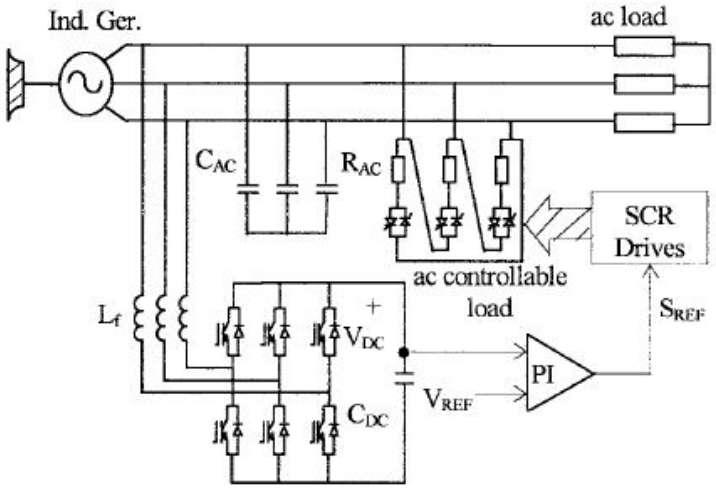

FIGURE 6.5: VSI-ELC with AC-side connected dump loads

Source [8]

On the DC side of the inverter, a capacitor C_{DC} works as a voltage source for the reverse-flow operation. When the village load is less than the generators power full-load output, some of the excess power will be stored in this capacitor. When the reactive compensation need increases, the bi-directionality provides the possibility of supplying this capacitance back to the AC side. In addition, adjustable resistors are connected to consume the resisting power to maintain the balance. These can be connected either on the AC or the DC side of the VSI, as shown in figures 6.5 and 6.6. In both cases, it is the feedback signal V_{DC} which describes the balance between the generated and the consumed power in the village load. The inductance L_f has a filtering function, described in appendix B, which represents a small voltage drop in this circuit.

As can be seen from the figures 6.5 and 6.6, the adjustable resistors working as dump loads has familiar configurations. The AC side solution uses anti-parallel connected thyristor controlled dump loads, which is the same principle as the solution presented in section 6.1. From this point of view, the VSI is only a complex reactive power

compensator in addition to the controlled dump load. The DC side solution uses a chopper controlled dump load like the one presented in 6.3. The argument for using the AC side dump load is to decrease the amount of active power flowing through the VSI, and hence decrease its power rating.

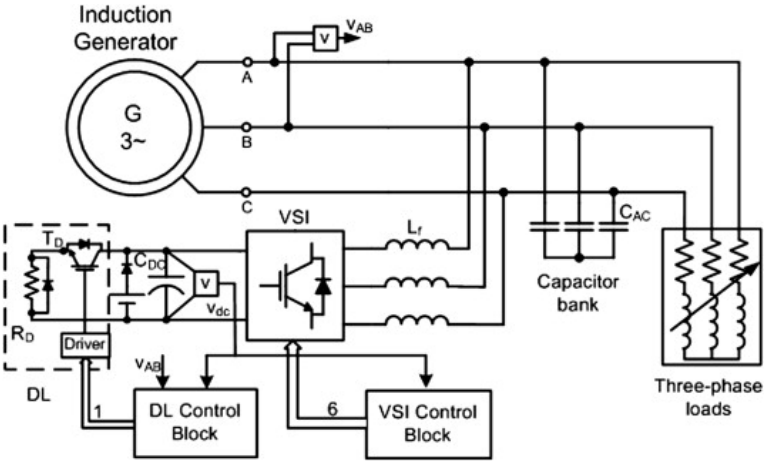

FIGURE 6.6: VSI-ELC with DC-side connected dump loads

Source [43]

The VSI is presented as the optimal option for isolated operation, as it is stated to be able to handle both unbalances in the system and any additional harmonics mitigation [8]. Unbalanced load is kept out of the scope of this work for limitation purposes, but is highly relevant for isolated operation. Since the software is intended to be free for downloading, the increaced complexity of the regulation algorithm is not a primary concern. For doing this in practice however, it will include a lot more sensors and complex equipment than the other alternative ELCs have, resulting in a higher cost.

[8], [43]

6.6 Discussion

Since it is the request from Remote Hydrolight to investigate the possibility of using the triac controlled technology with SEIG, it is used as a reference case in the further study. It is not expected to have a very good voltage regulation without any reactive compensation, so it is assumed that one of the options discussed in Chapter 5 will be added to the configuration.

Comparing the controlled rectifier option with the VSI, the latter seems to have most potential. Given that the objective is to find the optimal solution with high importance to it being cheap, it is however not evaluated further. For a similar use in island operation

in Norway this would possibly be the suggested solution, as it seems to be unique in its voltage and frequency stability.

The binary logic controller is not evaluated further as it physically will be more complex than the other with many big resistors, and the impression found in literature gives that it will provide a too poor voltage regulation. Even though the existing requirements in the rural areas are relatively low, it is desirable to go for a solution that can also meet higher demands in the future.

The uncontrolled rectifier seems like the cheapest and simplest alternative of the other possible options. Although it is expected to produce a higher amount of harmonics, it will have a better voltage control. This option is chosen to provide comparable results with the triac solution in a simulation environment to evaluate the differences in inductive load-sensitivity and harmonics production.

The question to be answered is if the simpler ELC solution will provide sufficient voltage control. Another point of view might be if the supposed necessary reactive compensation unit in a combination with a simple ELC will still be less complicated and provide sufficient compensation, or if the extra cost of installing one ELC unit controlling the whole system might be beneficial after all.

6.6.1 Reactive Compensation in Combination with ELC

If there is only resistive loads in the system, it may only be necessary to control the active power. The capacitor bank can be dimensioned to supply the full load reactive need for the generator. If this is sufficient depends on the reactive power consumed by the ELC. If this consumption causes a voltage drop in the system, reactive supply to balance this may be necessary. The choice of possible reactive power compensation will depend on the amounts of reactive power drawn, and the cost-benefit analysis of the improvement in voltage versus investment cost of the additional equipment.

All the three discussed methods presented in Chapter 5 will be interesting to test with the triac controlled ELC, but perhaps not with the uncontrolled rectifier ELC. As the latter is expected to have the best voltage regulation and the highest level of harmonics produced, the solution using the FC-TCR is probably not applicable.

Chapter 7

Simulation Models

The goal with the simulations is to create a simple fixed point model for analysing the existing ELC option using triac control, and to compare this with the uncontrolled rectifier solution.

This chapter covers the steps necessary to build comparable models from scratch. The analytical results are presented in the following chapter.

The simulations are done in the SimPowerSystems environment in Matlab/Simulink. The model configurations is set to the "OD23TB" option, and solver reset method is set to "robust" to make sure power electronics components are working properly. The Powergui block is set to "continous".

A pre-defined block for the induction machine is chosen from the Specialized Technology library of SimPowerSystems. A Y connected squirrel cage preset model is used, with frequency set to 50 Hz and machine parameters P_{base} = 4 kW and V_{base} = 400 V, resulting in I_{base} = 5.77 A. The same machine is used in all the simulations until section 8.2.

In this model, the turbine rotor speed is set to a constant value. As discussed in the introduction, the constant speed alternative is an approximation and a limitation of the results.

7.1 No Load

The constant speed of the generator should be of a value that gives a base frequency of 50 Hz in the system. First, the input to the machine is set to be
ω = 1.00 pu = 1500 rpm = 157.08 rad/s

The frequency is first measured by reading the phase voltage of one of the phases, and using a counting configuration to find the time of its zero crossings. The input speed of 157.08 rad/s gives a system frequency of 48.44 Hz. Since increased rotor speed results in increased system frequency when other parameters are kept constant, the value of the input constant speed ω to the machine is tuned up to $\omega = 160$ rad/s, giving a frequency of 50.01 Hz.

Further, a capacitor bank is connected to the system to provide reactive power for the self-magnetization of the rotor, and the initial no-load system is presented in figure 7.1. The star point of the capacitor bank is grounded as the simulation is unable to run without any connection point to ground.

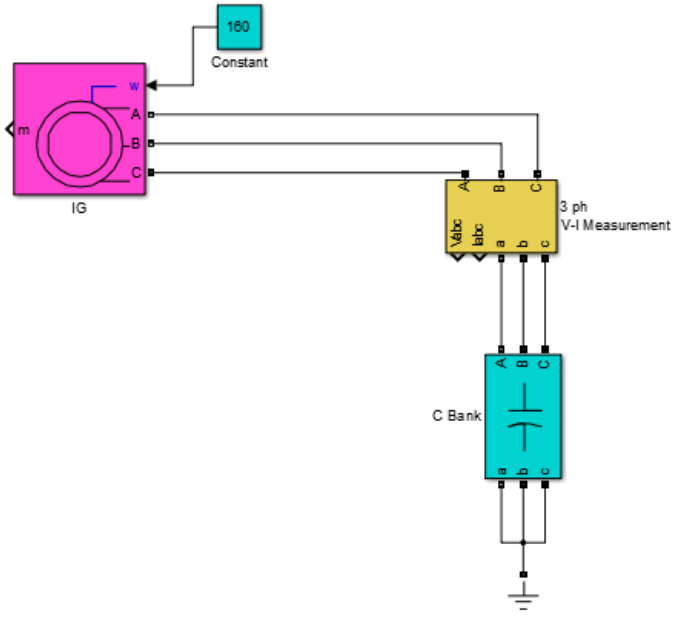

FIGURE 7.1: Simulation system (No-load)

The default magnetizing curve in the SimPowerSystems induction machine block has the same values for voltage and current independent of the generator size, implying that the magnetizing curve is not adjusted for changes in generator ratings.

First, there is a problem with the magnetizing curve starting at zero voltage and zero current, giving that there is no residual magnetism in the generator. With these conditions the generator will not start in isolated mode. In this case it will need to start connected to a voltage source or a battery that can provide the initial magnetizing current, for then to be disconnected when the desired value is achieved. This does not represent the system planned to be simulated, as it is a isolated system witch cannot connect to the grid and preferably not any other voltage source for voltage build up. Another problem

with the initial magnetizing curve is that at rated voltage, the magnetizing current is higher than the machines own rated current.

Because of these problems, the magnetizing curve is changed so it represents a realistic induction machine behavior. The new magnetizing curve implemented in the model is based on the results from the laboratory work in the project report [1], which is given in appendix C. To implement it in the simulation, it was first converted from SI units to PU, and then the rated values of the induction machine block in SimPowerSystem is used to adjust the curve according to the simulation machine. With these results, simulations are continued with an intersection point of 1.00 pu voltage that gives 0.725 pu current. With this the slope of the capacitance line is found, and hence the value of the capacitance needed to obtain rated voltage at no load: $C_{bank,noload} = 57.636\ \mu$F

After some tuning of the model parameters, it can be seen from the measurements that a value of C decreased to C = 53.8 μF gives the desired output of no-load voltage, and this value is set as the new $C_{bank,noload}$. The values for voltage, current and reactive power consumption with this capacitor bank is given in the table 7.1

$C_{bank,noload}$	53.8 μF
V_{ph}	230.6 V
I_{ph}	3.97 A
Q_{gen}	2746.8 Var

TABLE 7.1: Tuned parameter values - No load simulation

7.2 Resistive Load

As explained in section 2.3.2, the generator should be loaded with a resistive load a bit smaller than the rated effect of the generator. This is due to wear and stress on the generator if it is kept running at maximum capacity. Since oversizing the generator represents an increase in cost, the highest rated output within the given limit is chosen for the attached load, corresponding to the generator being 1.5 times the load rating.

Given that the rated output of generator in the model is 4kW, the full load is calculated to according to equation (7.1).

$$P_{tot} = \frac{P_{gen}}{1.5} = \frac{4k}{1.5} = 2.67kW \tag{7.1}$$

This value is used as a constant active power load in the system, and it corresponds to 890 W per phase. As described in Chapter 4, it is expected that an increase in active

power load will increase the reactive power demand. Thus, it is expected that an increase in the capacitor size is necessary to get a phase voltage of 230 V when the generator is loaded.

After trial and error, the value of the capacitor bank is increased from $C_{noload} = 53.8\ \mu$F to $C_{fullload} = 69.5\ \mu$F.

It is however not desirable to use constant-power loads in the simulations, so the load blocks are changed to the constant resistance type. The value for this resistance is calculated according to equation (7.2).

$$R_{ph} = \frac{V_{ph,RMS}^2}{P_{ph}} = \frac{230^2}{888.88} = 59.5125\Omega \tag{7.2}$$

As seen in Chapter 4, frequency is related to the active load. An increase in load will cause an increased slip in the generator, and hence a higher speed of the rotor is necessary to provide a frequency of 50 Hz in the system.

With a new input speed of w = 163 rad/s, 50 Hz is reached for the full-load case. An increased frequency corresponds to a changed magnetizing curve, where the voltage levels at the same currents is increased as shown in figure 4.3. This means that the value of the capacitor bank needs to be decreased in order to give the correct output voltage. Final values from the full-load tuning is given in the table 7.2.

P_{gen}	2684.5 W
Q_{gen}	3250.5 VAr
V	326 V
C	64.0 μF

TABLE 7.2: Tuned parameter values - Full resistive load

From this, it is found how much reactive power the system itself needs at full load. Additional reactive power requirements has to be supplied additionally if it results in a too large voltage drop.

7.3 Electronic Load Control (ELC)

The system including village load and an ELC unit in parallel is shown in figure 7.2

Voltage and current are measured at four connection points in the system: generator output, capacitor bank connection, ELC connection and village load connection. These values are used to analyze active and reactive power flow in addition to voltage stability. In plots showing system currents the Village Load current is left out when it is very similar to the Generator current.

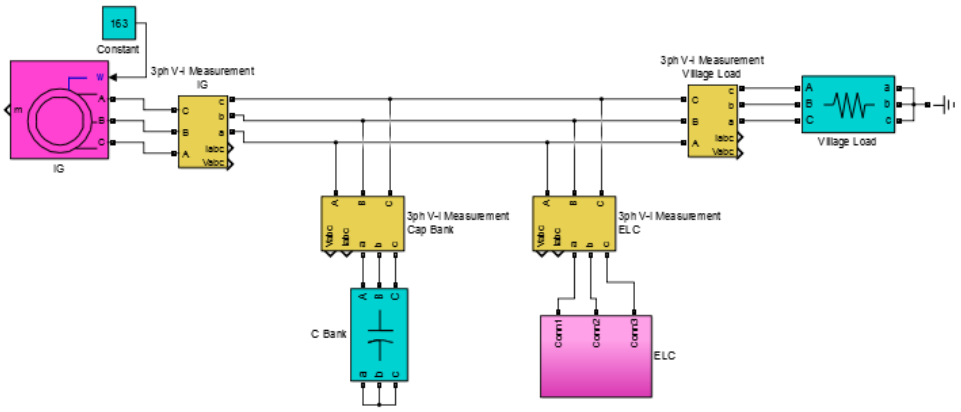

FIGURE 7.2: Simulation system (SEIG + ELC)

7.3.1 Thyristor-based ELC

Primarily it is interesting to investigate the reaction of the system using triac controlled dump loads, to see how the technology developed to be used with a synchronous generator will respond to a system using an asynchronous generator. According to the theory, it is expected that the induction generator is sensitive to changes in reactive power balance, and special attention is given to evaluate changes in voltage according to changes in active and reactive power.

The existing solution developed by Remote Hydrolight consists of a triac in series with a resistance at each phase, where the resistors are connected in star. In the simulation model, two thyristors in anti-parallel are used to represent the triac. The total value of the dump load in the ELC is dimensioned to be able to cover full load in case of complete loss of the village load. The foundation for the dimensioning is the same as in section 7.2, as the star connected dump load also will have 230 V across.
$R_{dump(star)} = R_{VillageLoad} = 59.5125\ \Omega$.

The calculations of the changes in village load in accordance with changes in firing angles of the ELC is given in Appendix B.

7.3.1.1 Gate Triggering of Thyristor

A PLL (Phase Locked Loop) from the SimPowerSystems library is used to generate a saw tooth signal going from 0 to 360 ^{o}, based on the period of the phase voltage. This signal is compared with a fixed firing angle in a relational operator block, and a pulse is generated when the saw tooth signal is greater than the firing angle. The PLL also gives a more accurate and faster frequency measurement than the previously mentioned solution from section 7.1, which counted zero crossings of the phase voltage. From this point the PLL is used for measuring frequency.

At first, the pulse generated was too wide, and caused the thyristors to conduct after the current reached zero and hence continuing throughout the period. To limit the pulse duration, a Monostable block, which generates a short pulse at the same time as the input pulse, was used to limit the length of the original pulse.

Another issue was that the signal was triggered only one time per period. It is necessary to trig one thyristor in the first half period, and the other in the second half. This was solved by splitting the signal into two and adding 180 ^{o} to the second firing angle signal.

For testing the accuracy of this system, the configuration was first attached to an ideal voltage source. After ensuring proper operation, it was attached to the existing system to provide the anti-parallel thyristors with gate signals.

The gate triggering subsystem is shown in figure 7.3:

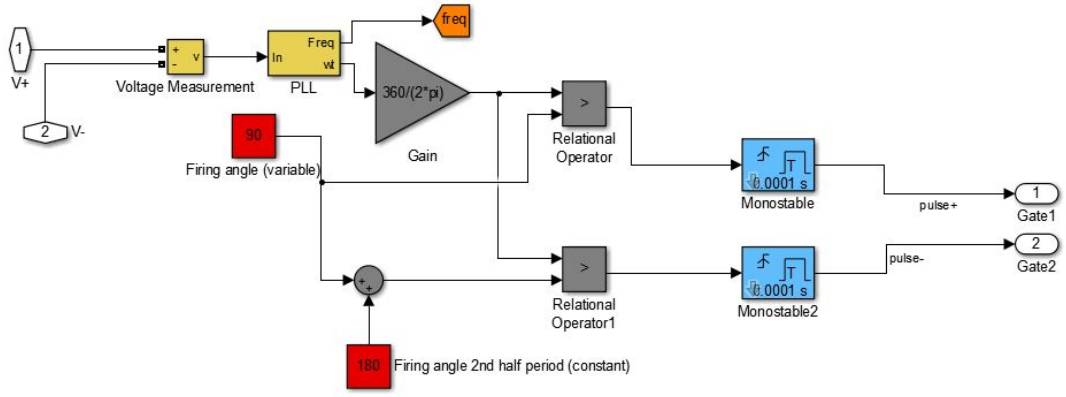

FIGURE 7.3: Gate triggering system for the anti-parallel connected thyristors

In figure 7.4 it is seen how the input sinusoidal voltage is transformed to the familiar thyristor controlled voltage waveform. The lower window shows the produced sawtooth

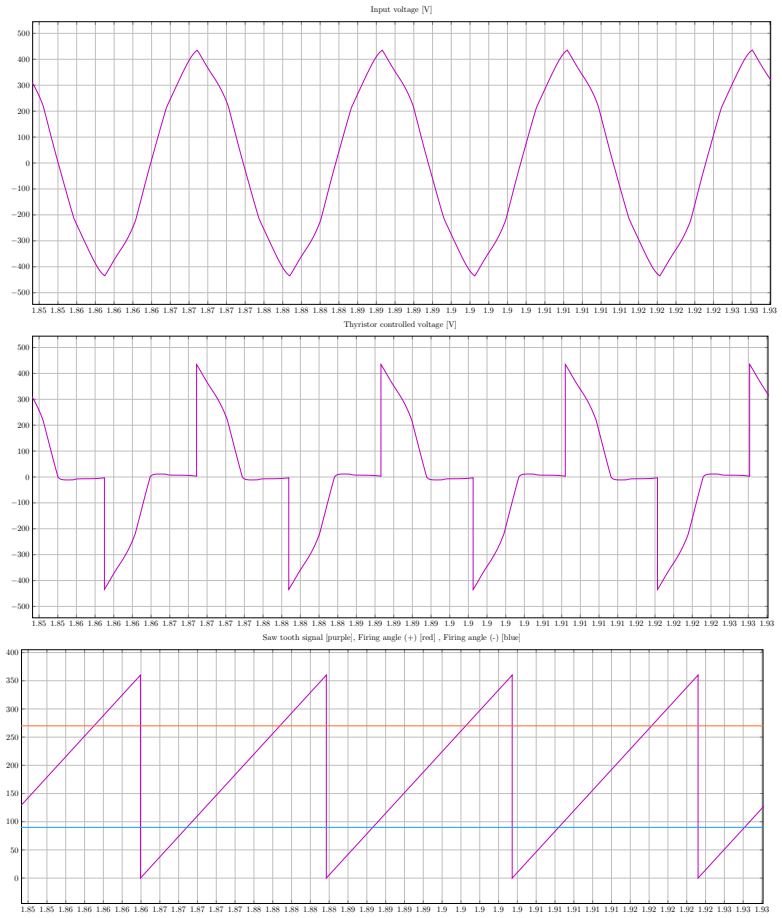

FIGURE 7.4: Gate triggering system for the anti-parallel connected thyristors

Top graph is input phase voltage, mid graph is resulting voltage over dump load, lover graph is sawtooth signal and triggering values

signal together with the constants 90 and 270 (180 + 90) ^{o}, and it is seen how the anti-parallel thyristor couple is triggering in both the positive and negative half period.

7.3.1.2 Delta VS Star Connected Dump Load

As explained in the introduction of this section, the simulation model is originally built with the dump loads connected with a shared neutral point in a star connection. This is because the original design developed by Remote Hydrolight uses this configuration.

It is interesting to evaluate how the system corresponds to the situation where the ELC is consuming half of the total load, still using the same parameter values tuned for full resistive load. The village load is in this case reduced to half of its original value, and the firing angle of the thyristors are set to 90 ^{o}, see Appendix B for details.

With the dump loads star connected, the resulting current measurements has an unpredicted behaviour. It can be seen from the current graphs that there is a problem

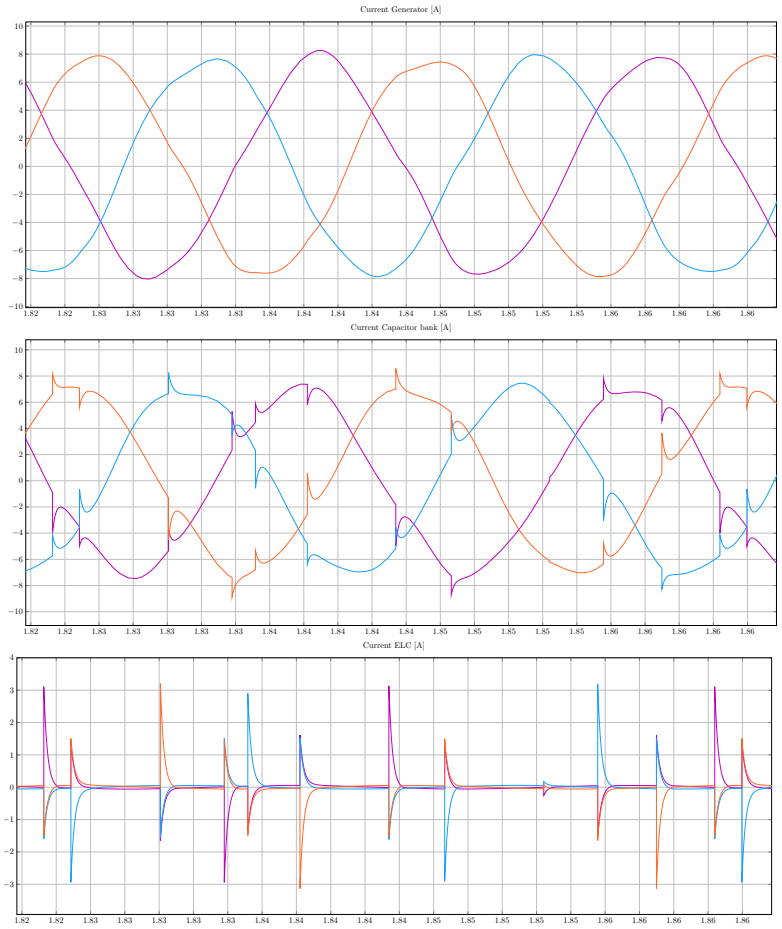

FIGURE 7.5: System currents at Y connected ELC at $\alpha = 90\ ^o$

Top: Generator current. Middle: Capacitor bank current. Bottom: ELC current.

when the system has to maintain Kirchoffs Current Law (KCL) in the neutral point: in order to keep the current 0, the triggering on/off of currents in the ELC is disturbed and causes big discontinuities in the current waveform in the whole system.

When one of the phases is triggered and the thyristors starts to conduct, it is observed that the current in one of the other phases goes straight to zero and the third is forced to have the opposite negative value. This can be seen in figure 7.5, which shows the currents in the system with the dump loads connected in star. There, the current at the generator is almost a perfect sinusoidal wave, because the ELC is almost not drawing any current that could disturb this waveform.

The observed result of this behaviour in the current is that there is practically no power drawn by the ELC at this firing angle. Since the village load is set to half value, this results is a system where the capacitor bank is over over-dimensioned. This results in an increase in RMS voltage, which is the opposite of what is expected from connecting the ELC.

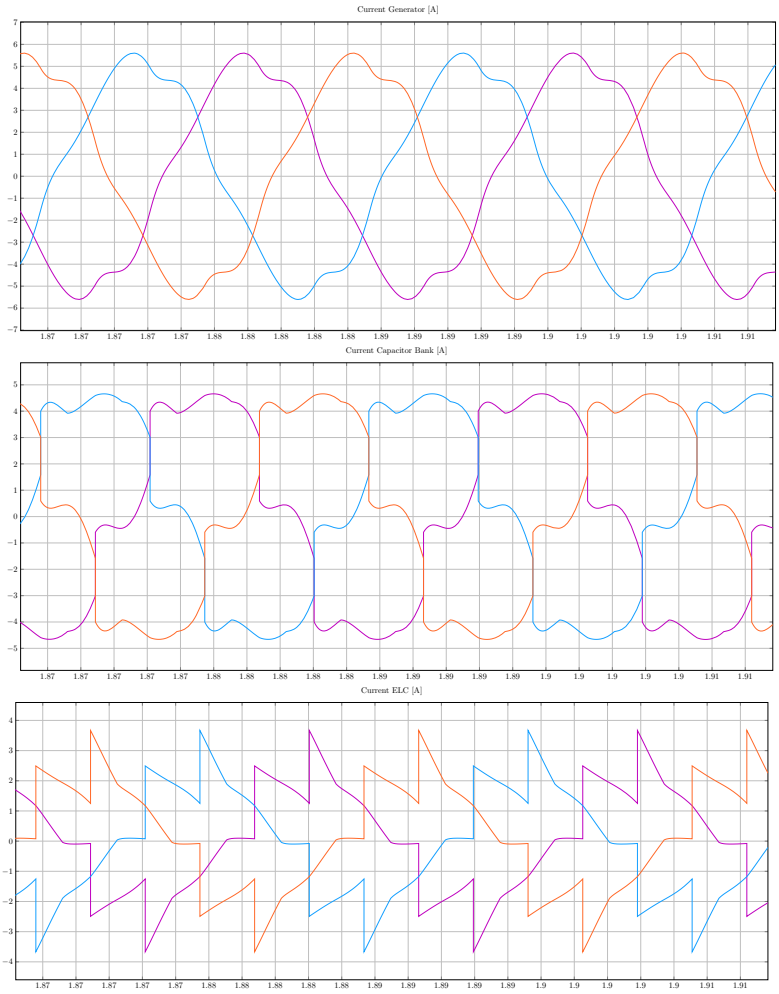

FIGURE 7.6: System currents at Δ connected ELC at $\alpha = 90\ ^{o}$

Top: Generator current. Middle: Capacitor bank current. Bottom: ELC current.

From this, is it desirable to see if the system acts differently when the KCL condition is not determinant in a neutral point after the gate triggering. To test this, the dump loads in the ELC are connected in delta instead of the original star connection.

The resistive value for the dump load in delta connection is calculated by star-delta conversion equation (7.3).

$$R_{dump(delta)} = R_{dump(star)} * 3 \tag{7.3}$$

Some disturbances in the currents are also observed in the delta connection, but not in the same amount or manner. Figure 7.6 shows the currents in the system with the dump loads connected in delta. The currents stabilizes after 0.25 seconds, consuming the same power as the village load. The star connected model, however, does not stabilize, and is consuming practically no active power for the $\alpha = 90\ ^{o}$ scenario.

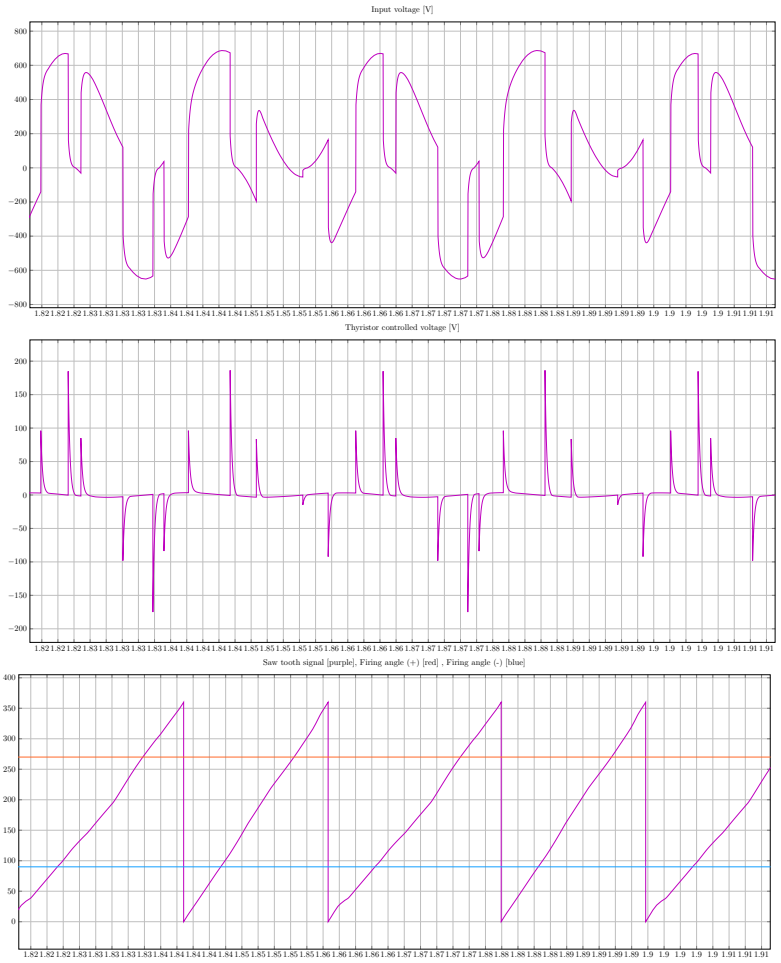

FIGURE 7.7: Gate triggering system for the anti-parallel connected thyristors - Error with star connection

Top graph is input phase voltage, mid graph is resulting voltage over dump load, lover graph is sawtooth signal and triggering values (cpmparable with figure 7.4)

Since the star connection of loads is the standard, some more investigation of the simulation model errors are needed before it can be rejected. Taking a look into the gate triggering block described in 7.3.1.1, it seems to be the high amount of distortion in the input voltage to the star-ELC that causes this unpredicted behaviour in the current. Figure 7.7 shows how the sawtooth signal produced has uneven periods, resulting in inconsistent triggering of the thyristors.

A model that does not draw any currents is not valid. This is also tested at different angles, and the result for the case of $\alpha = 60.5$ is evaluated. At this operating point, current is drawn by the ELC, but the waveforms are still not as expected. This results in less total power drawn in the ELC than predicted from theory, and a higher voltage drop that expected at this operating point.

-	-	P_{gen} W	P_{load} W	P_{ELC} W	Q_{gen} Var	$V_{ph,rms}$ V	$I_{ph,rms}$ A
α 90	Star	1604	1510	0	3738	245	5.48
	Delta	1414	703	711	1220	167	3.82
α 60.5	Star	1198	268.1	928.8	1153	163	3.49
	Delta	1996	398.5	1598	1955	198.9	4.73

TABLE 7.3: Comparing measured values: Delta VS Star

The results from the comparing tests between the delta connected and the star connected dump loads are given in Table 7.3.

Based on these results, the dump load is chosen to be delta connected in the further simulations as this is the only model that provides reasonable results. Figure 7.8 shows how the triacs and resistors are connected in the ELC. It is however not accepted as a viable result, so the comparison between delta and star connection will be a topic of interest in the laboratory tests as well.

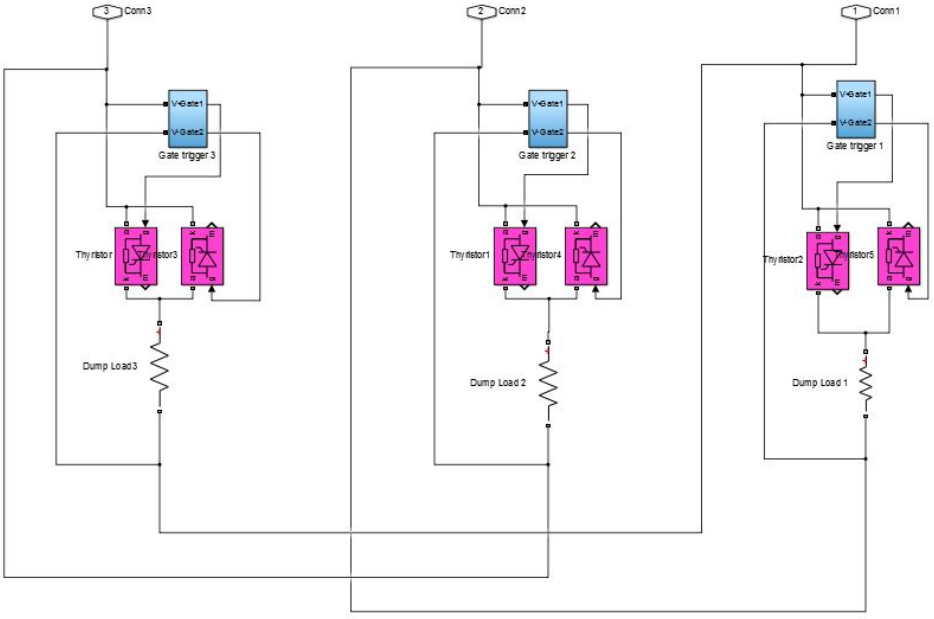

FIGURE 7.8: Subsystem showing thyristor controlled dump loads connected in delta

7.3.2 Uncontrolled Rectifier with Chopper

As concluded in section 6.6, the most interesting opponent to the triac controlled solution will be the uncontrolled rectifier. It is supposed to be of similar complexity, but expected to show a better voltage regulation.

The simulation model is shown in figure 7.9. This model is built with a three phase diode bridge to rectify the AC voltage into DC, and then a single IGBT switch is controlled with a duty cycle from 0 to 100 % to dissipate the desired amount of power to the DC-side dump load. The calculation of the parameters is given in Appendix B and presented in table 7.4.

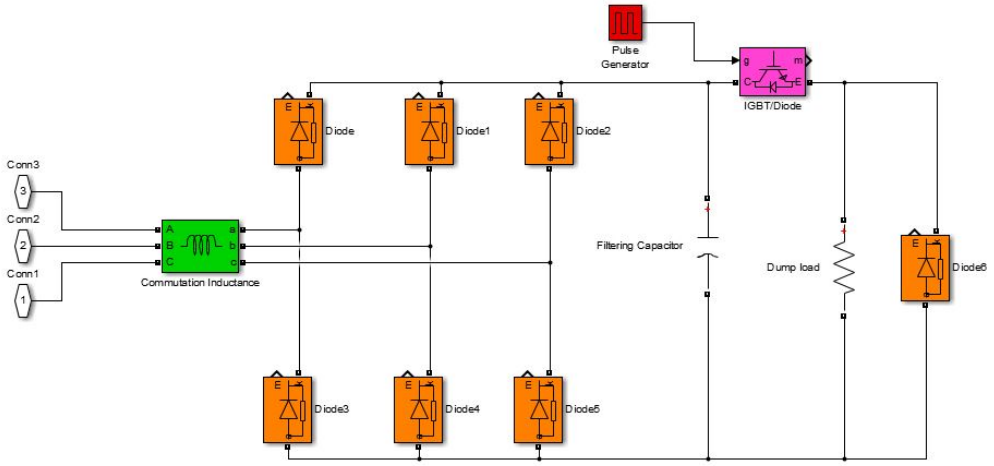

FIGURE 7.9: Simulation model of uncontrolled rectifier with chopper

Running the system with no commutation inductance connected results in high current peaks up to 30 A on the generator phase current, so it is assumed that this extra component is necessary for getting viable simulation results and it is included in further analysis.

R_{DC}	109.4 Ω
C_f	231 μF
L_s	12.7 mH

TABLE 7.4: Parameter values - Uncontrolled Rectifier Simulation Model

In parallel with the dump load a diode is connected to eliminate possible voltage peaks over the resistor when the supply voltage is suddenly changed by the IGBT chopper. This is because a resistive load in real life will never be purely resistive, but it will also contain some inductive value. This diode is called a free-wheeling diode or a flyback diode.

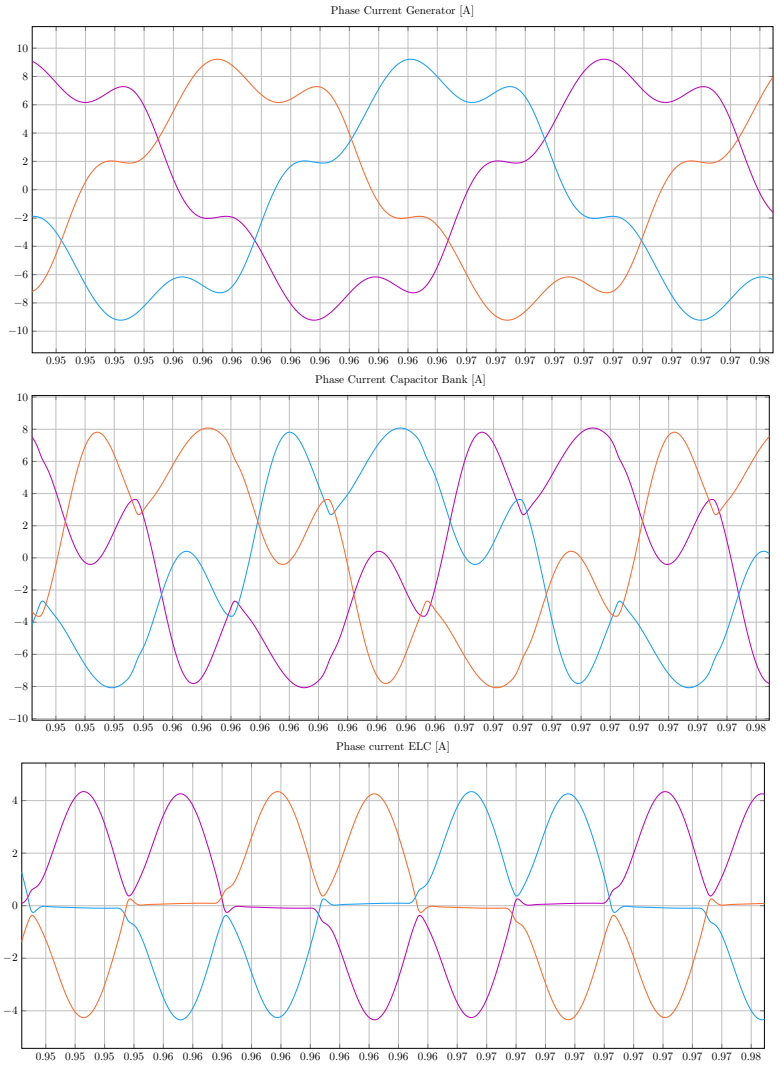

FIGURE 7.10: Waveforms in the uncontrolled rectifier ELC, obtained at Duty Cycle = 50 %

Top: Generator current. Middle: Capacitor bank current. Bottom: ELC current.

7.4 Current waveform distortion and harmonic measurements

Since the power electronic components that are used are non-linear loads, they will draw an non-sinusoidal current as explained in subsection 3.1.1. As seen already in figure 7.4, the output waveform after the thyristor chopping is not sinusoidal.

The distortion is also highly visible in the current of the diode bridge model, shown in figure 7.10.

SimPowerSystems provides a way to rapidly evaluate the harmonic content in either current or voltage. By connecting a ”To workspace” block to the voltage or current

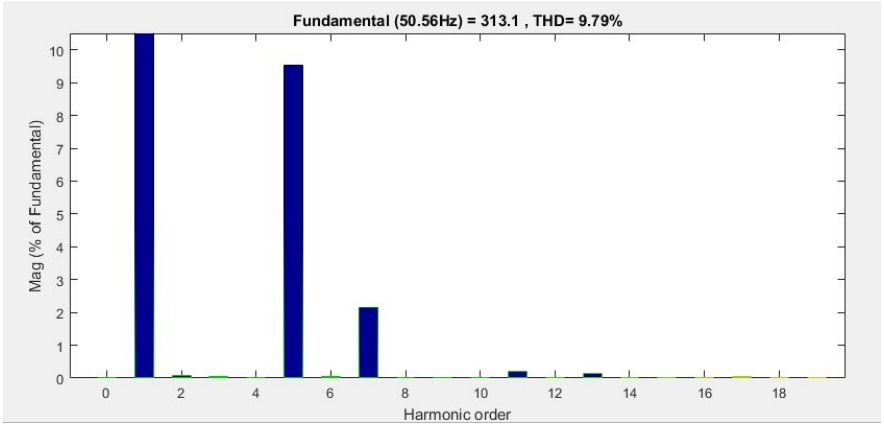

FIGURE 7.11: Output from SimPowerSystems FFT Analysis Tool

measurement in the point of interest, the data can be analyzed using FFT tool. It is important to save the data in the "To workspace" block using the format "Structure with time". The output gives THD in % and also the values of current or voltage peaks. Figure 7.11 shows the FFT analysis result for the voltage harmonics produced by the uncontrolled rectifier ELC at a duty cycle of 50 %, measured at the village load.

When analysing harmonics, one can choose to evaluate either harmonics in current or voltage. For this specific system, it is the voltage harmonics measured at the load that is of highest importance.

7.5 Discussion

Everything presented in this chapter is working accoring to what was expected from theory, with the exception of the Y-connected triac controlled ELC model. Even though the delta connected one are behaving as expected, it does not mean that it is functioning 100% as the star is based on the same principles. Testing this model in laboratory will help evaluate the viability of the simulation model.

For time-consuming reasons, and also given that the lab results are of higher interest, the simulation models was never developed to include the regulation. The fixed firing angle results presented in the next chapter will therefore give a guideline, but it lacks necessary parameters like response time. Implementation of regulation is left for further work.

Chapter 8

Results - Simulations

In this chapter, the main findings from tests performed on the simple fixed-point simulation models presented in the previous chapter are presented and evaluated. The results will give a basis for dimensioning and understanding a laboratory set-up. It will also be useful to evaluate differences in a simulation model and a laboratory test.

First, a comparison between the two ELC options are presented and evaluated. Further, the topic of connecting an induction motor as a load is covered. From these results, options for reactive power compensation are tested.

8.1 Thyristor Based ELC VS Uncontrolled Rectifier ELC

Both models are run in several simulations, evaluating voltage, power and harmonic distortions for the cases of the dump load consuming 0 - 100 % of the total load.

8.1.1 Voltage Variation

Based on the theory, it is expected to find that the triac solution will have the highest voltage drops due to its reactive power requirement. The results showing total reactive power levels and system voltage for the two models are presented graphically in figures 8.2 and 8.1.

From these, it can be seen how the triac solution has a maximum voltage drop of 26.7 %, while the diode bridge solution has 5.4 %. This can be evaluated closer by looking into the reactive power consumption at the ELC solutions supposed "worst case" scenarios, respectively $\alpha = 90\ ^o$ in the thyristor case and 100 % consumption in the diode bridge, given in table 8.1.

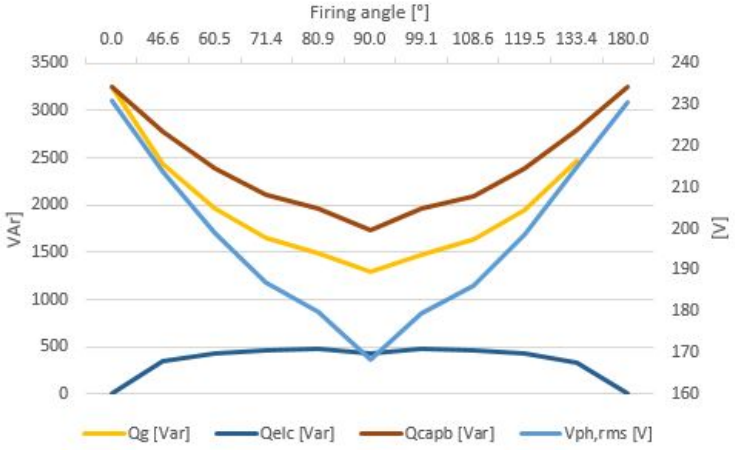

FIGURE 8.1: Reactive power and Voltage variations of Triac controlled ELC over changes in firing angle

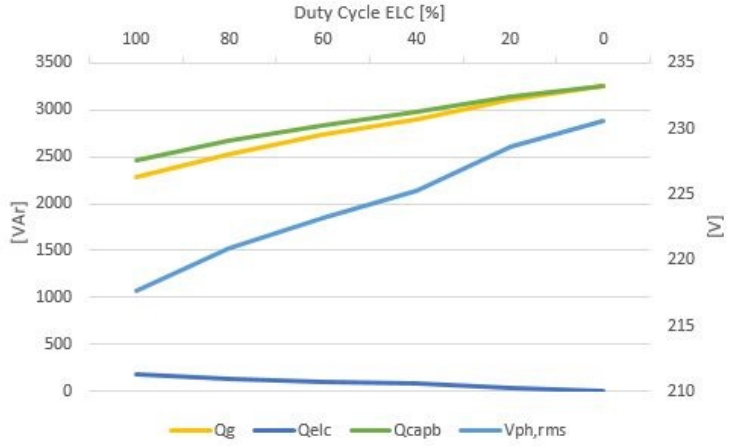

FIGURE 8.2: Reactive power and Voltage variations of Uncontrolled Rectifier ELC over changes in Duty Cycle

An important notice for this is however to mention the dependency in the relationship between reactive power and voltage: reactive power consumption in the system reduces the voltage, and a reduced voltage is limiting the actual reactive power consumption. The actual reactive consumption by the thyristor controlled ELC is therefore expected to be even higher at rated voltage, something to consider in a possible dimensioning of a compensation alternative. Had the voltage stayed constant it would have been expected

	Full Resistive Load	Triac ($\alpha = 90$)	Diode (D= 100%)
Voltage drop (%)	-	26.7	5.4
Q generator [KVar]	3250	1292	2284
Q ELC	-	433.4	184.2

TABLE 8.1: Comparing voltage drop and reactive power consumtion in "worst case"-scenarios of simulation models

to see a peak in consumed reactive power at $\alpha = 90\ ^o$.

Confirming further that the system operates as expected, the changes in active power in relation to voltage drop is also given in figures 8.3 and 8.4. Since the system is dimensioned with resistive values corresponding to full operating voltage, the total consumed power is reduced in accordance with voltage.

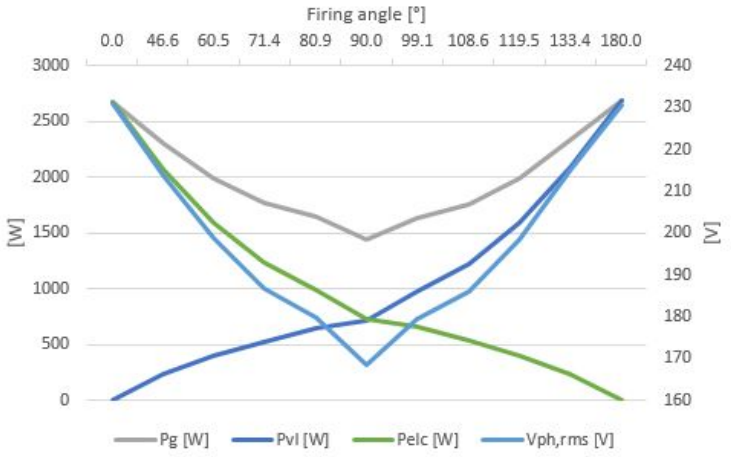

FIGURE 8.3: Active power and Voltage variations of Triac controlled ELC over changes in firing angle

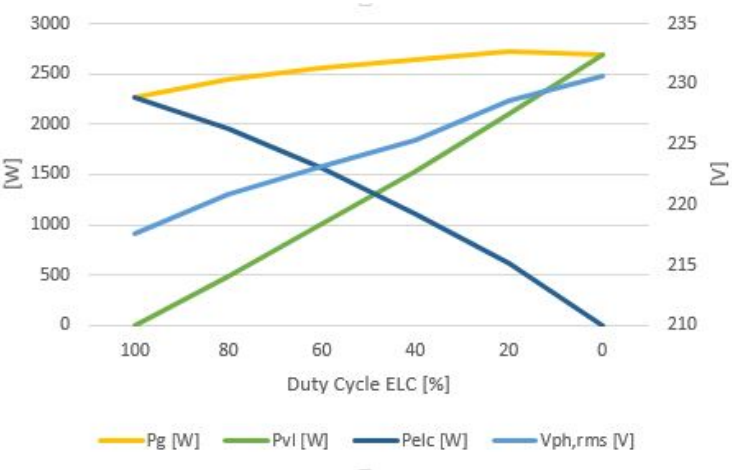

FIGURE 8.4: Active power and Voltage variations of Uncontrolled Rectifier ELC over changes in Duty Cycle

8.1.2 Harmonic Measurements

According to theory, the "worst case"-scenarios in relation to harmonics for respectively triac and diode-bridge will be at $\alpha = 90\ ^o$ and at Duty Cycle = 100 %. The measured results from voltage harmonics are shown in figure 8.5.

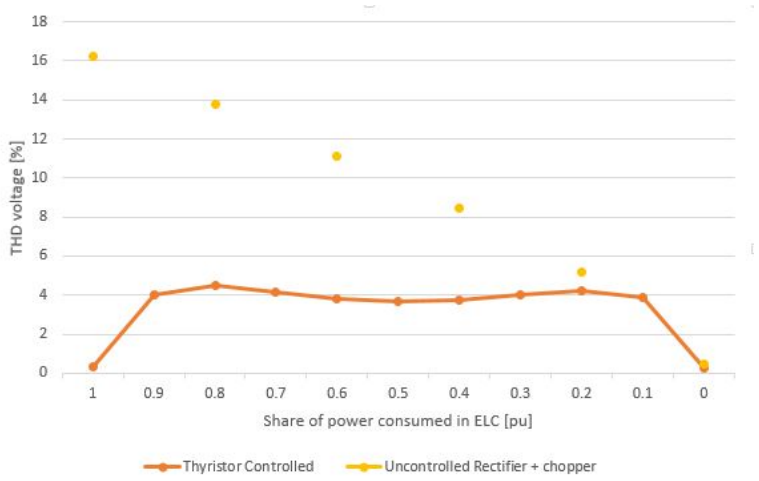

FIGURE 8.5: Computation of THD [%] measurements in the two simulation models

The uncontrolled rectifier is acting as expected, with a relatively high amount of voltage harmonics at the point where the ELC covers full load. The triac solution was expected to have a higher level of THDs than the result, approximately around 10 % at its worst case scenario [37]. By analyzing the current waveforms given in figures 7.6 and 7.10, it is confirmed that the model with the highest deviation from a sinusoidal waveform in the generator current will have the highest amounts of THD measured.

In order to analyze this further, the harmonic specter is studied using the SimPowerSystems FFT analysis. The triac controlled model is run at firing angle 90, and the uncontrolled rectifier is run with chopper set to 50 % to give comparable results. Figures 8.6 and 8.7 shows that the triac controller produces a high amount of harmonic distortions with a THD_i of 32.88 %, an a high variety of the specter. The uncontrolled rectifier solution produces an even higher amount, respectively 57.42 %, and here most of the harmonics are of the 5th and 7th type. With reference to the tuning made in Appendix B, it is expected to find that the higher order harmonics is already mitigated by the commutation inductance.

Given that, as discussed in section 3.1.1, the capacitor bank will filter most of the higher order harmonics, the total distortion in the system voltage of the triac controlled solution will be very low - even according to the requirements of the Norwegian central grid [5].

8.1.3 Comparing the Two Options

The triac controlled solution is, as expected, consuming a high amount of reactive power, resulting in a voltage drop. From the simulations, it might look like the elc will need reacive compensation to cover these losses. Adding an inductive load to the system will definately need compensation according to these results.

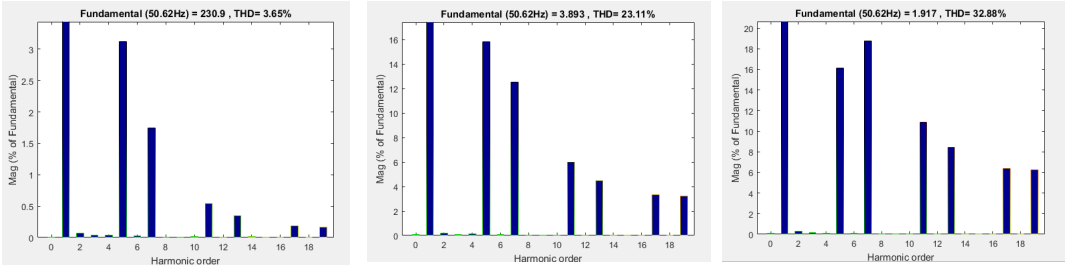

FIGURE 8.6: THD [%] measurement - Triac controlled dump load at α 90 degrees

Left: THDv at Generator. Middle: THDi at Capacitor Bank. Right: THDi at ELC.

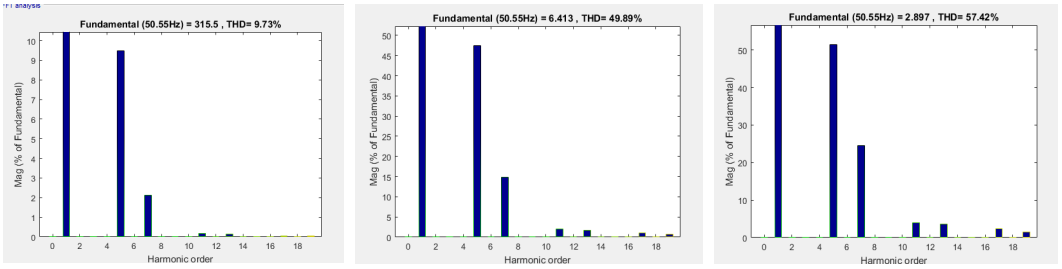

FIGURE 8.7: THD [%] measurement - Uncontrolled Rectifier ELC with Duty Cycle at 50 %

Left: THDv at Generator. Middle: THDi at Capacitor Bank. Right: THDi at ELC.

Uncontrolled has better voltage regulation, but a high harmonic distortion. Would be interesting to test also this one in a laboratory set-up, given that the objective of maintaining the voltage level is of higher importance than mitigating total harmonic content.

The triac on the other hands seems to have a more convienent relationship with the capacitor bank than the uncontrolled rectifier, as it is producing a high amount of current harmonics but it is mostly being neutralized by the capacitor.

Given that it is the triac solution that will be tested in the laboratory, it is this model which is kept for further analysis in this chapter.

8.2 Induction Motor as Load

As discussed in section 2.3.2, the most likely situation that will cause troubles for the ELC will be the starting of an induction motor.

The system is simulated with the ELC disconnected, as if assuming that the chosen ELC solution is able to maintain voltage and frequency during the scenario containing only varying resistive load. The village load is kept constant at full load value, assuming that the connection of an induction motor with no load attached will not result in a too high increase in total active power demand. The objective of investigation is the high current, and hence reactive power, demand characteristic of starting an induction motor.

Since SimPowerSystems does not provide a lower rating value than 4 kW for asynchronous machines, this will be the rating of the connected induction machine. The asynchronous motor block is connected to the terminal through switches, and the mechanical input is set to 0.2 Nm to simulate no-load torque [44]. Given that the motor is running at no-load, the resistive value in the village load is kept constant during the connection of IM.

The rating of the generator is tested for two different values, giving different ratios between the motor and generators size.

8.2.1 Ratio Motor/Generator: 0.53

The total system is first scaled up to match a 7.5 kW generator feeding a total village load of 5 kW. I_{rated} of the generator is calculated to be 10.83 A, and the magnetizing curve of the 7.5 kW generator is adjusted to these parameters.

The voltage is maintained at 400 V, but since rated current is increased the capacitance has to be re-dimensioned. This is done following the same procedure as in 7.1, and then adjusted for full resistive load. New C_{bank} is 119 μF.

The induction motor is connected in no-load mode at 1.3 seconds in the system, resulting in high current peaks and with a total voltage collapse as a consequence after a few seconds. The graphs are shown in figure 8.8.

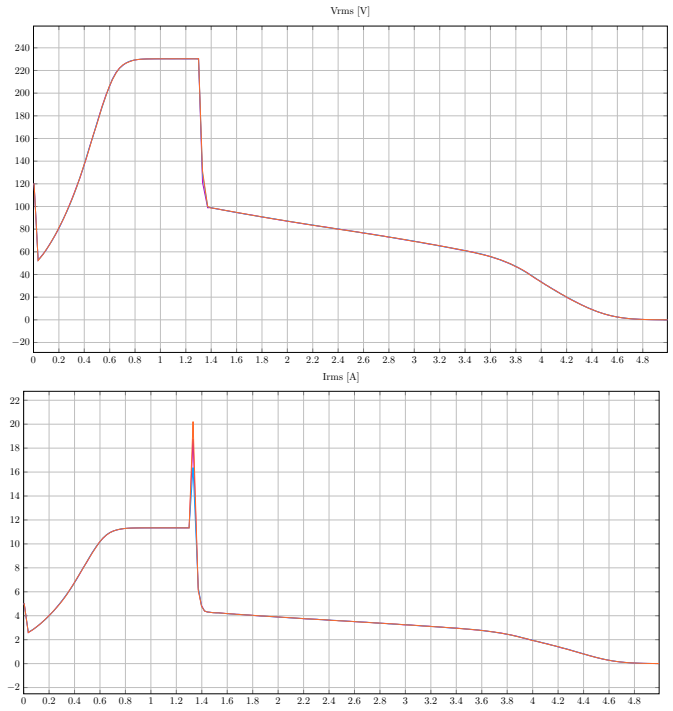

FIGURE 8.8: RMS Voltage and Current development during connection of induction motor (motor/generator ratio 0.53)

8.2.2 Ratio Motor/Generator: 0.27

To evaluate if the relative size of the connected motor was too large, the system is again re-tuned. In this scenario, the SEIG has ratings of P = 15 kW, V = 400 V and I = 21.6 A. The resulting new capacitor bank is C=222 μF, and full village load is $R_{VL} = 15.87\ \Omega$.

Using the same 4 kW induction motor as a load, the system is run again. The voltage build-up is slower, so the induction motor is switched in after 2.3 seconds. The rms voltage and current measured at the generator is presented in figure 8.9.

The voltage and current stabilizes, but at a lower operating point. The voltage drop is 15.5 %.

From this, it is found that some use of reactive power compensation will be needed for the case of starting an induction motor as a load, independent of the choice of ELC solution. It will however depend on the size of motor connected, which most likely will not be a known parameter for the actual implementation of a ELC. The challenge will be to find a solution that will be working properly for many different types of load connections, that is able to quickly provide the appropriate compensation.

Knowing that the available equipment for running similar tests in lab has a ratio of 0.25 (375 W induction motor, and 1.5 kW induction generator), the smaller ratio is kept for further simulations.

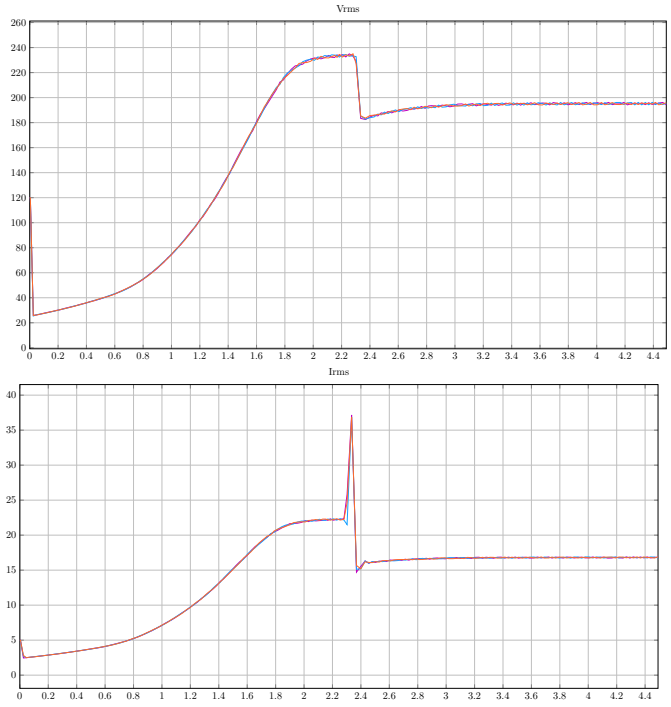

FIGURE 8.9: RMS Voltage and Current development during connection of induction motor (motor/generator ratio 0.27)

8.3 Options

Based on the knowledge provided by the literature study presented in the earlier chapters, there might be two options for compensating voltage loss caused by the consumption of reactive power from the ELC itself or other inductive loads: adding a reactive compensation unit or increasing the generator size. The case of switching in an induction motor at full resistive load is used as the case of comparison for the reactive compensation options.

8.3.1 Increased Generator Size

As seen in 8.2.2, the size of the generator relative to the load connected has a big influence on the system. In order to evaluate this further, the load attached to the triac controlled ELC solution is decreased. The value is set to the lowest of the boundaries given in section 2.3.2, namely generator being 2.5 times the load size.

$$P_{tot} = \frac{P_{gen}}{2.5} = \frac{4000W}{2.5} = 1600W$$

$$P_{phase} = \frac{1600W}{3} = 533.33W$$

With a full village load calculated as

$$R = \frac{V^2}{P} = \frac{230^2}{533.33} = 99.19\Omega$$

The system is tuned resulting in a new value for the capacitor bank: C_{new}=57.5 μF.

Running the simulation at the scenarios full village load and ELC at $\alpha = 90\ ^o$, the obtained results are given in table 8.2.

	Full Resistive Load	Triac ($\alpha = 90^o$)
P_{tot} = 2666.66 W	V = 230.7 V, I = 6.08 A	V = 167 V, I = 3.80 A
P_{tot} = 1600 W	V = 230.6 V, I = 4.88 A	Voltage collapse

TABLE 8.2: $Pgen$ = 4kW - Comparing operating points on different loading conditions

The operating point related to a full resistive load-scenario are plotted in the same graph as the induction generators magnetizing curve at no-load, given in figure 8.10. P_{load}=P_{gen}/1.5 is hereby called the 1.5-scenario, and P_{load}=P_{gen}/2.5 is the 2.5-scenario, accordingly.

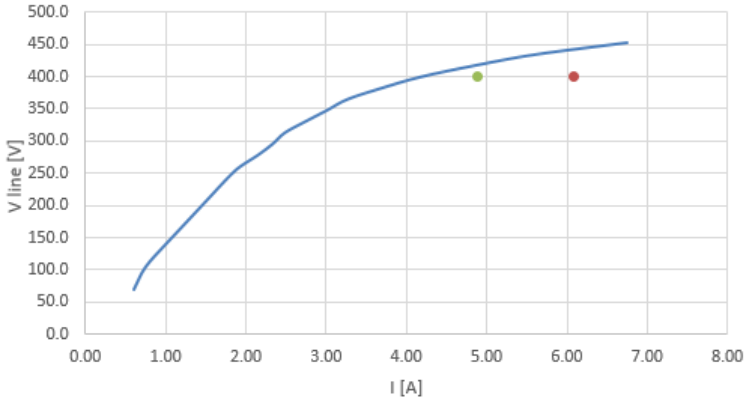

FIGURE 8.10: Full resistive load operation point of 1.5-scenario (red dot) and 2.5-scenario (green dot) in relation to no-load magnetizing curve

This phenomenon can be seen in relation to figure 4.7. The increased firing angle in the ELC will result in a lower power factor of the total attached load, and from this figure is can be seen how the terminal voltage of an induction generator varies with different load power factors as a function of active power output. For a lower power factor, voltage collapse will occur at a lower power output.

As seen in figure 8.10, the curve showing the relation between terminal current and voltage in the loaded situation will be on a lower level than the no-load curve. It will however have a similar shape, only displaced a bit lower and to the right. The capacitor bank of the 1.5- and 2.5-scenario is of different size, resulting in a different slope, with reference to the figure 4.3 from Chapter 4. It can be seen that the intersection point of the 2.5-scenario, represented by the green dot in figure **??**, is much closer to the systems no-load capacitance and hence the self-excitation line on the magnetizing curve.

Remembering that the reduction in power factor resembles an addition of an inductive load in parallel with the existing capacitor bank, the equation 4.6 can provide reason for why the 2.5-scenario collapses at firing angle 90 in the ELC. The resulting L from the ELC might be of such a big value that C_{eff} becomes smaller that C_{noload}.

Concluding this section, it seems like the SEIG system is more vulnerable for changes in reactive power if the total load is small compared to the rating of the generator. The smaller the load, the closer will the full resistive load operation point be to the no-load situation. An addition of reactive power might be a more sensitive issue at this

operation point than further out on the magnetizing curve. This is something to take into consideration when designing power ratings of an SEIG + ELC power system.

8.3.2 Switched Capacitor

From the simulation results, it is estimated that the induction motor draws approximately 2.4 kVAr at rated voltage. An additional capacitor bank is connected in parallel with the existing capacitor bank, with calculated value $C_{switched} = 47\ \mu$F to cover the induction motors consumption. The motor is switched in at 2.3 seconds, and the capacitor bank at 3.5 seconds. RMS voltage and current are shown in figure 8.11.

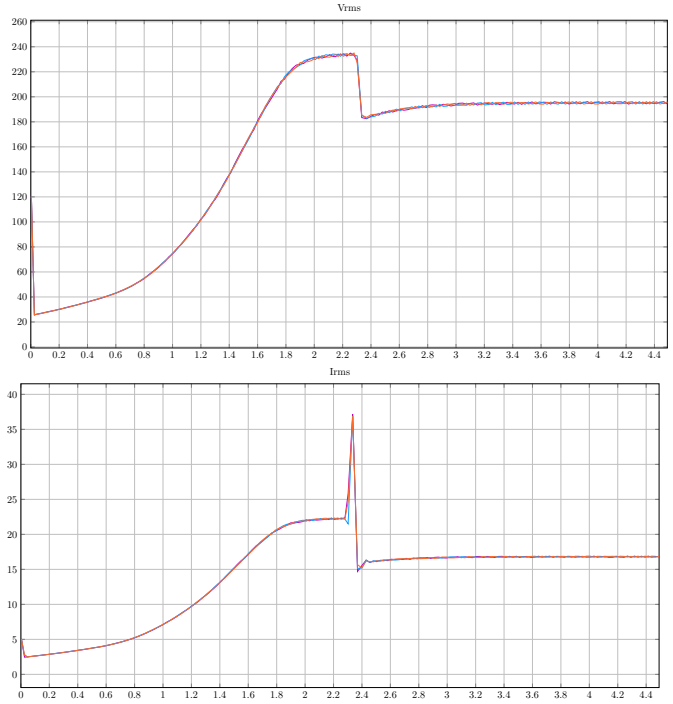

FIGURE 8.11: RMS Voltage and Current development during connection of induction motor and switched capacitor compensation (motor/generator ratio 0.27)

This test was included to verify that the calculated values of capacitor gives the expected voltage change when connected. An important notice about this test is that the capacitor switched has been calculated to fit the exact reactive power demand, and that this implementation in real life will not be able to fit as good as this simulation.

8.3.3 Series Capacitor

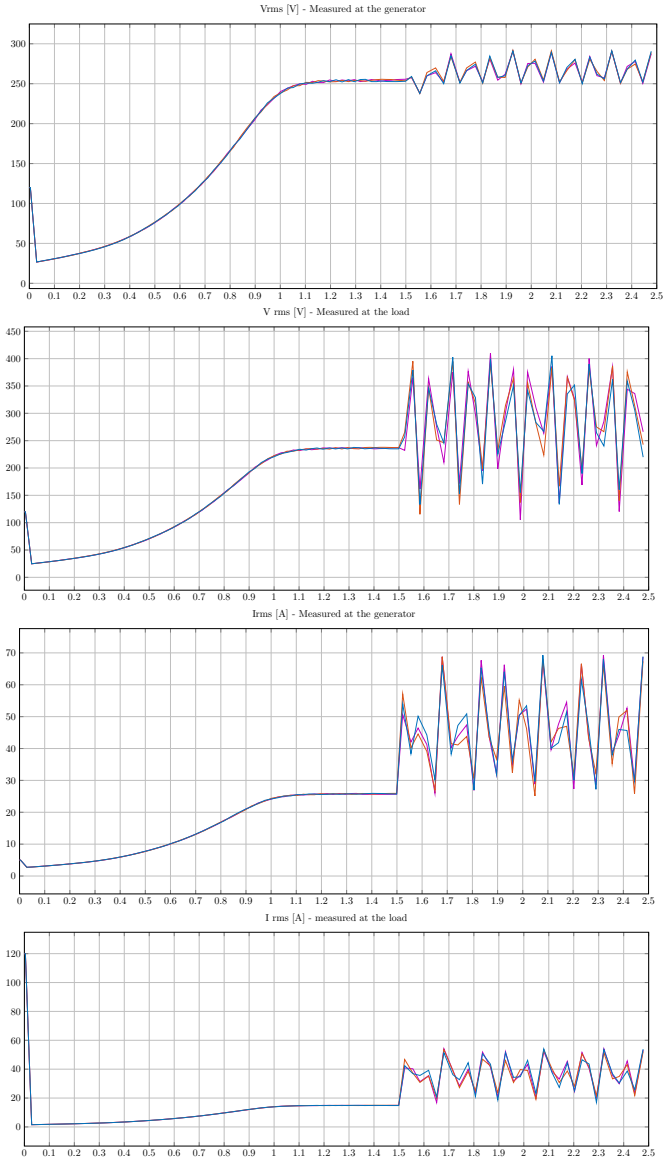

FIGURE 8.12: Voltage and current development in SEIG and IM load during series capacitor loading at k=0.4

For the sake of using this compensation method with an ELC, the series and shunt capacitors has to be dimensioned based on the systems requirement of reactive power. When all power produced by the generator is consumed by the village load, the reactive power demand is at its lowest and the short shunt combination must not provide a too high voltage. When the ELC is connected and consumes reactive power, the desire is a system that maintains voltage level within reasonable limits.

According to the finding in section 5.2, finding the right relation between the shunt and series capacitor is important for suitable voltage regulation and to avoid subsynchronous resonanses (SSR). No-load C for this system is 199 μF, so the shunt capacitor is reduced

to this value. The value of the series capacitance is tested for different values of k: 1, 0.8, 0.6 and 0.4. Figure 8.12 shows that for that given combination of k = 0.4, SSR is definitely present. The result are similar testing also the other combinations, only with varying degree of SSR.

8.3.4 FC-TCR

According to the findings in Chapter 5, the FC-TCR option is preferable when there is a big variation in the reactive power demand in the system, and when the accuracy in the voltage regulation needs to be high. Since the simulation model is built without regulation, the model was used to verify the calculations made when estimating the needed parameters for L and C in the parallel connection. The simulations showed satisfying results.

A firing angle control of the inductor was not implemented in the simulations for time-limitation purposes, but the intention is to test this option in the laboratory together with the other two reactive compensation options. Without the control, there is not possible to measure whether or not this configuration will add disturbances in the system.

8.4 Conclusions

The main findings from the simulation results can be summarized in the following paragraphs.

The uncontrolled rectifier-ELC has a much better voltage regulation than the triac controlled solution. It produces a higher amount of harmonic distortions, but this is not the most important parameter for controller design. The control design might be optimized to mitigate these harmonics if necessary, which might be an easier task than to try to control a higher voltage drop. This is seen in relation to the knowledge provided by Chapter 4, stating that the mutually dependant parameters in a SEIG system is difficult to separate and adjust. It would be interesting to further develop the uncontrolled rectifier simulation model to test it for different loading scenarios, and especially to implement a prototype of the controller for testing in the laboratory.

The connection of an induction motor as a load is as expected a critical situation for the controller, as the high inrush currents results in a large drop in system voltage. The need for compensation will be relative to the size of the motor, and it will be necessary to have a compensation that can handle big variations in reactive power demand at a fast response rate.

The relative size of the dimensioned full resistive load attached to the generator is important for the possible operation interval of the system. Testing with a low value of P_{tot} showed a higher sensitivity to changes in reactive power consumed by the ELC, as the existing operation point was very close to the no-load operation point. The addition of an assumed inductance most likely resulted in an efficient value of capacitor bank smaller than the rated C_{min} for the system, and the voltage collapsed.

When analyzing the reactive power compensation options, both the switched capacitor and the FC-TCR works as according the the calculated values. The series capacitor is however harder to dimension. As stated in most research papers used as theoretical foundation for this method in section 5.2, the trick with this method is to find the perfect ratio between shunt and series capacitance to avoid the subsynchronous resonance phenomenon. From testing several different ratios in the simulation, this has not been possible to avoid.

Chapter 9

Laboratory Setup for Testing Existing ELC Solution with SEIG

The existing ELC solution is developed by Remote Hydrolight for the purpose of it being used with a synchronous generator. The main objective of the laboratory work is to test its adequacy when used with an induction generator, and to detect what adjustments that might need to be done for this to function with a SEIG in the laboratory environment.

A picture of the whole set-up is given in figure 9.1, and schematic sketched of the laboratory set-up is given in figure 10.1 and 10.8 in the next chapter. The content of this chapter is summarized in the list under. The instruments used in the tests in this chapter is given in appendix A.

- The connection of the circuit board(s) in the ELC. According to the simulations, a delta connection of the dump loads were the best option, but the original set up is made for star connection so this issue has to be examined further.
- A capacitor bank has to be connected to provide for self-excitation and voltage build-up to rated voltage. The size of this needs to be determined, and its influence in the total system evaluated.
- The possible solutions for reactive compensation has to be dimensioned and tested with the existing system.
- Last, but not least, building the complete laboratory set-up is necessary for obtaining a physical understanding of the system and the different options.

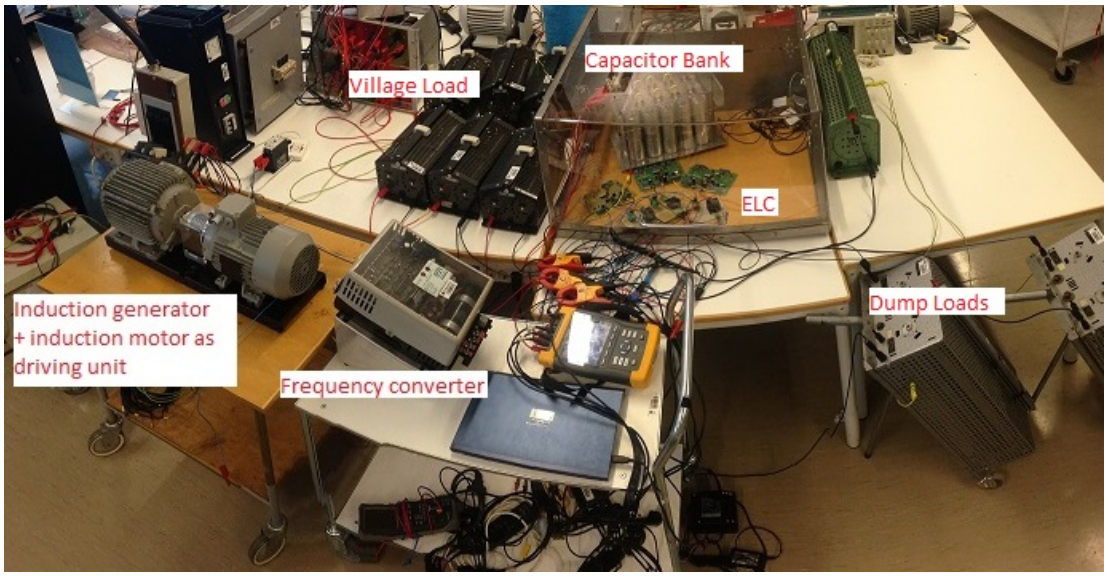

FIGURE 9.1: Picture of laboratory set-up for testing of original ELC circuit board with SEIG

This chapter is summarized with an explanation of the physical set-up used to provide the results presented in the next chapter.

9.1 Testing of Equipment

Before performing the laboratory testing of the whole system, the different components needs to be fixed and tested. This involves the signal transformer for power supply to the board, testing if the boards provides the desired gate signal and testing the operation of the chosen triacs.

9.1.1 Connection of Gate Signal Circuit Board: Delta/Star

The circuit board is designed for a 400 V star connected synchronous generator, and a star connection of the dump load and triacs. It has three phase inputs, one for each phase, and has three different gate outputs which corresponds to the phase. The board also has one input for the neutral. This gives 230 V over the connection between the phase and the neutral, and this is the max voltage for the board.

One board is used to trigger all the triacs in the system, where the triacs are connected to the dump load at the different phases (MT2), the corresponding gate signal and the neutral (MT1). The original setup is given in figure 9.2. For each phase in the given figure, two series connections of one dump load and one triac are connected in parallel. In the following tests, one triac and dump load are used for each phase.

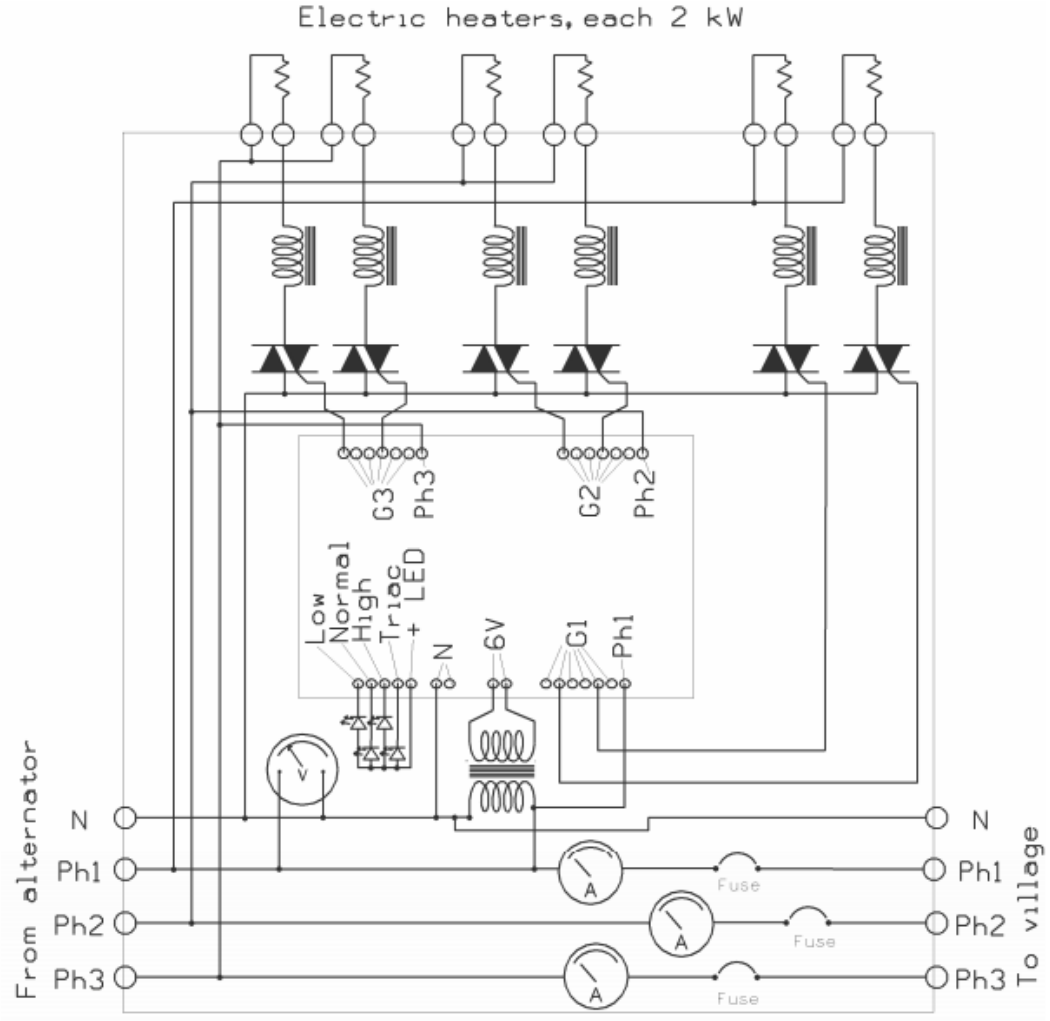

FIGURE 9.2: The ELC solution for the synchronous generator

Source: [2] p. 28

The circuit board demands the input from a neutral phase. This is also necessary so that the gate current sent to the thyristor can "exit" through the neutral phase. If the current doesn't have this return path, it will flow in the phase.

The induction generator does not normally have a neutral phase available for connection, but it is possible with some adjustments. The generator used in these laboratory tests is a 400V (Y)/230V (Δ), and a neutral wire is made available for the case of testing the generator in star connected mode.

According to the simulations, a delta connection of the dump load is preferable over the original star connection. It is desirable to test the difference between connection options also in the laboratory, to either validate or discard this result.

To be able to run the test with delta connected dump loads, the original neutral input has to be one of the other phases. This provides 230 V over the board, given that the generator is delta connected to provide a line voltage of 230 V. Also, three circuit boards has to be used instead of one and the processors has to be re-programmed corresponding to a single-phase load. The delta connection of the board is given in figure D.1 in appendix D. The following equipment has to be prepared in order to test both the star and the delta connected case.

9.1.2 Power Supply to the Gate Signal Circuit Board

The circuit board needs a 6 V input to operate. This is done by using a 230/6 V signal transformer connected, where the 230 V side is connected between two phases, or phase and neutral in the case of star connected generator, and the 6 V side is the input to the board. The transformer is soldered to a new board, and wires are connected to enable connection with the rest of the circuit/system. The signal transformer is tested, and it is discovered that this solution does not give enough current to drive the card. To provide a higher amount of current, an additional pair of conductors are connected from the secondary side of the transformer to the wires used for connection with the board.

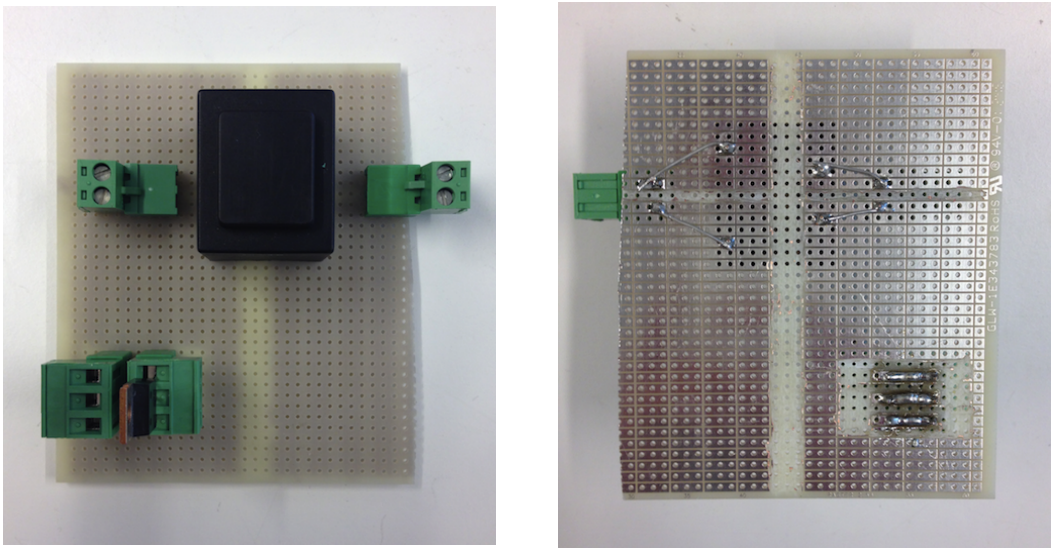

FIGURE 9.3: Board with signal transformer and triac

The left picture: Signal trafo: the black box, Triac: at the bottom left of the board, the green boxes are connection points for wires. The right picture: the other side of the board with the soldering

The plan is to use in total three of the 230/6 signal transformers for the case where three circuit boards are used. As there is only one such transformer available, two

230/9 V transformers are used for two remaining boards. These transformers are providing enough current to drive the board, so there is no need for an extra conductor to increase the current.

Figure 9.3 shows the transformers and the board, and the connection point for wires at both the primary and secondary side of the transformer. The triac is mounted at the same board. The first picture shows the top side, where the black box seen is the signal transformer. The green boxes are connection points for wires. The triac is at the lower left side of the board. The figure to the right shows the lback side of the board, where the connection point for the wires and for the transformer are connected by soldering. The silver colored conducting material on the lower side is removed with a drill between the primary and secondary side of the transformer to isolate the sides from each other. The same is done between the conduction points for the triac.

The three solutions with the transformers and the triac soldered to a board are all tested, to check if they conduct and that they provide the desired output. The tests provide satisfying results. A detailed description of the testing of the triacs are given in appendix E.

9.1.3 Testing the Gate Signal Output from the ELC Circuit Board

Before setting up the whole power system in the laboratory, a check to see if the circuit board will trigger a triac in series with a resistor is carried out.

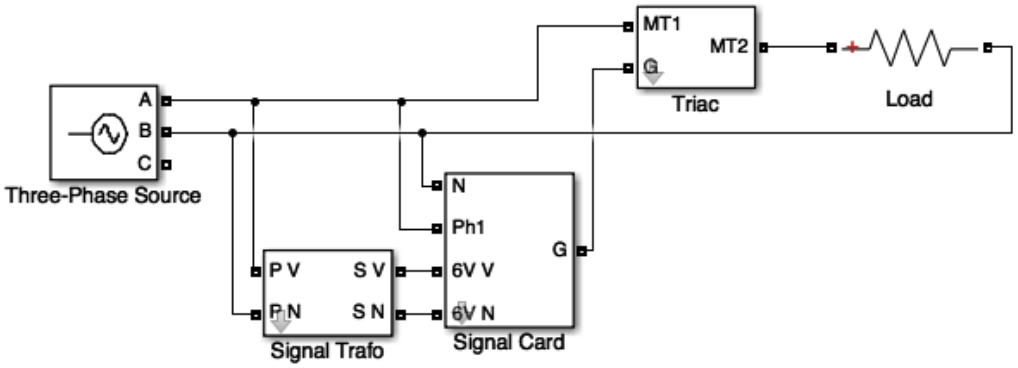

FIGURE 9.4: Block diagram for testing the circuit board working

There are three signal boards and three boards with signal transformers and traics connected. All the boards need to tested before the whole system can be put together. A block diagram of the test set-up is given in figure 9.4. From a voltage source of 230 V, phase A is connected to the phase connection at the signal board, to the signal

transformer and to MT1 at the triac. Phase B is used as a neutral in the system, and is connected to the neutral at the circuit board, to the signal transformer and to the resistor in the system. The resistor is set to 200 Ω. The signal transformer is used for the power supply for the signal card, and is connected to phase A and B of the voltage source at the primary side. The secondary side is connected to the signal card.

A principle circuit for the ELC for one phase is given in the top part of figure 9.5, and the layout for the three phase board with measurement points is given in the lower part. Both figures are marked with different circles with numbers, which are the points on the board where error searching is carried out. In table 9.1 the different measurement points are given, with an explanation of the ideal signal that would be measured here given the board is working properly. The operation of the signal board used in the laboratory test, and the source code for the microprocessor, is given in Appendix F.

The testing of this connection results in a time-consuming error search, as the output signal is not as expected and there is several points in the circuit where some error can occur. First, it is tested if the triac is conducting as expected. If this is the case, it is concluded that both boards are functioning properly. If the triac is not conducting, the next step is to measure the trigging signal provided by the signal board. This is done by connecting a resistor between the gate and the neutral, and measuring the signal with an oscilloscope. If there is no trigging signal, the following step is to check if the signal transformer is supplying the necessary power to the signal board. Next, the signal at the different measurement points given in figure 9.5 are measured, and then the measurements are compared with the expected signal given in table 9.1. From this test it is found that one of the triacs is not properly connected, and that one of the signal card is not working sufficiently. Both problems are solved, and it is now ensured that all the boards are functioning properly.

Measurement points	**Expected signal**
1-2: Connection points for the power supply	6 V AC
3-4: Power supply for processor	3 V DC
5-6: At point 5 the voltage is zero. Point 6 is connected to a 1 k Ω resistance	Trigger signal with an amplitude of 3 V
5-7: Point 7 is the other side of the resistor	Trigger signal with an amplitude of 0.7 V
8-9: To get a measurement of the gate signal, a resistance of 1 k Ω is connected between one of the gate connections (8) and the neutral (9)	Trigger signal

TABLE 9.1: Expected signals at different measurement points on the circuit card

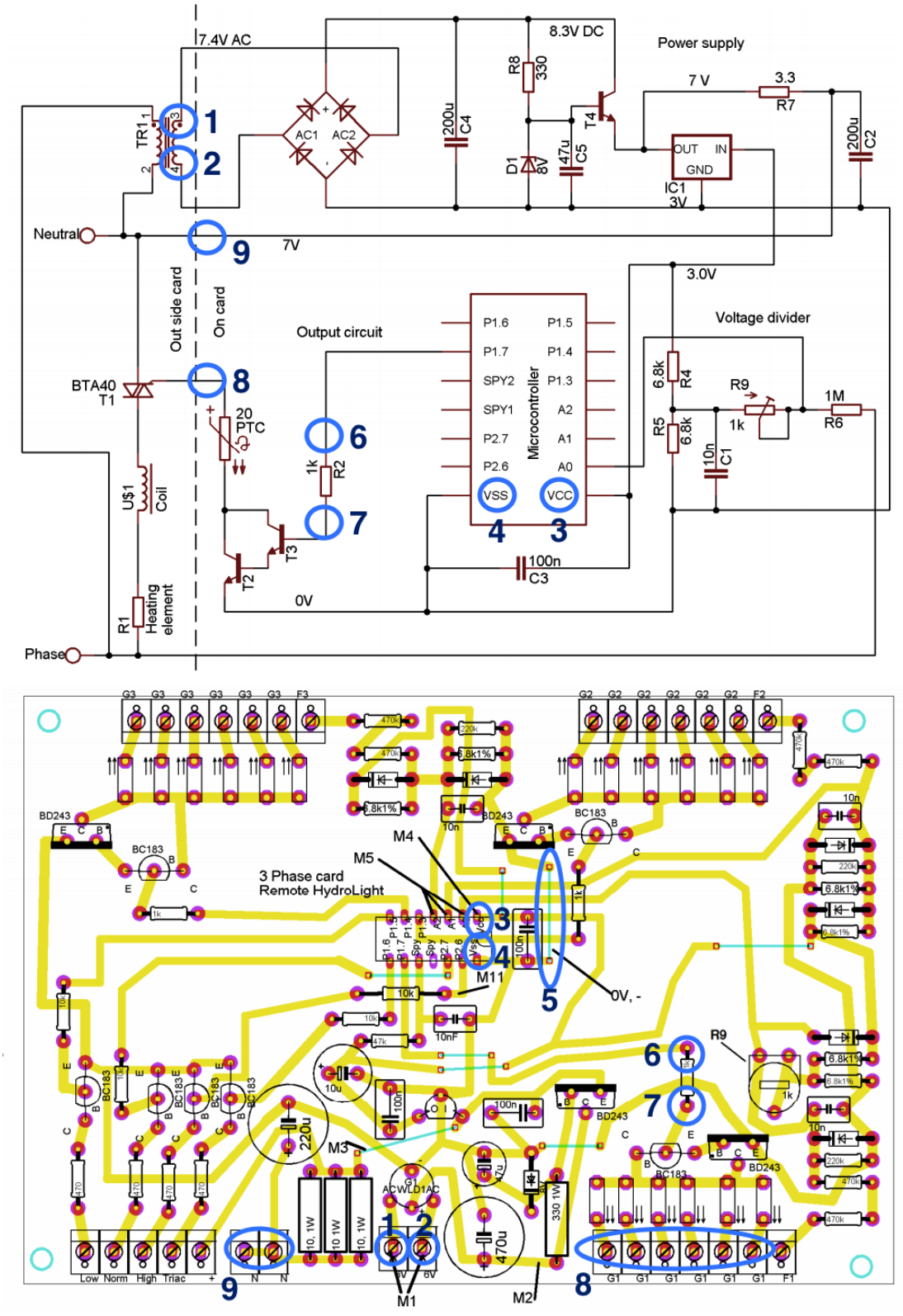

FIGURE 9.5: Top: Principle circuit ELC. Bottom: Tree phase card layout with measurement points corresponding to the above figure.

9.2 Tuning of Capacitor Bank for Laboratory Set-Up

To be able to test the complete system in the lab, the size of the capacitor bank which gives rated voltage at full load needs to be determined. A set up including a driving machine representing the hydro turbine, the generator, three loads representing full village load and a adjustable capacitor bank is used.

9.2.1 No-Load

Based on laboratory work done as a part of the project thesis [1] using a star connected generator, the theoretical no-load capacitor bank is calculated. The no load capacitor bank is calculated to be $C_{no-load,Y} = 34.76\ \mu$F and $C_{no-load,\Delta} = 104.28\ \mu$F.

A capacitor of adjustable size is connected to each phase, to check if the value calculated is correct. If the calculated value is corrected, self-excitation of the generator will happen when the driving unit is set between 1500-1580 rpm, and the voltage will be approximately
230 V.

The adjustable capacitors used in the experiment consist of one unit including five capacitors per phase, each of approximately 33 μF, which can be connected in parallel. Measurements gives the following values when adding another unit in the parallel connection: 1 = 33, 2 = 66, 3 = 99, 4 = 132 and 5 = 165 μF. In addition, there are three capacitors of 7 μF available.

Table 9.2 gives the results from the no-load test, where the capacitance value is tuned to obtain rated voltage in the system where the induction generator is connected in a delta configuration.

Test	C [μF]	f [Hz]	n [rpm]	V_{ph} [V]	I_{ph} [A]	Q [KVar]
1	66	50.1	1502	8.1	0.1	0.00
2	99	50.4	1519	223	4.0	1.53
3	106	50.5	1520	232	4.4	1.78

TABLE 9.2: Results from the no-load test (Delta connected generator)

In the first test, there is no self-excitation of the system, the capacitor value is too low. The value is increased, and the test is run again. In the second test, there is self excitation, but the voltage is below rated value. This implies that the capacitance needs to be slightly increased. By adding the small capacitances of 7 μF, increasing the capacitance from 99 μF to 106 μF, resulting in the desired output voltage. Thus, $C_{no-load,\Delta} = 106\ \mu$F.

Running the same test for a star connected generator, the no-load value is obtained at $C_{no-load,Y} = 33\ \mu$F.

During this test, it is also investigated if the self-excitation and the voltage-build up is dependent on whether the capacitors are connected from start, or switched in when the system has reached rated speed. The results shows that there is no practical difference.

9.2.2 Full-Load

Based on the theory and the simulation results, the capacitor value needs to be increased for the full load scenario, as the generator is consuming more reactive power at increased load.

From the simulation work, where a 4 kW star connected generator is connected to a 2.67 kW load, the no-load capacitor is found at C = 53.8 μF. The full load capacitor is C = 64.0 μF, corresponding to an increase of 18.96 %. If one can assume that the increase in capacitor value will be in the same range for the laboratory machine, the full load capacitor for the delta connected generator will be C = 126 μF. As this is just an assumption, a value of 99 μF will be used as a starting point.

The resistors used in this test have a rated current of 2 A. To make sure the current does not increase beyond that limit per phase, the generator speed is increased slowly while the phase currents are observed. The power flow in the system is also measured. The resistor values are calculated based on active power consumption of 1 kW in the system, 333 W per phase, resulting in a value $R_{fullload} = 53\ \Omega$.

The speed of the generator at rated load, which is 1.5 kW, giving a frequency of 50 Hz is 1580 rpm. As the full load in this test is 1 kW, that the speed that gives rated frequency is a bit lower than 1580 rpm. It will however be between 1580 and 1500 rpm.

During the tests, it was experienced that the voltage build-up took place. It did however not reach up to the expected values. At the measurement of frequency, it is registered that a value higher that 45 Hz is never reached in any of the tests. By measuring the rotational speed of the driving unit, it is stated that there must be some sort of torque limit in the equipment. The total load on the generator and hence also the value of the capacitor bank is therefor reduced, but without any significant improvement. The final conclusion drawn from these tests is that the driving unit is not strong enough to run a loaded generator, and that is has to be changed. All the test results are given in table G.1 in Appendix G, with an explanation of the tests.

9.2.2.1 Induction Motor as Driving Unit

Tthe driving unit is changed with an induction machine with rated effect of 3 kW. The induction machine is run as a motor, and is driving the rotor of the induction generator in the system. To control the speed of the rotation, the induction motor is connected to a frequency converter. This is used to set the speed. The speed is not displayed, but can be measured using the tachometer. The results confirm that the induction motor is strong enough to run the system.

The results from this test is given in table 9.3.

Test	R [Ω]	C [μF]	f [Hz]	n [rpm]	V_{ph} [V]	I_{ph} [A]	P [kW]	Q [KVar]	S [KVA]
1	53	132	50.66	1564	232.5	6.15	1.01	2.23	2.45

TABLE 9.3: Results from the full-load test with induction motor as driving unit

9.2.3 Results

The capacitance values can now be found. The results of the capacitance tuning are presented in table 9.4, where the difference between measured no-load and full-load capacitance is given in %.

Generator connection	calculated no-load [μF]	no-load [μF]	full-load [μF]	Diff [%]
Star (simulated) 4 kW, 400 V	57.64	53.8	64.0	18.95
Star 1.5 kW, 400 V	34.76	33	40	21.21
Delta 1.5 kW, 230 V	104.28	106	132	24.53

TABLE 9.4: Capacitor bank values tuned for different operations and systems

9.3 Reactive Compensation

9.3.1 Switched and Series Connected Capacitors

Based on results from simulations and theory, and additional adjustable capacitor of the same values as the one presented in section 9.2 is prepared. This is because of the estimates of a series capacitor being of value similar to the no-load shunt capacitance, or higher.

For the case of testing switched capacitors in the lab, a set of three 7 μF capacitors is prepared. Given the possible danger of remaining voltage in a capacitor that has been switched out, a 10 kΩ resistor is soldered to the terminals of each capacitor, to work as a discharging resistor.

9.3.2 FC-TCR

As discussed in Chapter 5, it is an interesting option to also test the FC-TCR compensation as it is the one of the investigated options that has the best potential for a smooth voltage regulation.

The smallest available inductor at the University equipment storage that was able to handle the given current limits was of value 16 mH. This value is much greater than the one needed, and this results in a higher consumption of reactive power in the inductor. Therefore, a greater capacitor is needed, so that the total reactive power from the FC-SVC is balansed.

As long as the thyristor controlling the inductor is working in the operation range that provides the correct amount of reactive effect from this unit, this can work sufficiently. However, it only works if the firing angle of the thyristor always operates within the range providing an amount of reactive effect that the system can handle. If the thyristor is not conducting, the reactive supply will be too high for the system, resulting in too high voltage. If on the other hand, it is conducting all the time, the unit will consume reactive effect, which may lead to voltage collapse in the system.

To be able to test FC-TCR in the lab, it is crucial to have a thyristor connected to the inductor which always operates within the desiring range of firing angle. Therefor, the thyristor and the firing pulse generator needs to be tested.

9.3.2.1 Testing Firing Pulse Generator

The voltage can become very high in the inductor if the current is switched off. Before testing the reactive power at different firing angles from the FC-TCR, the pulse generator has to be tested to assure proper functioning of this device.

The device available is old and bulky, and is shown in figure 9.6. It consists of six thyristors of two per phase, a pulse generator and an inlet for each of the three phases so that the pulse generator can set the firing angle corresponding to the immediate waveform. The test is run with the thyristors connected in anti-parallel, and in series with a star configuration of three resistors, each of 200 Ω. The system is fed by a voltage source of 400 V. This is because the input of the device used demanded 400 V, so is will only be possible to test this compensation method in the case of the induction generator being star connected and hence providing 400 V. A transformer is used to isolate the system from the grid for safer testing in the lab, connected between the voltage source and the system.

FIGURE 9.6: Practical set-up of three phase controlled thyristors for FC-TCR

In figure 9.6, the system is shown with an external box for controlling the firing angles of the thyristors. First, the original pulse generator was used, but it was found that it was no longer working. Instead of the original adjustment where a specific angle was set, the new box consists of the two options "Ramp up" and "Ramp down". When the device is turned on, it always starts with a firing angle of 0 ^{o}, and then the "Ramp up" and "Ramp down" can be used to set the desired angle. However, it is not possible

to connect and start the device at one specific firing angle. It is not possible to use this firing pulse generator and the thyristors in a FC-TCR with the available capacitor and inductor, as this will result in an excessive reactive power supply of several kVars when the firing angle is 0 ^{o}. Therefore, this method for reactive compensation cannot be tested in lab.

9.4 Evaluation

When evaluating the delta connection in relation to the original star configuration, the practical difference is the need for either three or one of the circuit boards. The delta configuration uses three, which results in a more complicated laboratory set-up where it might be harder to error-search if something goes wrong in any of the connections. The ELC-delta configurations is given in figure 9.7 to give an impression of the physical set-up. When used on site it will however most likely be implemented in a box, and the practical difference in using one or three cards will be the price of the card itself.

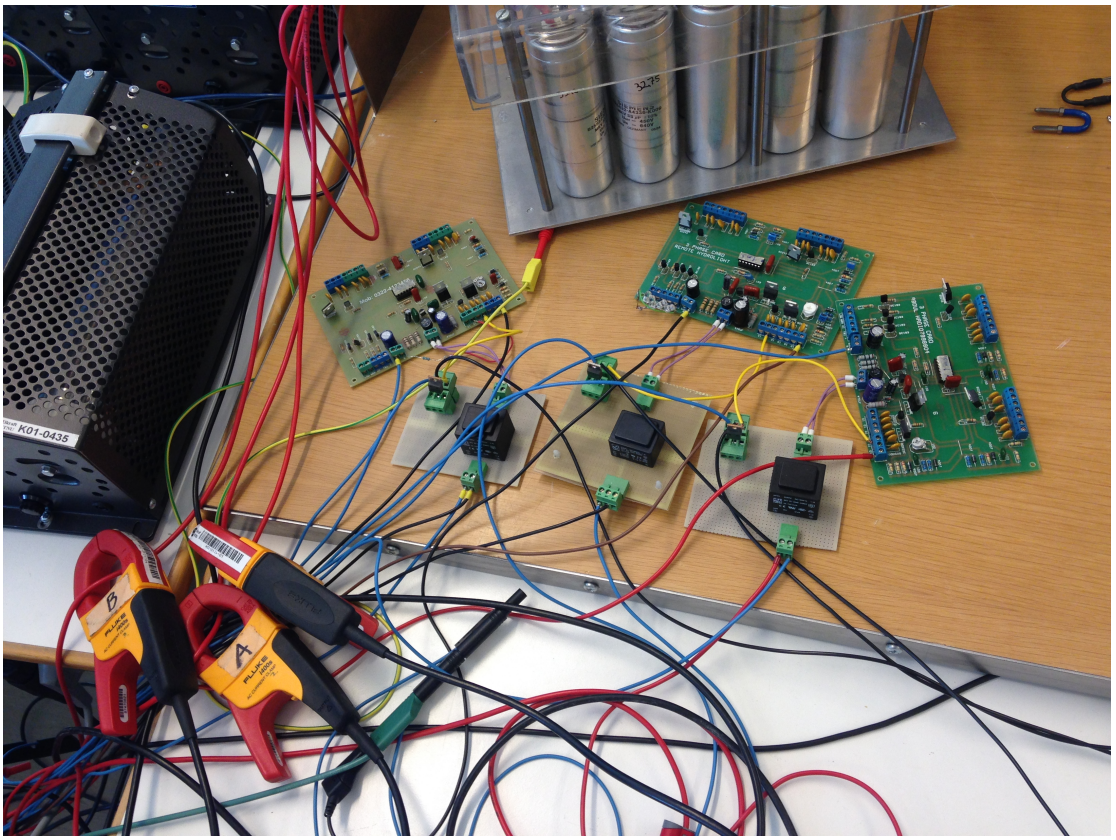

FIGURE 9.7: Connection points of delta-connected ELC

Another visible difference between the two set-ups at this point is the value of the capacitor bank needed. The star connected ELC will need a star connection of the generator, and therefore a higher voltage across the capacitor bank. This will, as proven

in this chapter, result in three times lower capacitance value and hence be affecting the total price of the system. The resistors used as village load in this laboratory set-up will, of the same argument, be three times higher R-value for the star. The village load will however not be a system cost. As a result, the delta configuration will be more expensive than the star configuration.

An important experience from this chapter is the provided understanding of the physical sizes of a laboratory set-up. It is supposed to simulate an entire pico hydro power system, as shown in figure 9.1 in the introduction of this chapter, and this takes up a lot of space and available equipment.

The most peculiar finding in this preparation work is the seemingly contradiction when it comes to inductor size. When using FC-TCR for a small amount of reactive compensation, it results a large values for X_c and X_l. This is due to the equation for reactive power delivered by an reactance, which is inversely proportional with the reactance squared. For the capacitance, a large value of reactance is equivalent with a small value of capacitance. For the inductor however, the inductance size is proportional with the reactance, giving and increased inductance for increased reactance . This relation is proportional, so the smaller reactive compensation needed, the larger will the value of L in the FC-TCR be. A larger value of inductance is proportional with the size of the inductance. Hence, an reduction in amount of reactive compensation leads to an increased inductance and hence an increased inductor size.

Finally, the limitations with the setup has to be emphasized. The frequency converter is used to set a given frequency of the system. This is a limitation in the first place, as the actual system will have an almost constant torque input, not speed. This frequency was in addition not possible to set exactly, but determined by the operation point set by this converter. During some of the tests presented in the next chapter, it was necessary for safety reasons to turn the system completely off when changing measurement point. Therefore, there is some error in all measurements.

The different parts of the system are now tested, and the laboratory tests can be carried out. The results are given in the next chapter.

Chapter 10

Results - Laboratory Testing

In this chapter, the results from laboratory testing are given and evaluated. The tests are done using the set-up developed and explained in the previous chapter. The induction generator used for the tests has a rated effect of 1.5 kW. The results are compared with the simulations and related to the theory given in the previous chapters.

There is not many articles studying the ELC with a triac controlling the dump load at each phase, connected to a SEIG, which shows experimental results on the behavior of this system. It is therefore decided to carry out a thorough laboratory investigation of this system under different operation conditions. First, test are performed using fixed firing angles. This is done to see if the operation of the ELC at different firing angles causes variations in the voltage level of the system. In addition, it is desirable to evaluate the differences between delta/star and also the viability of simulation model. As the simulation results suggest that the a delta connection is preferable compared to a star connection of the ELC, both configurations are tested in lab to examine this.

Further, the SEIG is tested with an induction motor as load, both with only village load connected and with the ELC operating with a phase delay of 5 ms, which is equal to a firing angle $\alpha = 90\ ^o$ when the system is operating at 50 Hz. At this operation condition maximum voltage drop is expected.

The results are discussed, and the last part covers possible compensation methods for achieving better voltage levels in the system. This is done both for the situation where the ELC is causing voltage drop, and when an induction motor is connected. Possible reactive compensation is evaluated in this context.

Finally, an evaluation of the possible use of triac controlled solution with SEIG is given, where the different options for compensation are compared.

Moreover, the laboratory results are compared to the simulation results, to investigate the viability of simulation results.

10.1 Fixed Firing Angle Measurements

The objective of this test is to check if the ELC operating at different firing angles is causing a voltage drop in the system. The tests are performed with the existing circuit board to see in practice how it works with the SEIG. The general operation principle of the circuit board is given in Appendix F. Based on the simulation results it is desirable to test both star and delta connected dump load. This gives the possibility to check whether there is a difference between the power quality in the two configurations of the ELC.

The evaluation is done by measuring voltage and current waveforms and RMS values, and harmonics at different points in the system. Figure 10.1 shows the system with the induction generator, the capacitor bank, the ELC and the resistive village load. The current measurements are done in the lines connected to the respective component. The current measured for the ELC is done in the lines going to the ELC, which are shown in figure 10.1, and not internally in the ELC.

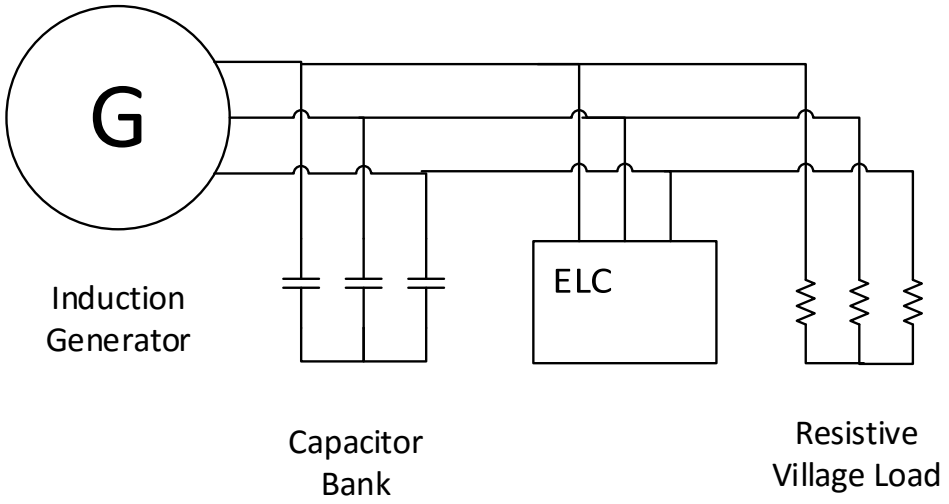

FIGURE 10.1: Induction generator with capacitor bank, resistive village load and ELC

The tests are performed using the same values of four different firing angles. The different firing angles are obtained by programming the processors with the source code given in appendix F. The choice of the firing angles that the ELC is tested with is explained in the previous chapter. The different phase delays (PD) and the corresponding firing angles, given a frequency of 50 Hz, is given in table 10.1. Together with the resistive values of the village load corresponding to the different firing angles. In addition, the power division between the village load, P_{vl}, and the dump load, P_{dl}, is given.

PD [ms]	α [^{o}]	P_{dl} [W]	P_{vl} [W]	$R_{vl,Y}$ [Ω]	$R_{vl,\Delta}$ [Ω]
1	18	8.3	991.7	19061.5	6353.8
4.5	81	598.1	401.9	394.8	131.6
5	90	500	500	318	105.6
7.5	135	90.7	909.3	174.5	58.2

TABLE 10.1: Phase delay and corresponding firing angles given a frequency of 50 Hz. Corresponding resistive vl and the power division between the vl and the ELC

From table 10.1, it can be seen that the resistance is very high in the case of a $\alpha = 18\ ^o$ and only 8.3 W goes to the dump load. As a good approximation, it is therefore chosen not to connect the village load in this scenario.

The resistance of the dump load and the parallel capacitance is constant throughout this test. The dump load is the same size in both configurations, $R_{vl,Y} = R_{vl,\Delta} = 159$ Ω. In section 9.2.3 the full load capacitor bank is determined to be $C_Y = 40$ μF and $C_\Delta = 132$ μF.

If the induction generator is star connected the rated values for voltage and current are V_Y=400 V and $I_Y = 3.45$ A, while a delta connection corresponds to $V_\Delta = 230$ V and $I_\Delta = 6$ A.

Before the ELC is connected, both star and delta configurations are run with full village load connected. The values obtained are used as a base case for comparison, as there will be no additional reactive power consumption in the system other than what the induction generator is consuming at rated voltage. The results are given in table 10.2.

	R_{vl} [Ω]	f [Hz]	V [V]	I [A]	P [kW]	Q [KVar]	S [KVA]	PF
Y	159	51.18	405	3.3	0.99	2.08	2.30	0.43
Δ	53	50.44	233	6.1	1.00	2.23	2.45	0.41

TABLE 10.2: Results from the Y and Δ connected induction generator with full village load (ELC not connected)

10.1.1 Setting the Frequency in the System

As can be seen in table 10.2, the voltage is not exactly at the rated value. This is due to difficulties with setting the frequency at exact values in the system. When setting the rotor speed at the induction generator by adjusting the frequency converter, the speed cannot be adjusted continuously, but jumps between different values normally separated by a corresponding frequency of 0.5 Hz. In further tests in the system, the voltage values given i table 10.2 are used as the rated voltage and the same goes for the corresponding frequency. From testing with different frequencies in the system, it is observed that the voltage level is very sensitive to changes in frequency. As the frequency values given in table 10.2 are used as the rated frequency, this value is tried to obtained when testing at different firing angles. As this is not always possible, the voltage levels in the system are affected by this, resulting in an uncertainty in the measurements. The variations in voltage are limited to $\pm$ 1.5 % from the desired value. This is applicable for all the measurements done in the laboratory.

10.1.2 Comparing Delta and Star Connection of ELC

Both configurations are tested for the four different firing angles, and frequency, voltage, current, active and reactive power, power factor and THD are measured at the different measurement points given in figure 10.1. The measurements are done with a power quality analyzer (FLUKE 434, see Appendix A). Tables giving all the obtained values for both configurations are given in appendix H, while the most important data are given in this section.

Table 10.3 shows the voltage level at different firing angles and rated frequency and the corresponding per unit value.

α [^{o}]	Voltage Δ		Voltage Y	
	[V]	[pu]	[V]	[pu]
no ELC	233	1	405	1
18	231	0.989	400	0.988
81	216	0.925	368	0.909
90	217	0.931	369	0.911
135	222	0.955	388	0.958

TABLE 10.3: Voltage level at different firing angles for Δ and Y configurations

As can be seen in table 10.3, the per unit voltage drop is approximately the same for the two configurations, with a minimum voltage at $\alpha = 81$ [^{o}] of 0.925 and 0.909 for the Δ and Y connections, respectively.

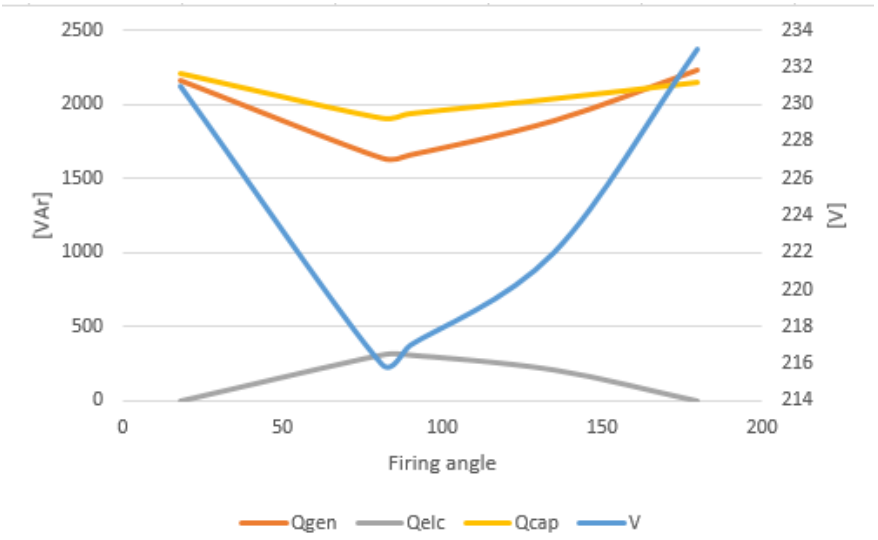

FIGURE 10.2: Reactive power and Voltage variations of Δ connected ELC over changes in firing angle - Lab results

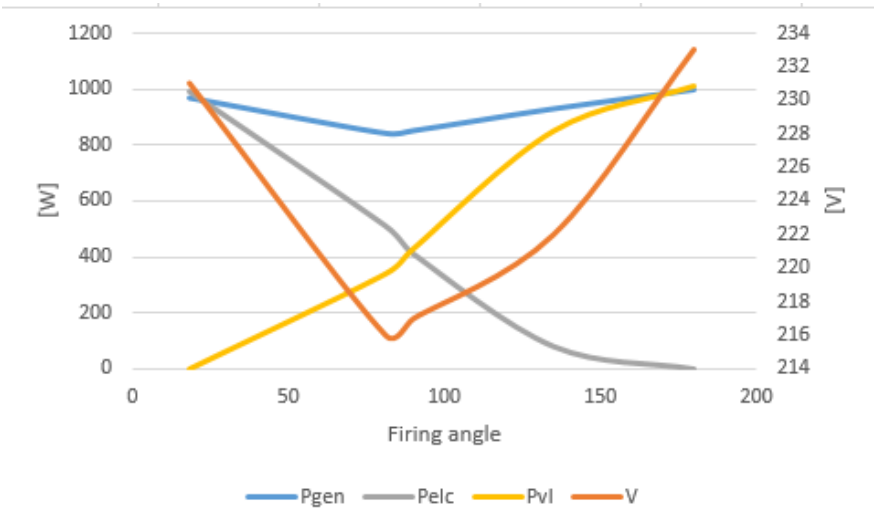

FIGURE 10.3: Active power and Voltage variations of Δ connected ELC over changes in firing angle - Lab results

Q-V and P-V graphs for the Δ connection is presented in 10.2, showing similar relations as figures 8.1 and 8.3 from the simulation results. It is decided to only give the graphs for the Δ configuration, as this is the only graphs obtained from the simulations. With the voltage drop is only down at 216 V at the worst case for the delta connected ELC, it is very close to being within the limit given at 220 V. The star connected ELC has a more severe voltage drop, with 368 V at the worst case compared to the limit given at 383 V.

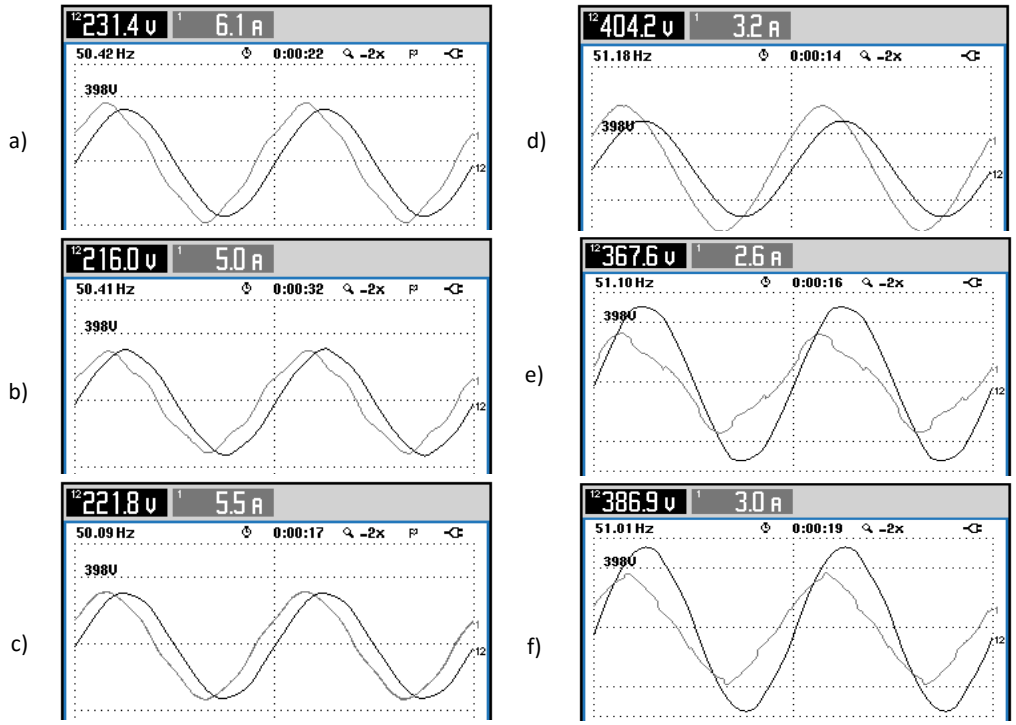

FIGURE 10.4: Phase Voltage and current waveforms at the generator for only village load connected, $\alpha = 90\ ^o$ and $\alpha = 135\ ^o$, for Δ and Y connection.

Δ: a) only VL, b) $\alpha = 90\ ^o$ c) $\alpha = 135\ ^o$,
Y: d) only VL, e) $\alpha = 90\ ^o$, f) $\alpha = 135\ ^o$

In addition to looking at the voltage value, it is important to consider the waveforms in the system. Figure 10.4 shows the voltage and current waveform at the generator for one phase for both configurations, at only VL connected and with the ELC operating at $\alpha = 90\ ^o$ and $\alpha = 135\ ^o$. Waveforms for $\alpha = 81\ ^o$ is not included due to the close resemblance to $\alpha = 90\ ^o$.

The voltage waveform is close to a sine wave for both configurations. For the current waveform however, there is some distortion. The current waveform for the Y connection has a higher degree of distorting. For both configuration, the current waveform is furthest from a sin at $\alpha = 90\ ^o$. It is interesting to look at the current waveform measured at the different components in the system at this scenario. For both configurations, figure 10.5 shows the voltage and current waveform at the village load and the current waveform measured at the generator, the capacitor bank and the ELC..

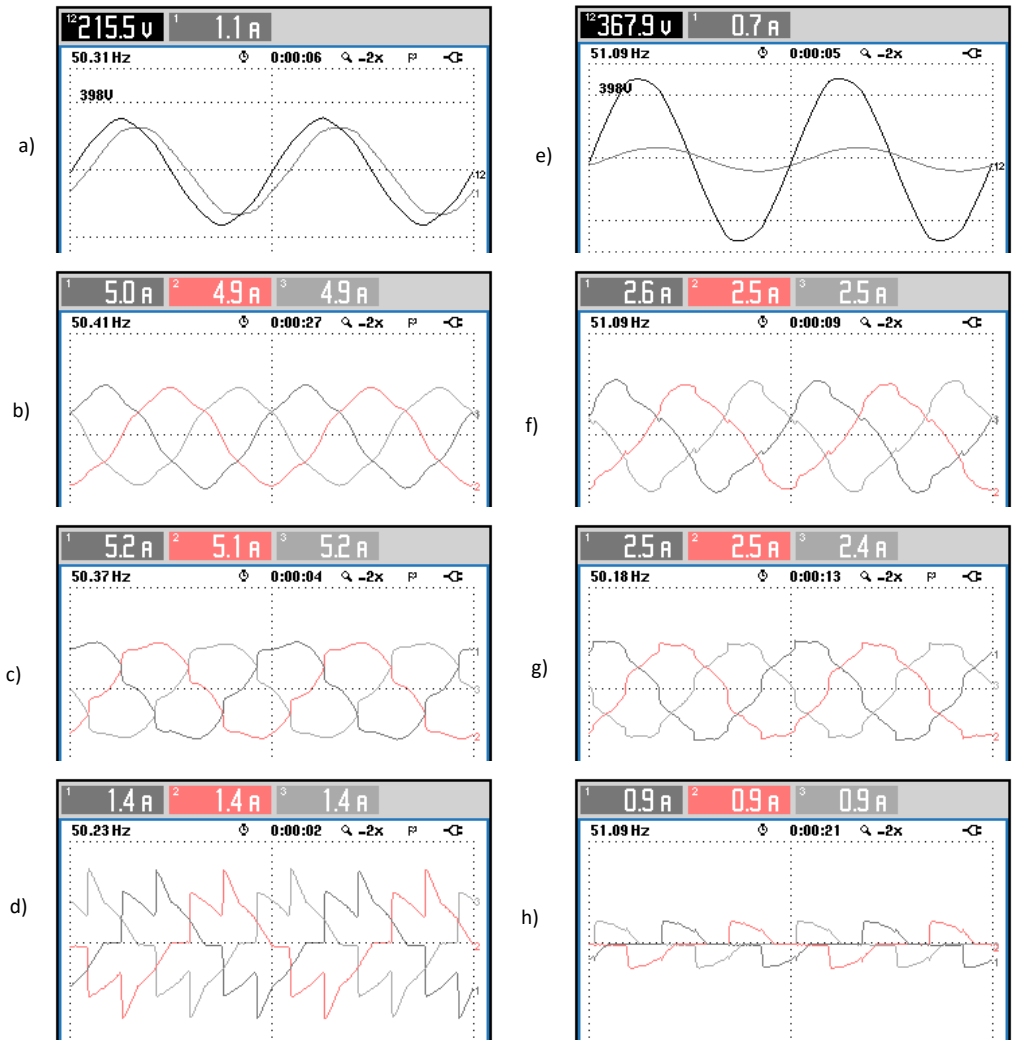

FIGURE 10.5: Delta and Y connection. Phase Voltage and current waveforms at the village load, together with current waveforms at the generator, capacitor bank and the ELC , $\alpha = 90\ ^{o}$

Δ: a) V and I at VL, b) I at Gen, c) I at C_p, d) I at ELC
Y: e) V and I at VL, f) I at Gen, g) I at C_p, h) I at ELC

As previously mentioned, the generator current deviates from a sine wave. In both cases, the voltage waveform resembles a sine wave quite accurately. The current waveform at the village load has the same shape, as the village load is purely resistive. As can be seen in figure 10.5, the ELC current is distorted in both cases. The current at the capacitor bank, C_p, balances this distortions, resulting in a less distortion current waveform at the generator terminals. This is naturally related to the analysis presented in the next section.

Just like in the simulation model, the voltage harmonics in the system with the triac controlled ELC are very low. Voltage THD is maintained under 3 % for both delta and

star connection.

Figure 10.7 shows the harmonic spectres measured at different points in the laboratory set-up. As in the simulation results in section 8.1.2, the ELC is producing a high percentage of current harmonics. These are mostly filtered in the capacitor bank, resulting in a low amount of current THD measured at the generator. This is seen as sinusoidal voltage waveforms with a relatively small amount of deviation in both laboratory and simulations. The star connected dump loads has the lowest value of voltage THD even though the ELC is producing the highest percentage of current THD, which is explained given the relative value of the system current: The star connected system has a lower rated generator current, and the ELC in this case draws a small amount of current compared with the other components.

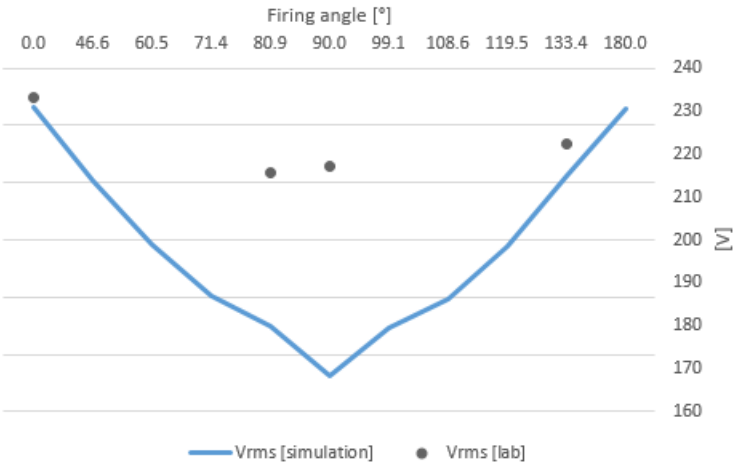

FIGURE 10.6: Voltage variation in triac controlled dump load for different values of firing angle - Lab results compared with simulation

10.1.2.1 Evaluating Simulation and Laboratory Results

Figure 10.6 shows the differences in measured voltage drop in the simulation model and laboratory set-up. The laboratory ELC is working far better than expected, with a voltage drop of only 9.4 % at the worst case in the star connected ELC. The Δ connected ELC has a voltage drop of only 6 %.

The waveform analysis shows that the Y connected ELC has a higher amount of distortion than the Δ one, but it is far from being as distorted as the simulation model, which could not run properly because of this. On the contrary, the Y connected ELC has the lowest voltage THD, since the rated current of the Y connected system is significantly lower than in the Δ case. Since the Y connected simulation model did not run properly, it was not possible to obtain comparable results.

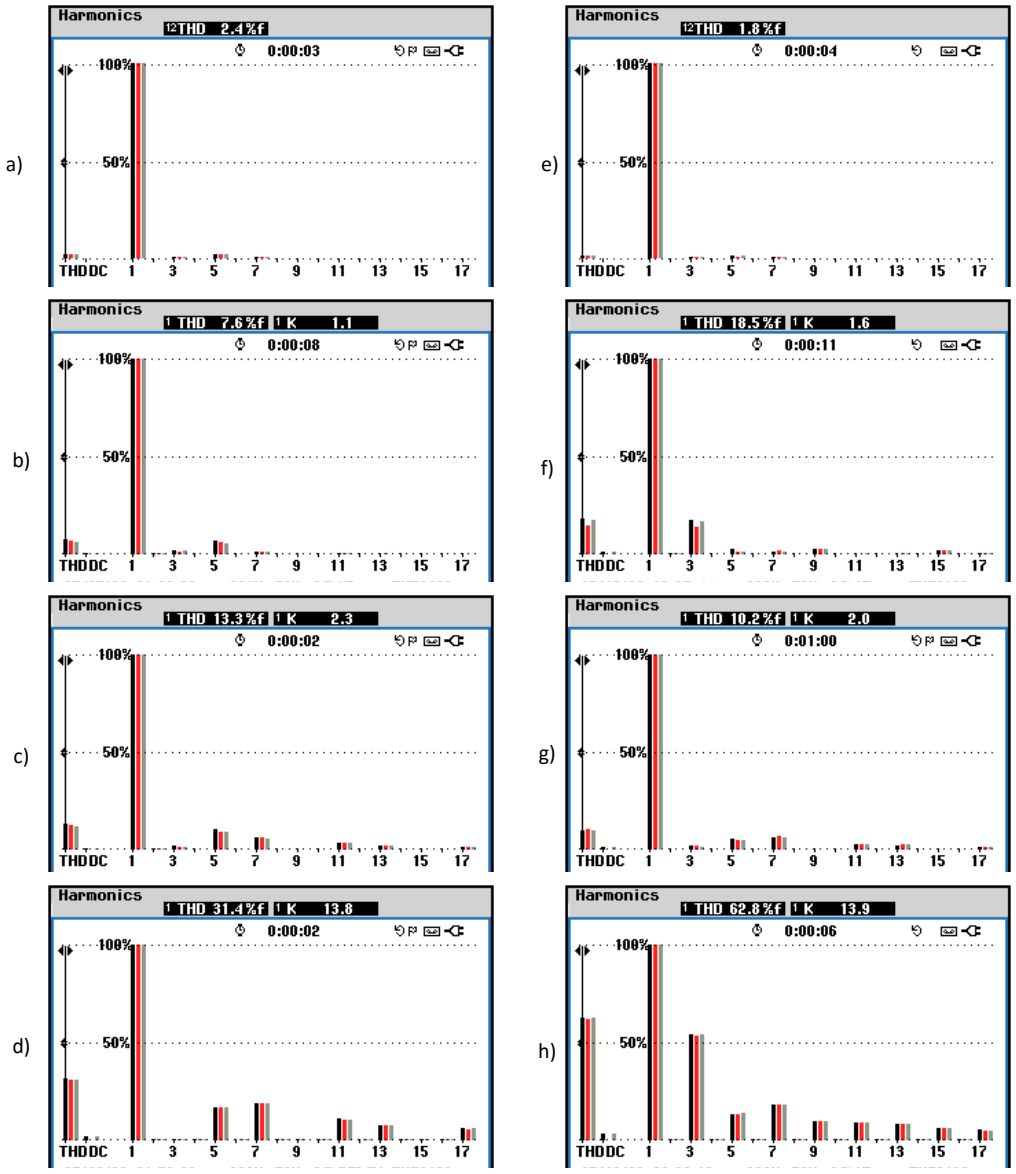

FIGURE 10.7: Delta and Y connection. Harmonics measurements at different points in the laboratory set-up, $\alpha = 90\ ^o$

Δ: a) THD voltage Gen, b) THD current Gen, c) THD current C_p, d) THD current ELC
Y: e) THD voltage Gen, f)THD current Gen, g)THD current C_p, h)THD current ELC

The choice of either Y or Δ configuration seems to mostly be a matter of taste and requirements from the surrounding system, as there is no significant difference. For Remote Hydrolights sake, it will be simpler to continue using the Y configuration they already have designed their circuit board for. It does however have a higher distortion in the ELC current, and a slightly higher percentage of voltage drop.

The curious fact that the laboratory results shows better voltage regulation indicates that there is improvement potential in the simulation model.

10.1.2.2 Frequency Change for Obtaining Rated Voltage

As seen in the laboratory tests and expected from the theory, the voltage in the system is very sensitive to changes in frequency. It is therefore interesting to see how much the frequency needs to be changed in order to obtain rated voltage is the system, when the ELC is operating at different firing angels. These measurements are not done for $\alpha = 18$ [^{o}], as this results in only a small voltage drop. The results for both Δ and Y configuration are given in table 10.4.

α [^{o}]	f at V_{rated}			
	Δ		Y	
	[Hz]	[pu]	[Hz]	[pu]
no ELC	50.44	1	51.18	1
81	51.89	1.029	53.07	1.037
90	52.01	1.031	53.20	1.039
135	50.97	1.011	52.18	1.020

TABLE 10.4: Changes in frequency to obtain rated voltage for Y and Δ configuration

The frequency change is highest for both configurations with $\alpha = 90\ ^o$. The frequency change at this angle is 1.031 pu and 1.039 pu for delta and star, respectively. The frequency increase is a bit higher for the star configuration at all the firing angles

10.1.3 Discussion

At the worst case scenario of the Y-connected ELC, the frequency is increased with 4 % in order to restore rated voltage at firing angle 90 degrees.

As discussed in section 2.3.2, the resistive load will not be influenced by an increase in frequency. By first impression, increasing system frequency seems like an interesting option given the sensitivity of the voltage in relation to the frequency. A small increase in frequency can help maintain voltage levels during periods when this is dropping because of reactive power demand from the loads. The main objective is to maintain voltage level, remembering the limits given in subsection 2.3.1 that said the voltage can vary $\pm$ 4.35 % and the frequency up to $\pm$ 10 %.

One important consideration in this discussion is the lack of evidence of using increased frequency in the literature of SEIG operation. Normally, keeping the nominal frequency is part of the objectives as the frequency limits given for the specific research articles on SEIGs are stricter than the ones presented here.

One possible way of using the frequency to regulate the voltage could be to over-dimension the dump loads of the ELC. This will give the ELC room for adjusting the frequency by changing the total power balance in the system, resulting in changed rotor speed. For the case of addition of an inductive load in the system, resulting in an inevitable voltage reduction, the ELC could reduce the total active power seen from the generator in order to increase system frequency. The practical implementation will be a topic left for further work, as it will need more investigation. It is important to keep in mind the complexity of the mutual dependant parameters, and even though increased frequency was easy using the specific lab set-up in this thesis including a frequency converter, there might be other obstacles when testing with a constant torque.

Based on the simulation results, the expected voltage drop from connection of an induction motor is higher than from the ELC operation only, and it is assumed that some type of reactive compensation will be needed. This is covered in the following section. An interesting point of view there will however be the possible use of frequency regulation in addition to reactive compensation, so this topic is kept for the further analysis of laboratory results.

10.2 Induction Motor as Load

Equivalent to the simulation results presented in Chapter 8, the alternatives for reactive compensation in the laboratory will be tested in relation to the possible connection of an induction motor as a load. The system overview is given in figure 10.8.

The induction motor (IM) connected has a power rating of 375 W, resulting in a power rating ratio of 0.25 between IM load and SEIG. This is similar to the ratio presented in section 8.2.2 of the simulation chapter. This power ratio does however not apply during the tests, as the IM is not loaded, and the power drawn by the motor will only be equal to the losses in the motor. As in the simulations, the induction motor is connected without disconnecting any active load. This is due to the small amount of active power the induction motor will consume at no load, and thus this will not have much. The topic of interest when connecting the induction motor is the transient start-up characteristics with a high consumption of reactive effect.

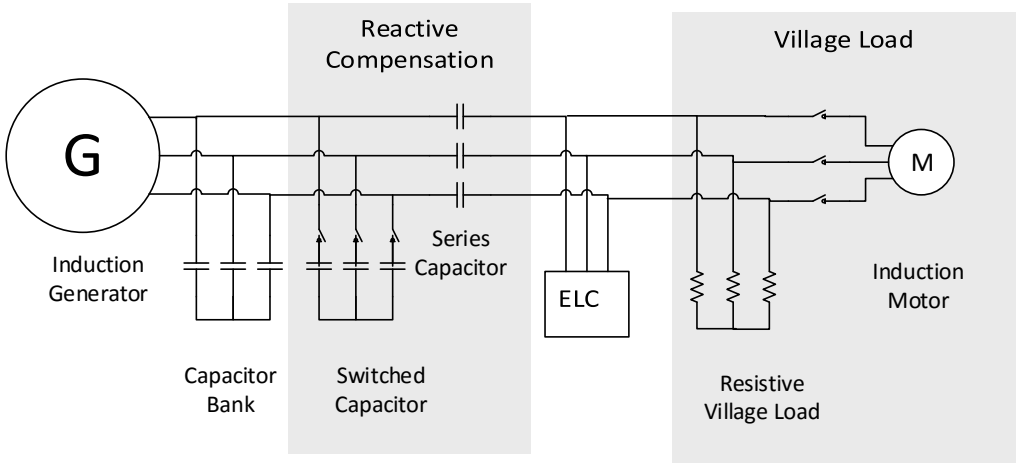

FIGURE 10.8: System overview including IM load and reactive power compensation options

First, the parameters for the IM load when it is connected directly to the 400 V grid is presented in table 10.5. When the induction motor is connected to the system, the values of the different parameters are referred to this base case.

V [V]	I [A]	f [Hz]	P [kW]	Q [kVar]	S [kVA]	PF
405	1.0	49.97	0.13	0.66	0.67	0.20

TABLE 10.5: IM connected to 400 V grid

10.2.1 No Compensation

Based on the results from section 10.1, it is seen that there is not much difference in voltage variation for Δ and Y connection. As the existing ELC system developed for a synchronous generator is star connected, further tests are carried out with Y configuration of both the induction generator and the ELC. The choice of Y connection is also related to the available equipment in the laboratory. It was originally planned to test reactive compensation by FC-TCR, where the thyristors was dimensioned for 400 V. Even though the FC-TCR was never tested connected to the SEIG system, the other compensation methods were evaluated for the Y configuration, as it was planned to compare the results for this scenario.

The IM is being switched in after the system has reached steady state operation. First, it is tested without the ELC connected, and with full resistive village load. Next, the induction motor is switched in with the ELC working at the worst case, with $\alpha = 90\ ^{o}$. The latter is the case where the voltage level is lowest, and there is already a lack of reactive power in the system. The test is performed to investigate the worst timing of connecting an induction machine, and to see whether the system collapses or reaches a lower voltage level. After these testes are carried out, the need for reactive compensation may be determined, a method for compensation can be chosen, and the parameters dimensioned.

Figure 10.9 shows the transient behavior of the voltage in the system when the IM is connected when the ELC is operating at $\alpha = 90\ ^{o}$. The voltage is 370 V before the induction motor is connected. When the IM is connected the voltage is reduced to approximately 120 V, and the voltage level is not stable.

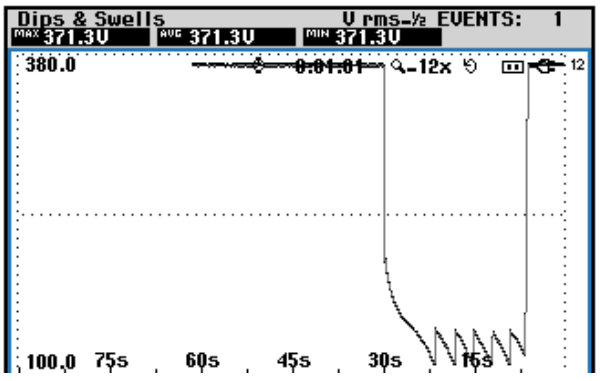

FIGURE 10.9: Transient voltage measured at generator output during connection and disconnection of IM at ELC with $\alpha = 90\ ^{0}$

IM connected at t = 30 s, disconnected at t = 5 s

The transient graph in figure 10.9 and the measurements are obtained by using fluke 343 Power Quality Analyzer, see appendix A for further information about the instrument. The numbers to the right in the white window the graph is plotted on shows the dimension of the vertical axis, which here represents the voltage in the system. The number in the lower corner is the lowest axis value, while the number in the top corner is the highest axis value. The time is shows at the horizontal axis. The time shown at the left side on the axis represents the time when the measurement starts, while the time t = 0s, at the right side, is the time when the measurement are stopped. The numbers given in the black boxes at the top of the figure is the value of the graph at t = 0s, when the measurements are stopped. The three numbers represents the three different phase values. This graph format, and the given explanation, applies for all the following graphs in this chapter.

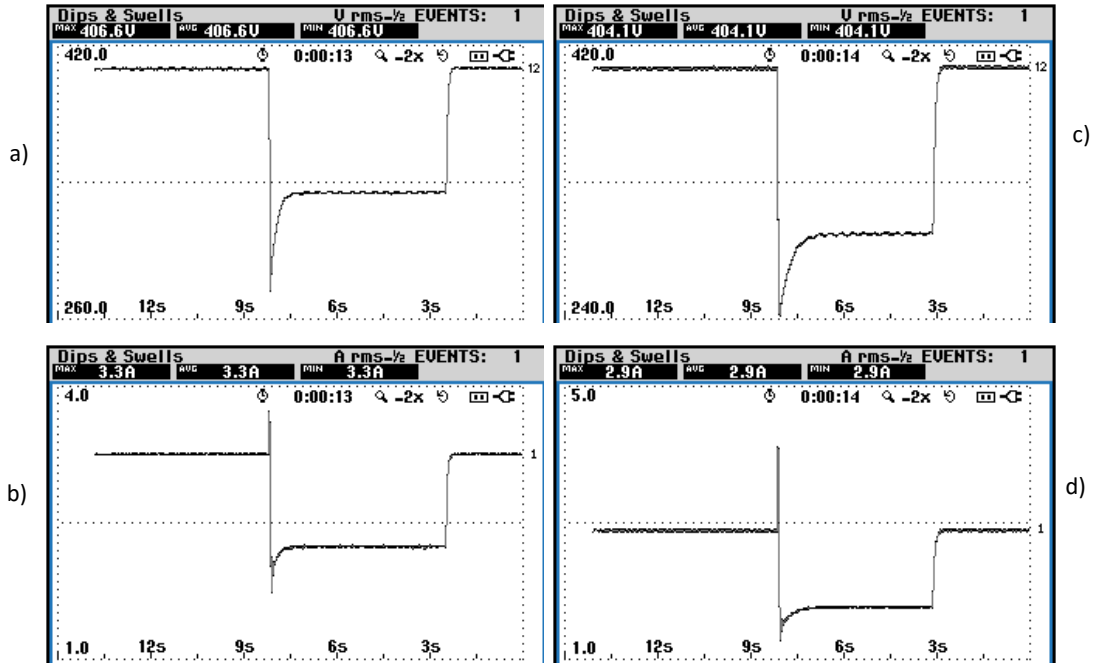

FIGURE 10.10: Transient rms voltage and current measured at generator output during connection and disconnection of IM

Left: Only village load connected, a) voltage, b) current. IM connected at t = 8 s, disconnected at t = 2.5 s.
Right: ELC connected at firing angle 90, c) voltage, d) current. IM connected at t = 8 s, disconnected at t = 3 s

For further comparison between the case with only the village load connected and the village load and the ELC at 90 degrees, the frequency is increased in the latter case in order to obtain rated voltage before the induction machine is connected. Figure 10.10 shows the transient response of both current and voltage when the IM is connected and disconnected. The graph to the left corresponds to only village load connected, while the graph to the right is for the ELC with $\alpha = 90\ ^o$.

The graphs have similar shapes, but it is visible how the ELC connected one is more sensitive to the changes in reactive power resulting in a lower voltage when the IM is connected, even though both tests starts at rated voltage. The voltage drop for ELC with $\alpha = 90$ degrees, is however, much smaller when the induction motor is connected at rated voltage.

For the case with only village load connected, the current and the active and reactive power is measured at the different parts of the system, before and after the connection of the IM. Given that the results from the previous section showed that only a small increase in frequency is necessary for obtaining rated voltage, this is also tested for the case of connection of an IM as load. The results are given in table 10.6. MP in the table is short for measurement point. In this column, the abbreviations for the different MP is given. Gen is for generator, C_p is the parallel connected capacitor bank, vl is the village load, IM is the induction motor load and vl+IM is the total load. The same abbreviations are used in the following tables in this chapter.

In this table, the frequency increase giving rated voltage in the system is given in the column to the right. Current and active and reactive power is also measured at this frequency. As the table shows, the frequency is increased with 7.5 % from the base value to obtain rated voltage when the induction motor is connected.

MP	Before IM connected f=51.20 Hz, V=402 V			IM connected f=51.34 Hz, V=330 V			IM connected, f incr f=55.09 Hz, V=405 V		
	I [A]	P [kW]	Q [kVar]	I [A]	P [kW]	Q [kVar]	I [A]	P [kW]	Q [kVar]
Gen	3.2	0.98	2.05	2.2	0.73	1.07	2.9	1.09	1.72
C_p	2.9	-0.03	2.03	2.4	-0.03	1.39	3.2	-0.04	2.21
vl	1.4	0.99	0	1.2	0.67	0	1.4	1.01	0.04
IM	-	-	-	0.6	0.07	0.31	0.7	0.10	0.49
vl+IM	-	-	-	1.4	0.75	0.30	1.7	1.12	0.48

TABLE 10.6: VL and IM

Table 10.7 gives the current and the active and reactive power at the generator for the same scenarios as the previous table. Only the generator values are given here for simplifying purposes. The important data here is the necessary frequency increase up to 56.53 Hz to obtain rated voltage with both the ELC at 90 degrees and the induction motor connected. This is an increase of 10.5 % from the base frequency.

MP	Before IM connected f=53.03 Hz, V=404 V			IM connected f=53.49 Hz, V=297 V			IM connected, f incr f=56.53 Hz, V=400 V		
	I [A]	P [kW]	Q [kVar]	I [A]	P [kW]	Q [kVar]	I [A]	P [kW]	Q [kVar]
Gen	2.9	-	-	1.8	0.50	0.76	2.5	0.85	1.50

TABLE 10.7: VL and ELC at $\alpha = 90\ ^o$, IM connected at V_{rated}

The measured active power at the generator is very low in this case because of the limitations in the test: the frequency deviates significantly from the base of 50 Hz, so the ELC which is programmed to open the triacs after 5 ms will draw less power than expected, since the period is reduced from 20 ms to 17.85 ms. This results in the ELC having a actual firing angle of 101.754 ^{o}, resulting in the ELC consuming 370 W instead of 500 W, given rated voltage. As well, the IM equivalent reactance is increased with frequency, resulting in less current going here, and hence less power.

The system current is, as predicted from section 4.3, lower for the same rated voltage at an increased frequency. This is due to the fact that an increase in frequency gives increased voltage corresponding to a specific magnetizing current level. Thus, with increased frequency, the operation point for the rated voltage will be at a lower current value. This is seen also in the values of total reactive power is lower measured at a higher frequency.

10.2.2 Discussion

When considering the IM as a load, the shortcomings of the method of increasing frequency is more visible. For large voltage drops when the IM is connection, the frequency needse to be increased between 7.5 and 10 % from its base value, depending on the existing operation point of the ELC at the time the IM is connected. This is very close to the frequency limit given at ± 10 %, and not an operation point one would want the system to be operating at. Based on these results, there is definitely a need for reactive compensation in the system during connection of an IM.

10.3 IM with Reactive Compensation

In the previous section, a severe voltage drop is observed when an induction motor is connected as load. Some compensation is necessary to increase the voltage level during the connection of this load, in order to stay within the limits for system voltage presented in section 2.3.1.

Based on the difficulty to determine what caused what when both the ELC and the village load is connected, and then the IM and the compensation is connected, the next test will be performed without the ELC and with only the village load. This reduces the number of variables that influence the system, and hence it will be easier to see the actual impact of the reactive compensation methods.

Reactive compensation in form of switched capacitor and series capacitor is tested, and the results are given in this section. Based on the need of additional reactive power in the system, the amount of reactive compensation is calculated, and used to dimension the capacitance values. It is not expected that this solution will contribute to steady state harmonics at higher frequency than the fundamental, because there is nothing switching the current at each period. Thus, THD is not looked into when evaluating these options.

10.3.1 Switched Capacitor

From the previous section, the need for reactive compensation is calculated. This is used to calculate the size of the switched capacitor by using equation (4.5). The test is performed with the switched capacitor $C_{sw} = 7\ \mu$F, which is a bit below the calculated value based on the need of reactive compensation. It is therefore expected that the connection of this capacitor will increase the voltage, but the voltage will not reach rated value. Normally, this solution would consist of several capacitors, and then the optimal combination would be switched in depending on the need of reactive effect. This results in a voltage control in fixed steps.

First, the induction generator with the capacitor bank and the village load connected is started and allowed to reach steady state operation with rated voltage and frequency. Then, the IM is connected followed by the capacitor. Both are connected to the system by a switch, and are connected in parallel with the other components. Figure 10.8 shows the switched capacitors connected to the system. This test is run without the series capacitor shown in the figure.

Table 10.8 shows the voltage, current and active and reactive power at the different points in the system before the IM is connected, when IM is connected and when IM and C_{sw} is connected. The current and active and reactive power at vl and vl+IM is not measured when the switched capacitor is connected.

MP	Before IM connected f= 51.16 Hz, V=403 V			IM connected f=51.28 Hz, V=331 V			IM + C_{sw} connected f=51.28 Hz, V=380 V		
	I [A]	P [kW]	Q [kVar]	I [A]	P [kW]	Q [kVar]	I [A]	P [kW]	Q [kVar]
Gen	3.3	0.98	2.05	2.2	0.72	1.07	2.9	0.96	1.67
C_p	2.9	-0.03	2.03	2.4	-0.03	1.37	3.2	-0.04	2.13
vl	1.4	0.99	0.00	1.2	0.67	0.00	-	-	-
IM	-	-	-	0.5	0.07	0.31	0.7	0.10	0.46
vl+IM	-	-	-	1.4	0.75	0.30	-	-	-
C_{sw}	-	-	-	-	-	-	0.5	-0.01	0.31

TABLE 10.8: VL, IM and C_{sw}

When C_{sw} is connected the voltage increases from 331 V to 380, and is almost within the operating limits for the system. The increased voltage results in an increased reactive power supplied from C_p, from 1.07 kVar to 1.67 kVar. The supply from C_{sw} is 0.31 kVar. Thus, the connection of the capacitor results in a total reactive power increase from 1.07 kVar to 2.09 kVar.

As well, the active power supplied by the generator increases. The village loads consumes 0.86 kW, which is less than rated village load. The lack of power delivered to the resistive load is a result of the low voltage level in the system. If the voltage level in the system is within operation range, the resistive loads will work sufficiently. When evaluating the supply to the resistive loads, it is the voltage level that is essential.

When the IM is connected to a 400 V grid, its active power and reactive power consumption is 0.13 kW and 0.66 kW, from table 10.5. For the IM connected in this laboratory power system, the active power consumption is increased from 0.07 to 0.10 kW when C_p is connected, and the reactive power consumption is increased from 0.31 to 0.46 kVar. Thus, the power delivered to the IM is closer to the ideal values when the switch is connected, but still improvable.

The transient voltage and current response measured is given in figure 10.11. a) and b) shows the voltage and current response measured at the generator. c) and d) shows the voltage and current measured at the IM. First, the system is operating at rated voltage, then the IM is connected, resulting in a transient voltage dip and a current peak in the system, caused by the IM starting characteristics. The system is fast stabilizing at a reduced voltage, the current at the generator is also reduced. Next, C_{sw} is switched in.

This results in an increase in the voltage in the system, and an increased current at both the generator and the IM. C_{sw} is then disconnected, followed by the disconnection of the IM. The system goes back to original steady state voltage and current values.

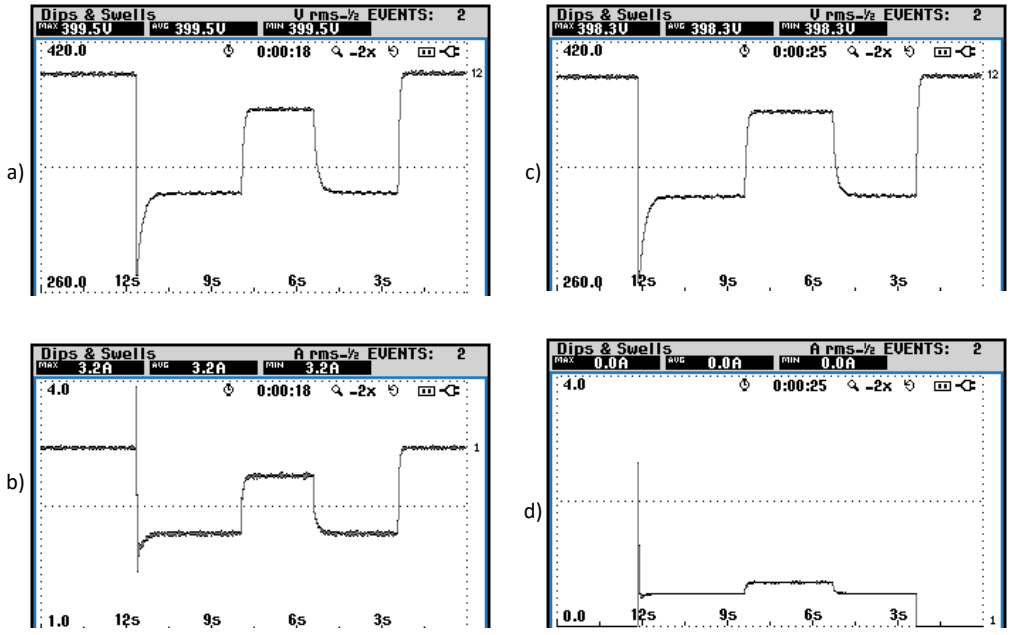

FIGURE 10.11: Transient voltage and current response when IM and C_{sw} is connected and disconnected

Left: Measured at the generator, a) voltage, b) current. IM connected at t = 11.5 s, C_{sw} connected at t = 8 s, C_{sw} disconnected at t = 5 s, IM disconnected at t = 2.5 s
Rigth: Measured at the IM, a) voltage, b) current. IM connected at t = 12 s, C_{sw} connected at t = 8.5 s, C_{sw} disconnected at t = 5 s, IM disconnected at t = 2.5 s

A test is carried out to see if the system is able to start with both the IM and C_{sw} connected from start. The rotor speed is increased up to normal operation speed, but there is no voltage build-up. The speed is then further increased, but still without any voltage build-up. The system needs to start, and reach normal operation values before the IM and C_{sw} can be connected.

As the switched capacitor is not able to provide a sufficient voltage level alone, it is investigated how much the frequency needs to be increased to reach rated voltage in the system when the capacitor is connected. The results are given in table 10.9, where the frequency, voltage, current and active and reactive power measured at the generator are given for before the IM is connected, when the IM is connected, when the IM and C_{sw} is connected and when the IM and C_{sw} is connected and the frequency is increased.

Before IM connected f=53.18Hz, V=406V			IM connected f=53.50Hz, V=295V			IM + C_{sw} connected f=53.14Hz, V=384V			IM+C_{sw}+f incr f=54.35Hz, V=407V		
I [A]	P [kW]	Q [kVar]	I [A]	P [kW]	Q [kVar]	I [A]	P [kW]	Q [kVar]	I [A]	P [kW]	Q [kVar]
2.9	0.87	1.85	1.8	0.49	0.76	2.6	0.85	1.54	2.9	0.94	1.78

TABLE 10.9: IM and ELC 90. Comparing compensation options. Values measured at the generator

A frequency increase from 53.14 Hz to 54.35 is necessary for reaching a voltage of 407 V. This corresponds to a increase from 1.038 pu to 1.062 pu, related to the frequency resulting in rated voltage when only the village load is connected. As can be seen, the active power is increased from 0.85 kW to 0.94 kW. This small increase is due to the change in firing angle, which is caused by the increased frequency as explained previous in this chapter. A frequency of 54.53 Hz an a phase delay of 5 ms results is a firing angle $\alpha = 98.15\ ^o$. At this firing angle, the ELC consumes 0.41 kW. As well, the increased frequency results in an increased reactance in the IM, resulting in less current flow to the IM, and thus less active power.

10.3.2 Series Capacitor

According to the theory given in chapter 5, series connected capacitance can provide reactive power according to the the current drawn by the load. It is interesting to investigate if this solution works with a almost constant active power load, and a varying reactive load. This solution may however result in subsynchronous resonance (SSR) when an inductive load is connected. SSR is unwanted due to the resulting oscillations in voltage and current, and oscillations in the speed and torque of the IM. The parallel capacitor, C_p, needs to be adjusted when a series capacitor, C_s, is connected in the system. This is necessary to balance the reactive power. When a series capacitance is introduced in the system, this will also supply reactive power. Hence, the parallel capacitance supply of reactive power must be reduced accordingly. The parallel capacitor is reduced to the no-load value. The factor k, which is the ratio between the parallel capacitance and the series capacitance, should be in the range 1-0.4 according to the theory. It is found that the SSR is possible to avoid in the system given an optimum combination of the capacitors.

In the simulation results presented in section 8.3.3, no combination between C_p and C_s was possible to obtain, resulting in SSR during connection of IM at all the tested values of K.

10.3.2.1 Series Compensation with C_p = 33 μF and C_s = 33 μF

The first test is run with C_p = 33 μF and C_s = 33 μF, which is equal to k = 1. The frequency is adjusted to obtain rated voltage at the generator before the IM is connected. A frequency of 49.98 results in a voltage of 403 V. Table 10.10 gives the measured values in the system before and after the connection of the IM. The measurement point denoted as C_s + vl + IM is the point on the generator side of C_s, while the measurement point denoted as vl + IM is at the load side of C_s.

MP	Before IM connected f= 49.98 Hz				IM connected f= 48.87 Hz			
	V [V]	I [A]	P[kW]	Q[kVar]	V [V]	I [A]	P[kW]	Q[kVar]
Gen	403	3.2	0.72	2.10	364	3.3	1.15	1.75
C_p	403	2.3	-0.03	1.62	364	2.1	-0.02	1.30
C_s+vl + IM	403	1.2	0.72	0.46	364	1.9	1.12	0.43
vl+IM	344	1.2	0.73	0.00	400	1.9	1.14	0.66
vl	344	1.2	0.73	0.00	400	1.4	1.00	0.00
IM	-	-	-	-	400	1.0	0.14	0.65

TABLE 10.10: IM, VL and Series Compensation with C_p = 33 μF and C_s = 33 μF

Before the IM is connected, the voltage at the generator side is 403 V. At the load side however, the voltage is 344 V. This is outside the allowed operating range for the voltage. The village load is only consuming 0.73 kW due to the low voltage level. When the IM is connected, the voltage level and the frequency in the system is changed. The frequency is reduced from 49.98 Hz to 48.87 Hz. On the load side the voltage is increased to 400 V, which is within the operation limits. This results in 1.00 kW to the resistive village load. The IM consumes 0.14 kW and 0.65 kVar, which is very close to consumption when the IM is connected directly to a 400 V grid. The voltage drops to 364 V at the generator side when the IM is connected.

The transient voltage and current response when the IM is connected is given in figure 10.12. a) and b) shows the voltage and current response, respectively, measured at the generator. c) and d) shows the voltage and current response measured at the load side of C_s.

A high voltage and current peak is observed when the IM is connected, as can be seen in figure 10.12. At the load side there is first a voltage dip, followed by a voltage peak before the voltage stabilises.

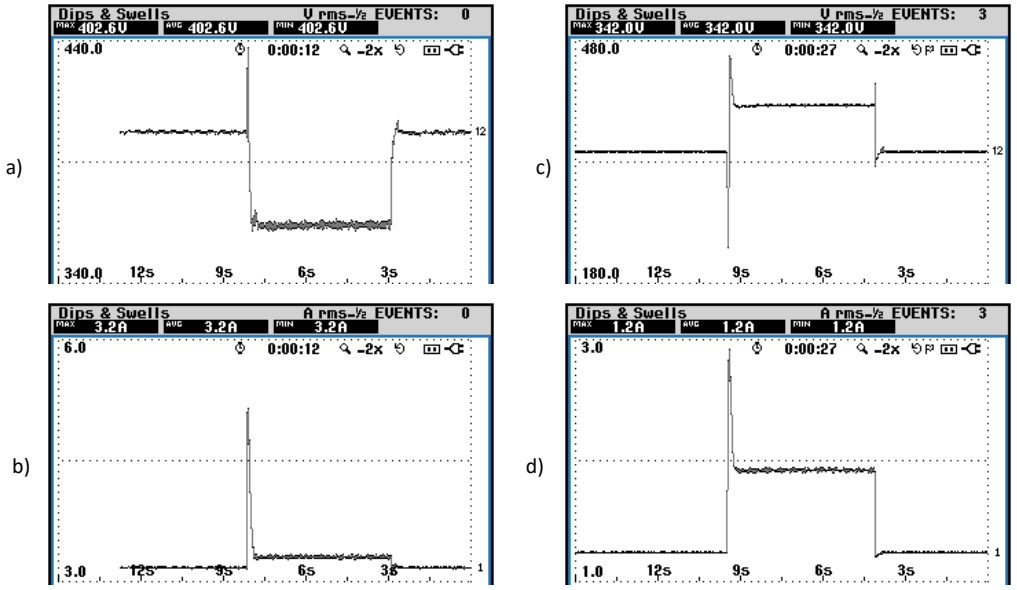

FIGURE 10.12: Transient voltage and current response when the IM is connected in a system with Series Compensation with $C_p = 33$ μF and $C_s = 33$ μF

Left: Measured at the generator, a) voltage, b) current. IM connected at t = 8 s, disconnected at t = 3 s
Right: Measured at the load side, a) voltage, b) current. IM connected at t = 9 s, connected at t = 4 s

As the voltage level is too low at the load side before the IM is connected, this is not a well functioning solution. The load is mostly going to be purely resistive, or only a small share of inductive load. The case of the IM connected will not be the normal loading of the generator. The system needs to be designed to work sufficient both with and without the IM connected.

To reduce the voltage difference on the generator and load side of the series capacitance, the capacitance is increased. This results in a reduction in the reactance, and hence a lower voltage drop over the component.

10.3.2.2 Series Compensation with $C_p = 33$ μF and $C_s = 40$ μF

A new test is performed, with $C_p = 33$ μF and $C_s = 40$ μF, resulting in k = 0.825.

The frequency is again adjusted to provide rated voltage at the generator before the IM connected, where f = 50.21 Hz and V = 399 V. As it is most interesting to look at the values measured at the generator and at the load side of the series capacitors, this is the values given in table 10.11.

MP	Before IM connected f = 50.21 Hz				IM connected f = 49.40 Hz			
	V [V]	I [A]	P[kW]	Q[kVar]	V [V]	I [A]	P[kW]	Q[kVar]
Gen	399	3.2	0.76	2.04	343	2.9	1.01	1.40
vl+IM	361	1.3	0.80	0.07	384	1.7	1.02	0.53

TABLE 10.11: IM, VL and Series Compensation with $C_p = 33$ μF and $C_s = 40$ μF

This solution results in a lower voltage differentiation on the two sides of the C_p when the IM is not connected. However, the voltage level at the load side without the IM connected is 361 V, which is not within the allowable operation range. The voltage values when the IM is connected is not improved. The voltage at the generator side is reduced to 343 V while the voltage at the load side is increased to 384 V, which is within allowable operation rate. As the voltage at the load side is not within the desired voltage range when the IM is not connected, this combination of capacitor does not provide satisfying voltage levels in the system.

Figure 10.13 shows the transient voltage and current response measured at the load side when the IM is connected. SSR is now observed at the load side. In the right part of the figure, the voltage and current oscillations when the IM is connected is shown.

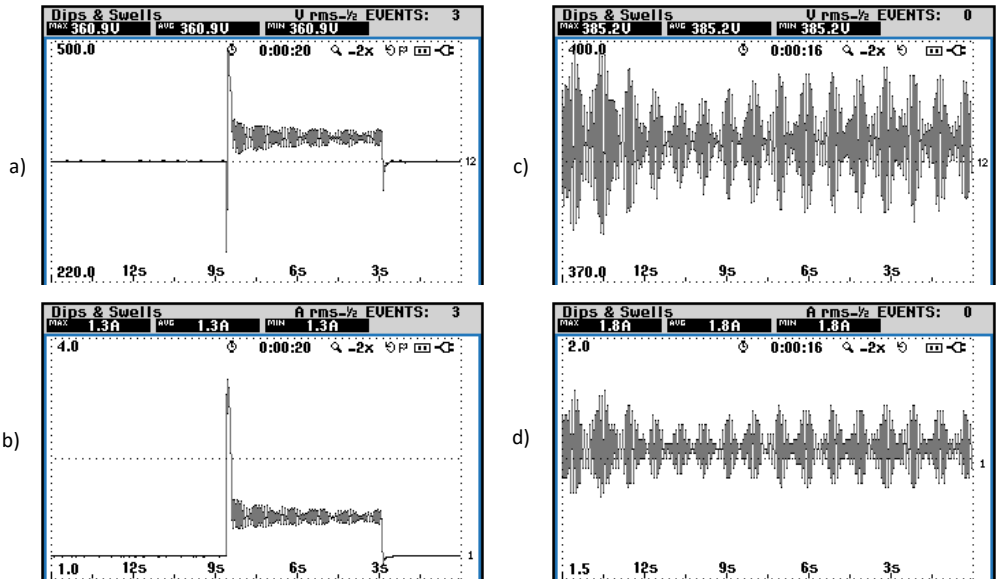

FIGURE 10.13: Transient voltage and current response when the IM is connected in a system with Series Compensation with $C_p = 33$ μF and $C_s = 44$ μF

At the load side: Voltage, a), and current, b), response when IM connected at t = 8.5 s, disconnected at t = 3 s. Voltage, c), and current, d), oscillations when the IM is connected.

This is not a sufficient solution due to the unsatisfactory voltage levels in the system and the presence of SSR. The combination of the capacitors needs to be changed.

10.3.2.3 Series Compensation with Cp = 36.5 μF and Cs = 66 μF

Next, the C_s is further increased. This will result in less reactive power delivered from the C_s to the generator, hence C_p is also increased to provide an increased amount of reactive power. The next combination tested consists of C_p = 36.5 μF and C_s = 66 μF, resulting in k = 0.55. The values measured at the generator and the load side of C_s before the IM is connected is given i table 10.12.

MP	Before IM connected f = 51.44 Hz				IM connected f = 49.46 Hz			
	V [V]	I [A]	P[kW]	Q[kVar]	V [V]	I [A]	P[kW]	Q[kVar]
Gen	402	3.1	0.90	1.98				
vl+IM	386	1.4	0.93	0.04				

TABLE 10.12: IM, VL and Series Compensation with C_p = 36.5 μF and C_s = 66 μF

As can be seen from table 10.12, this combination of C_p and C_s seems promising before the IM is connected. The voltage at the load side is 386 V, which is within the allowed operation range. When the IM is connected, severe SSR is observed, both at the generator and the load side of the Cs. Due to this, the voltage, current and active and reactive power is varying, and it is not possible to determine a value for these parameters. Thus, there are no measurement of these values when the IM is connected.

Figure 10.14 shows the transient voltage and current response measured at the generator and at the load side of the C_s. The oscillation due to the SSR is van be seen in the graphs. The voltage oscillates between 290 V and 330 V at the generator side, while the current oscillates 2.2 A and 4.8 A. At the load side, the voltage oscillates between 220 V and 480 V, and the current oscillates between 1.2 A and 3 A. Due to the heavy presence of SSR in the system, this is also not a satisfying combination of the capacitors.

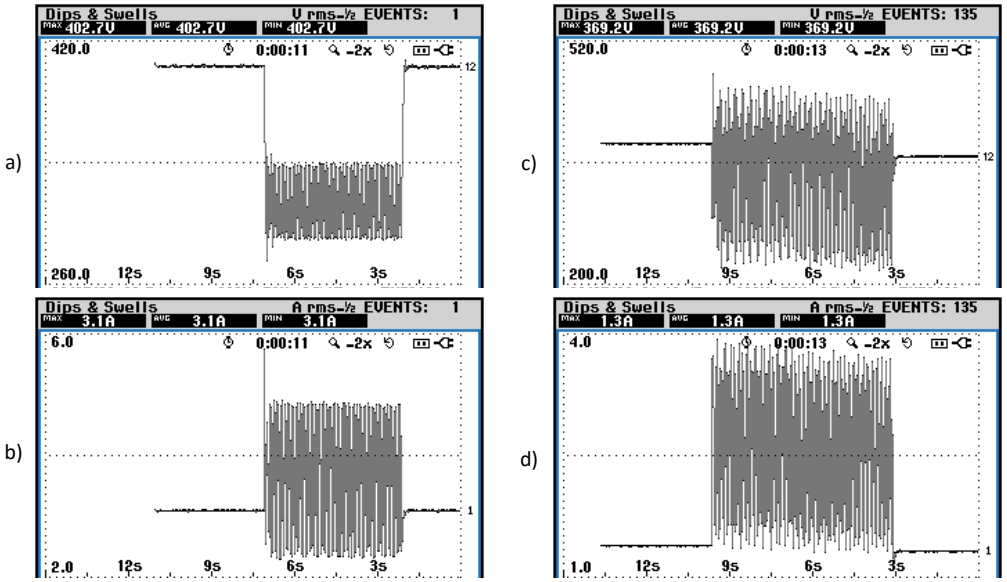

FIGURE 10.14: Transient voltage and current response when the IM is connected in a system with Series Compensation with $C_p = 36.5\ \mu$F and $C_s = 66\ \mu$F

Measured at Gen, a) voltage, b) current. IM connected at t = 7 s, disconnected at t = 2 s
Measured at load side, a) voltage, b) current. IM connected at t = 9.5 s, connected at t = 3 s

10.3.2.4 Evaluation of the Different Combinations of the Capacitors in Series Compensation

In the first combination tested, with k = 1, a voltage difference between the generator side and the load side of C_s is observed. Before the IM is connected, the generator voltage is 403 V, while the voltage on the load side is only 433 V. This is not a sufficient voltage levels for the loads, as the minimum voltage level is 483 V. When the IM is connected however, the voltage at the load side is increased to 400 V, while the generator voltage is reduced to 364 V. As the voltage at the load side always needs to be within the allowable voltage range, this combination is not working as desired.

A new test is performed with k = 0.825. C_s is increased, resulting in a reduction in its reactance value, and a decrease in voltage variation on the generator side and the load side is expected. The resulting voltage at the load when the IM is not connected is 361 V and when the IM is connected, the voltage is 384 V. Thus, it is still outside desired operation range when the IM is not connected. As well, a small amount of SSR is observed at the load side of system.

C_s is further increased, and C_p is slightly increased, resulting in k = 0.55. As expected, this leads to an increased voltage at the load side before the IM is connected. However,

when the IM is connected, a severe amount of SSR is observed in both sides of the system. This is not acceptable operation conditions for a power system.

10.3.3 Discussion - Reactive Compensation Options

As there is a need for reactive compensation when the IM is connected as load, two different options are tested. First, reactive compensation by switched capacitor is tested, then series capacitor is tested.

In the laboratory, the need for reactive compensation is first determined, and this is used to calculate the value of the switched capacitor. As the capacitor available in lab has a bit lower capacitance than the calculated value, it is assumed that the compensation will result in a voltage lower than rated value. First, the test is performed with only the village load connected. When the capacitor is switched in, the voltage is increased from 331 V to 380 V, and is almost within the allowed operation range. Then, the test is performed with the ELC operating at $\alpha = 90\ ^o$. Before the IM is connected, the frequency is adjusted to obtain rated voltage in the system, f = 53.18 Hz. When the capacitor is switched in, the voltage is increased from 295 to 384 V. The voltage is just within the allowable voltage range. A further increase in frequency, to
f = 54.35 Hz results in rated voltage in the system. Thus, the frequency which results in rated voltage is reduced from 56.53 Hz to 54.35 Hz when the capacitor is connected.

In a real system, one or more capacitors are available for connection in a solution with switched capacitors for reactive compensation. An increased number of capacitances results in better voltage regulation, but also in increased costs. As the inductive load in the system is most likely only going to be an IM, a few number of capacitors can be used, which are dimensioned to match typical IM sizes. If this solution does not provide desired voltage levels, a slight increase of reduction in frequency can be used to further adjust the voltage level.

The second solution tested is series compensation by short-shunt configuration. Three different combinations of Cp and Cs are tested. The ratio between Cp and Cs is k, and according to theory this should be in the range 1-0.4. The different combinations used in the tests results in k = 1, k = 0.825 and k = 0.55.

As found in the simulation results, it is a very complex task to tune the series capacitor for obtaining a good rated voltage and at the same time avoid the SSR phenomenon.

It seems as the reduction in voltage drop when the k is reduced goes on the behalf of the presence of SSR in the system. Reduction in voltage drop leads to an increase in SSR in the system. With the different combinations of capacitors tested, it is not possible to

obtain a satisfying balance between voltage levels in the system an the amount of SSR. The amount of SSR produced is dependent on the parallel and the series capacitance as well as the inductive load connected. Thus, the system might be optimised for one load combination. If the load later is changes, SSR may be observed in the system. As there is no control of the size of IM connected to the system or the other inductive load, SSR will be a probability, even though it is not observed for a specific load combination.

From these results, is is found that an increase in k is necessary to increase to voltage at the load when the IM is not connected. An increase in k results in an increased level of SSR in the system. As a k resulting in desired voltage levels, both when the IM is connected and disconnected, and without a high level of SSR is not found, this is not a desirable solution for reactive compensation.

10.4 Conclusion

The measured voltage drop at $\alpha = 90\ ^o$ is 9.4 % for Y connection, and 7.7 % for Δ. When the ELC is Y connected and the IM is connected, the voltage drop is 17.4 % for the case of full resistive load. When the system is operating at rated frequency giving a voltage level of 370 V and with the ELC at $\alpha = 90\ ^o$, the voltage is reduced to 120 V when the IM is connected. This is equivalent with a 70 % deviation from the rated voltage. When the system is operating at an increased frequency resulting in rated voltage and the IM is connected, the voltage drops to 297 V, corresponding to a voltage drop of 26.5 %. It is therefore seen that the voltage level the IM is connected at is critical for the amount of voltage drop. In the simulation, the voltage drop was 26.7 % for only ELC connected at 90 ^{o}. When the IM is connected, a transient current peak and voltage dip is observed in both the lab and the simulation, but the system is fast stabilizing at a new current and voltage level so it is not given further attention to the topic.

	Before IM connected	IM connected	IM + f incr	IM + C_{sw}	IM + C_{sw} + f incr
V [V]	406	295	399	384	408
f [Hz]	53.18	53.50	56.53	53.14	54.47

TABLE 10.13: IM connected with ELC firing angle = 90 ^{o} and different compensation options, system voltage and frequency

A continuous error of measurements is the frequency, which is not possible to adjust correctly with the frequency converter used. All the parameters is however calculated for 50 Hz, giving for instance that the firing of the thyristor will happen a slight moment later than calculated if the frequency is increased. This is because it is coded using timing in ms instead of angle.

The frequency is not that affected by the different loads connected, it is the voltage that suffers the greatest variation with different loads connected. The frequency can however be adjusted to minimize the voltage drop. In lab, the speed of the turbine is adjusted to provide the desired frequency in the system. In reality, an assumption about constant torque is viable. Then, the speed of the turbine is dependent on the loads connected, as described in the theory. There is no option of just changing the speed of the rotor to get the desired frequency by a switch, as done in the lab. In a real system, the rotor speed can be changed, resulting in frequency change, by adjusting the electrical power connected to the system. To increase the frequency, active load can be removed from the load. Thus, to always have the possibility of increasing frequency, there must be active load in the ELC available for disconnection.

The switched capacitor works as expected, and the quality of the voltage regulation provided depends on the amount of capacitors connected. This is again depending on the total costs. As the inductive load in the system is most likely will be an IM, a little number of capacitors can be used dimensioned to match typical IM sizes. If this solution does not provide desired voltage levels, a slight increase or reduction in frequency can be used to further adjust the voltage level.

The hypothesis for the series capacitor was that it could be a good solution because of the simplicity. In reality, it is too difficult to tune for this given set-up. Trying to improve the voltage level at the village load connection point resulted in increasing SSR. It might be possible to find a suitable combination of capacitance values, but that would be for the specific load size tested. The system will need to handle different load connections, so series capacitance is discarded as an option.

Chapter 11

Conclusion

The main challenge of controlling an induction generator in isolated operation is all the mutually dependant parameters, and the difficulty to determine their relations when no parameter can be assumed 100 % constant. The relations of highest importance in the investigations presented in this thesis is the dependency between voltage level, reactive power balance and frequency.

A higher share of inductive loads gives a smaller range of operation before voltage collapse for the isolated induction generator. The reactive power consumption of the generator increases with the active power load. If the active load is balanced by an ELC, there will not be changes in the voltage and frequency related to active power variations, and the problem is reduced to balancing the reactive consumption of the inductive loads.

There is not many examples of the triac-controlled ELC solution used with SEIG found in the literature, and the sources listed covers only resistive load. This might only be because the triac control is seen as an old technology, but its cost-efficiency makes it interesting for rural applications. The main findings in this report points in the direction of this technology being suitable for the objective, but that some adjustment might be necessary for being able to handle different load connections.

The simulation of the triac controlled ELC showed a poor voltage regulation, and the results implied that a compensation unit might be necessary even for normal operation with only resistive village load. Testing in the laboratory however, the voltage drop decreased significantly for a similar test using fixed firing angles.

The uncontrolled rectifier ELC solution showed much better voltage regulation than the triac solution in the simulations, and it would be very interesting to test also this one in a laboratory set-up to see if also this will improve in the lab. From these results it is

assumed to be a better option than the triac solution, but continued tests on this option is left for further work.

The simulation model was not able to provide reliable results for the star connection alternative of the triac controlled ELC, and it was stated that the big discontinuities in the voltage waveform sabotaged the proper operation of the designed simulation block that provides the gate signal to the thyristors. Both the delta and the star configuration of the ELC was tested in the laboratory. The waveform in the star connected ELC was proved worse also in this test, and this configuration had a bit larger voltage drop. This was however so insignificant that the choice of either star or delta configuration is left without giving a specific recommendation. Since Remote Hydrolight already uses the star configuration in their design, they can continue without any big troubles.

When comparing disturbances caused by harmonic components, the measurement of THD in % is used. The simulations show that the triac controlled solution produces a significant amount of current THD, but the interaction with the connected capacitor bank is beneficial for the type of harmonics produced. This results is a low voltage THD measured in the system. A similar characteristic is seen also in the laboratory result. The uncontrolled rectifier-ELC solution tested in the simulation produces 4 times higher voltage THD at its worst case compared to the triac solution, and this is the main drawback found of the former solution.

When simulating different ratings of load size it was discovered that the SEIG system seems to be more vulnerable for changes in reactive power if the total load is small compared to the rating of the generator. The smaller the load, the closer will the full resistive load operation point be to the no-load situation. A shortage of reactive power might be a more sensitive issue at this operation point than further out to the right on the magnetizing curve. This is something to take into consideration when designing the ratings of the power system.

The connection of an induction motor as a load is the most likely "worst case"-scenario of load connection in a system like the one studied. It is testes in both lab and simulations. In all cases the connection results in a severe voltage drop caused by the inrush current and reactive power consumption. A too high ratio of motor size vs generator results in total voltage collapse. Some type of compensation will be necessary in order to maintain system voltage during connection of a motor.

When testing the connection of IM in the laboratory, is was found that the voltage level at the connection time was decisive for the following voltage drop. When the ELC was operating at $\alpha = 90\ ^o$, the voltage drop was significantly less in the case of connection at rated voltage compared to connection at rated frequency. At the latter

operation condition, the voltage level was below rated value before the IM was connected. Maintaining the average voltage level within a relatively strict limit will be important for being able to handle large imbalances that might occur.

Increased frequency was used as a method to provide rated voltage at loading conditions with increased reactive power consumption. This was done easily in the laboratory by adjusting the frequency converter, but this will be a more complex task in a more realistic laboratory set-up. This investigation was done as a consequence of the results finding that the voltage level was very sensitive to small increases in frequency. It was found possible to maintain the voltage measured at the village load within given limits even when the IM was connected, and at the same time keeping the frequency within given limits as well. There is not much literature found on the topic given that the existing research on utilization of SEIG has frequency stability as one of the main objectives. Given the wide tolerances provided for this thesis, it is seen as an interesting option, perhaps in combination with reactive power compensation.

Of the reactive compensation options studied, the switched capacitor has the most potential. The quality of the voltage regulation provided by this unit depends on the amount of capacitors connected. This is again affecting on the total costs. As the inductive load in the system is most likely an IM, a small number of capacitors can be used dimensioned to match typical IM sizes. If this solution does not provide desired voltage levels, a slight increase or reduction in frequency can be used to further adjust the voltage level.

The series capacitor alternative turned out to be a too complex task to tune for the given set-up. Trying to improve the voltage level at the village load connection point resulted in increasing SSR. If a suitable combination of capacitance values is found, it would only be perfectly tuned for one specific load size tested. The system will need to handle different load connections, so series capacitance is discarded as an option.

11.1 Recommendations

This thesis has been assigned to Engineers Without Boarders NTNU by Remote Hydrolight, and as a final summary some recommendations is given.

To answer to the request provided by Remote Hydrolight, it can be stated from this thesis that the option of using their existing triac controlled ELC combined with an SEIG is possible.

From the results obtained, it is seen as most reasonable to use the ELC without any compensation during normal operation with resistive village load, and including one or more switched capacitors in the scheme in case of any large disturbances like the connection of an induction motor. More research is necessary on the topic, but if it is found suitable, the use of variable frequency to adjust smaller voltage changes is interesting. This can possibly be used with the switched capacitor to provide a more smooth adjustment than the step-wise regulation it represents.

Suggestions for further work is given in the next chapter.

Chapter 12

Further work

In the event of this thesis being the basis for continued studies, some elements noticed as possible good options for further work is listed:

- Improve the simulation models to include regulation to provide a more realistic result considering also reaction time of the system
- Implement fixed torque input to the turbine/generator in both simulation model and laboratory set-up
- Investigate the possible practical implementation of voltage control by varying the frequency level
- Test the uncontrolled rectifier ELC in the laboratory set-up
- Analyze the possible improved utilization of the energy dissipated in the dump loads. Suggestions might be battery storage, or better utilization of the heat produced by the existing heating elements

Appendix A

Instrument List

Instrument	**NTNU Elkraft identification number**
Arbitrary waveform generator, TTi TGA1244 40 MHz	B03-0411
Control unit for driving machine LEY-BOLD	B03-0504
Differential Probe, High Voltage, Tetronix P5200A 50 MHz	I06-0514
Digital Storage Oscilloscope, four channels, Tetronix TDS 2014B	G04-0345
Driving machine	A03-0086
Frequency converter Hitachi Ltd	B03-0141
Induction machine 1 kW Y692/Δ400	A03-0098
Induction machine 1.5 kW Y400/Δ230	no identification number
Induction machine 3 kW, Y380/Δ220	Elkraft lab N.T.H. A3-57
LCR meter ESCORT, ELC-131D	H01-0089
Power Amplifier, TOE 7610 DC-100KHz	B03-0479
Pulse Generator, TTi TGP110 10 MHz	B03-0522
Tachometer	NO6-0090
Three-Phase Power Quality Analyzers, FLUKE 434	H02-0124
Thyristors with firing angle generator	Elkraft N.T.H. P4-23
True RMS Multimeter FLUKE 175	S03-0451

Table A.1: Instrument List

Appendix B

Dimensioning Selected ELC Solutions

As concluded in chapter 6, it is interesting to compare and evaluate the triac controlled solution and the uncontrolled rectifier solution. This appendix gives the reader an understanding of the measures done to calculate the parameters for simulation, and also the necessary voltage and current ranges for components for the option of building a laboratory set-up.

First, the given range of voltage and current is calculated assuming the ELCs will be connected to the same system with identical rated values. Following, individual component dimensioning is provided for the two alternatives. The values are used in the simulation model presented in chapter 7.

B.1 Voltage and Current Range of Components

The assumed SEIG is connected in a Y configuration, with a rated line voltage of 400 V and total rated power of 4 kW.

A 10 % variation of terminal voltage from the SEIG gives a dimensioning RMS line voltage of V_{RMS} = 440 V, and hence a peak line voltage $V_{peak} = \sqrt{2}\ V_{RMS}$= 622.3 V

The current rating of the components used in the load controller has to be dimensioned by the rated power output and the line current.

$$I = \frac{P_G}{\sqrt{3}V} = \frac{2666W}{\sqrt{3} * 400} = 3.85A \tag{B.1}$$

In the dimensioning, one have to consider a distortion factor of the input current of the ELC. This will always be less than 1, and a value of 0.955 is found in reference [40].

It is also necessary to account for the crest factor, the measure of extreme peaks in the current waveform. Normally it will be between 1.4 and 2.0, and the latter is used for worst-case dimensioning purpose. The dimensioning line current can therefore be set as

$$I = \frac{3.85}{0.955} x 2.0 = 4.03 x 2.0 = 8.06A$$

Including also a safety factor of 2, the rating for this system is of ca 1200 V and 16 A.

This should be in accordance with Remote Hydrolights focus on maintaining a high security margin on the components used, as discussed in 2.2.

B.2 Parameter Design

B.2.1 Thyristor

The dump load is calculated from the desired power output at rated voltage, the relation is given in equation (B.2). The SEIG is designed to handle a full rated load of $P_G = \frac{4kW}{1.5} = 2.666$ kW.

$$R_{dl} = \frac{V_{phase}^2}{P_G} \tag{B.2}$$

B.2.1.1 Calculating Firing Angle

The value of the firing angle α of the thyristors is calculated based on the power that is needed to be dissipated in the dump loads, given in equation (B.3) [45].

$$P = \frac{V_{peak}^2}{2\pi R_{dump}}(\pi - \alpha + 0.5sin(2\alpha)) \tag{B.3}$$

To simulate changes in load from zero to full value of the village load, the resistive value of the village load is changed corresponding to the changes in firing angle. The calculated values are given in table B.1

α [degrees]	R_{vl} [ω]
0.0	∞
46.6	595.1
60.5	297.6
71.4	198.4
80.9	148.8
90.0	119.0
99.1	99.2
108.6	85.0
119.5	74.4
133.4	66.1
180.0	59.5

TABLE B.1: Firing angle values with corresponding changes in village load

B.2.2 Uncontrolled Rectifier

To calculate the rating of the DC side dump load in the uncontrolled rectifier, the DC voltage is calculated from (B.4).

$$V_{DC} = \frac{3\sqrt{2}V}{\pi} = 1.35V = 540V \tag{B.4}$$

The dump load is then calculated from the desired power output at rated voltage:

$$R_{DC} = \frac{V_{DC}^2}{P_G} = 109.4\Omega \tag{B.5}$$

B.2.2.1 Filtering Capacitor

As mentioned in 6.3, a filtering capacitor is used to keep voltage ripples at a low level.

An increased size of capacitor means increased price as commented in section 3.2, and it is desirable to find the minimum needed value of capacitance for this reason.

From the equation below, it can be seen how the choice of filtering capacitor C_f is connected to a ripple factor RF of the voltage, given in percent. An acceptable value of RF would be around 5 %.

$$C_f = \frac{1}{12fR_D}x(1 + \frac{1}{\sqrt{2}RF} = \frac{1}{12x50x109.4}x(1 + \frac{1}{\sqrt{2}0.05}) = 231\mu F \tag{B.6}$$

B.2.2.2 Commutation Inductance

The proper use of series connected inductance in combination with the parallel connected capacitance from the already exciting capactior bank can provide a second order low pass filter that will deliver a sinusoidal waveform at the SEIG terminal. Without this filter the high order harmonics could possibly damage the generators internal windings, as discussed in 3.1.1, and the commutation inductance is mostly used to protect the generator [8].

More specifically, the dc-side current I_d is normalized by the per phase short-circuit current [7]. Choosing an appropriate value of L_s will improve total power factor and decrease the THD in the current.

$$I_{shortcircuit} = \frac{V/\sqrt{3}}{\omega L_s} \tag{B.7}$$

The regular approximation value of L is 5 - 10 % of Zbase. The value of L is calculated given a system with $V = 400$ V, and an assumption of $S_N = 4000$ VA.

$$Z_{base} = \frac{U_N^2}{S_N} = \frac{400^2 V}{4kVA} = 40\Omega \tag{B.8}$$

$$L_{10\%} = 0.1\frac{Z_{base}}{\omega} = \frac{2.6\Omega}{100\pi} = 12.7mH \tag{B.9}$$

Using this value in equation (B.7), the relation between I_{DC} and $I_{shortcircuit}$ is found as

$$\frac{I_{DC}}{I_{shortcircuit}} = \frac{\frac{540V}{109.4\Omega}}{57.36\Omega} = 0.08 \tag{B.10}$$

Figure B.1 shows the benefits of choosing parameters with this relation.

When adding the L to the system, the commutation of current from one diode to the next in the bridge is no longer instantaneous. Instead, there is a commutation interval u where one phase current drops to zero while the next gets time to build up

This results in a small voltage drop each sixth ($\pi/3$ radians) part of the period, during each current commutation in the six pulse bridge, with the value

$$l\delta V_d = \frac{3}{\pi} w L_s I \tag{B.11}$$

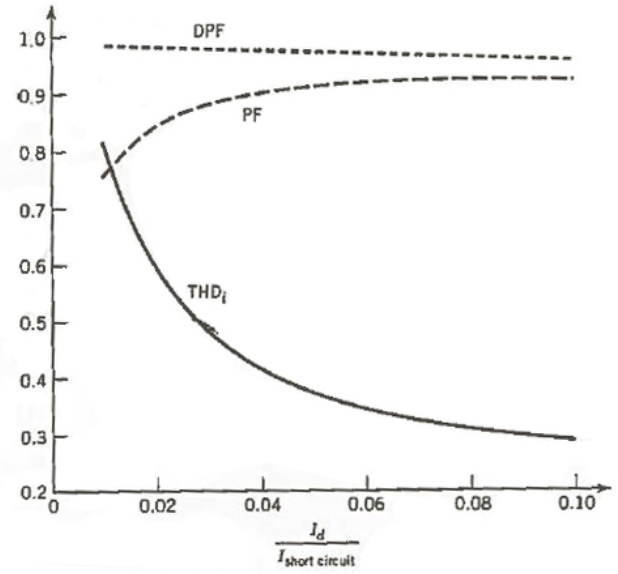

FIGURE B.1: THD, DPF and PF in the rectifier

Source [7] p. 94

Giving that the actual average DC voltage will be

$$V_{DC} = 1.35V_{LL} - \frac{3}{\pi}wL_sI \tag{B.12}$$

[7], [40], [39]

B.2.2.3 Duty Cycle Values

Similar to the thyristor controlled alternative, changes in village load is calculated following the corresponding changes of duty cycle of the IGBT chopper. Calculated values are given in table B.2

Duty Cycle ELC [%]	Village Load [ω]
1	∞
0.9	595.1
0.8	297.6
0.7	198.4
0.6	148.8
0.5	119.0
0.4	99.2
0.3	85.0
0.2	74.4
0.1	66.1
0	59.5

TABLE B.2: Duty cycle values with corresponding changes in village load

Appendix C

Magnetizing Curve for the Laboratory Machine and the Corresponding No-Load Capacitor Bank

The magnetizing curve given here is form the preliminary report [1], and was obtained through laboratory testing.

The magnetizing curve from a 4 pole 1.5 kW Δ connected induction machine with rated values 230 V and 6 A is measured at 50 Hz frequency is shown below as the green curve in figure C.1. This is an approximation since the frequency measurement was not completely accurate, but it shows the basic shape and dimensions of the curve. The values for the points at the curve is given in table C.1 together with the frequency they where measured at.

From the magnetizing curve, we find the intersection point between the curve and the desired output voltage. In figure C.1, the $V_{rated-phase}$ is 230 V, and this corresponds to I_m of value 4.35 A. It is important to consider the current level at the operation point, as is shall not exceed rated values for the machine.

Further, the same intersection point is used to find the slope of the needed reactive power to obtain that operation point. This is seen in figure C.1 as the blue line.

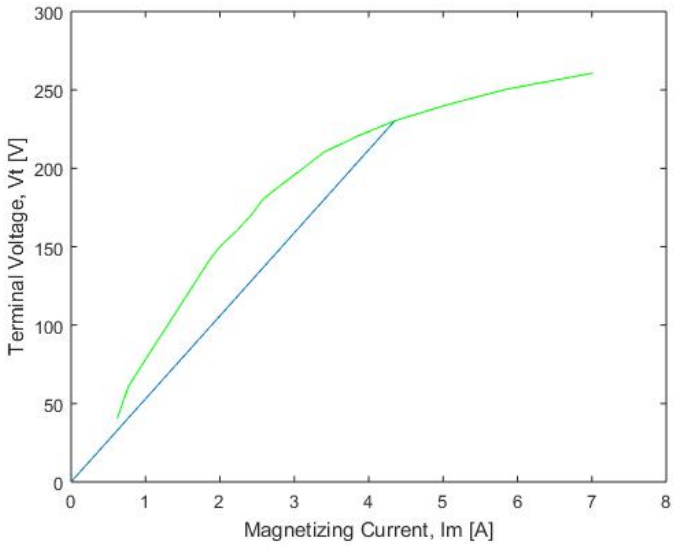

FIGURE C.1: Plot of magnetizing curve(green) and corresponding C-curve(blue)

Source: Prosjektoppgaven

Voltage [V]	Current [A]	n_r [rpm]
260.8	7.02	1501.0
250.2	5.83	1498.0
240.2	5.03	1496.0
230.3	4.35	1495.8
220.5	385	1499.6
210.1	3.39	1497.6
200.1	3.12	1499.3
190.1	2.84	1500.4
180.3	2.58	1500.3
170.2	2.42	1497.1
160.3	2.23	1497.1
150.0	2.00	1492.6
140.7	1.85	1494.3
120.1	1.57	1497.4
100.1	1.30	1493.9
80.3	1.03	1494.1
60.8	0.77	1487.0
40.5	0.62	1476.3

TABLE C.1: Voltage and Current values for the Magnetizing Curve (from no-load test)

Appendix D

Schematic Figure of Delta Connected ELC

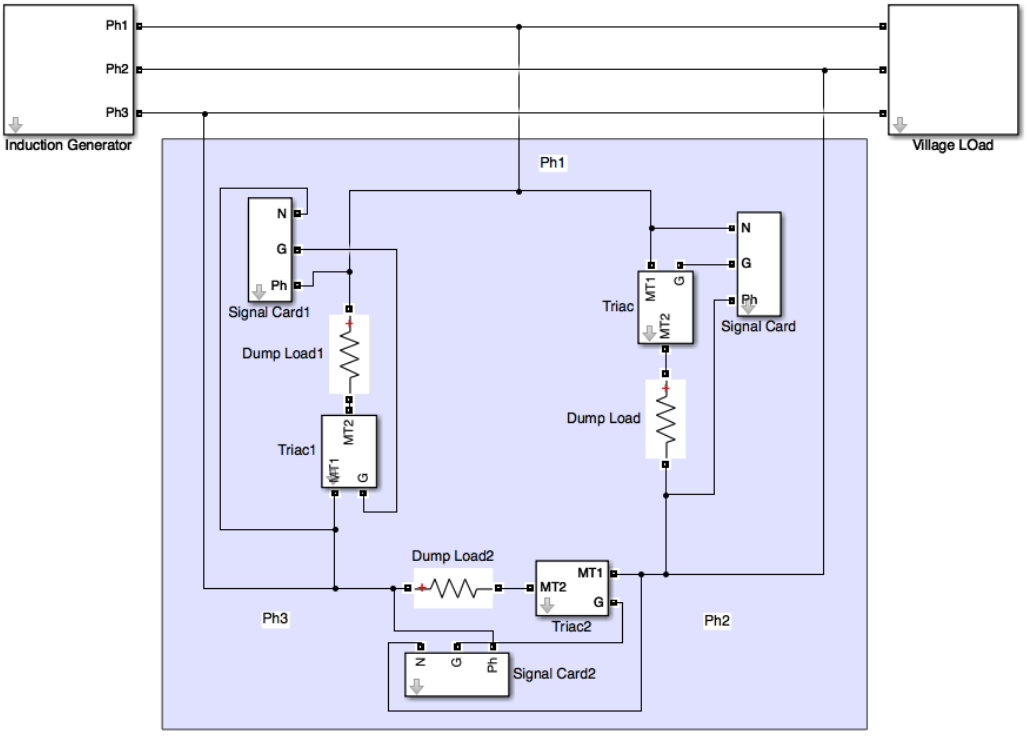

FIGURE D.1: The delta connected ELC solution for the laboratory test

Appendix E

Triac Testing

Before connection with the system, it is necessary to observe that the triacs are working as expected. The triac chosen is a TBA140 triac, with repetitive peak off-state voltage of 600 V and RMS on-state current of 25 A [46], which is concidered to be sufficient for these tests. Estimates for current and voltage which the triac will be subject to in a long-term system is given in Appendix B. Before using the triac in the system, a test circuit is set up in the lab for understanding how the triac works. The instruments used in this test are listed in Appendix A.

A pulse generator is used to provide a trigger signal to the gate, and the triac is placed in series with a resistor, between an arbitrary waveform generator which is providing the driving voltage for the circuit.

The output of the pulse generator is set to a square voltage signal, with a frequency of 50 Hz and 1 V amplitude. The resistor in the circuit is a 56 Ω resistor. The signal generator is providing a sinusoidal voltage at 50 Hz.

An oscilloscope is connected across the resistor by a differential probe to measure the voltage. If the triac is conducting, there will be a voltage across the resistor with the same frequency as the voltage source. The waveform will be disturbed by the firing angle. If the triac is not conducting, there will be no voltage across the resistor.

First, the test rig does not give any output. After error searching, it is found that the pulse generator is not powerful enough to provide the current needed, due to the high output impedance of the pulse generator. From the data sheet for the triac, it is found that the current running through the anode and cathode needs to be equal or greater than 100 mA for the triac to conduct [46]. To generate a high enough current, a power amplifier is connected to the signal generator.

Following, a voltage in phase with the voltage source is seen over the resistor. Still, it is not as expected, as the voltage signal is seen both when the trigger signal is on and off. In addition, the waveform of the voltage corresponds exactly to the waveform of the signal generator, and is not disturbed by the firing angle of the triac. As the triac should only conduct when a trigger signal is sent to the gate, something is wrong with the setup.

Error searching detects that when the triac is conducting only when the gate is connected to the ground point in the circuit, implying that there must be some leakage currents flowing from the grounded point to the gate in the set up, resulting in a constant triggering of the triac. To avoid this current flow, a resistor of 82 Ω is connected between the gate and the trigger signal.

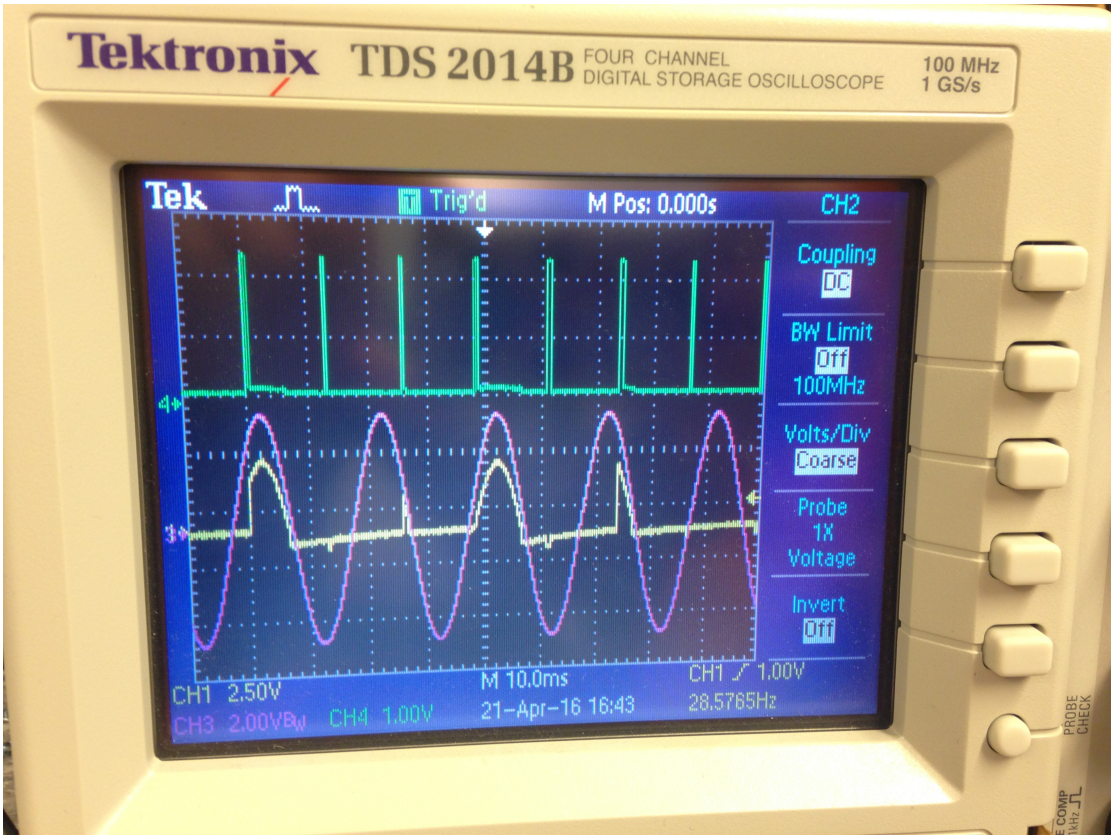

FIGURE E.1: Waveform output from triac signal testing

Green signal: gate pulse, purple signal: voltage from waveform generator, yellow signal: the resulting voltage waveform across the resistor

After correcting these errors, it is observed a voltage over the resistor only when the triac is trigged, shown in figure E.1. The graph is obtained by using the oscilloscope listed in the instrument list in appendix A. The purple waveform is the voltage signal from the waveform generator, the green signal is the trigging pulse, and the yellow waveform is the voltage over the resistor. As the trigging signal and the driving voltage is not

provided by the same signal generator, they are not completely in phase. This results in the trigging of the thyristor at different phase delays. The goal of this test is however to check if the triac is conducting when trigged, which is now observed. The trigging at different phase delays will not be an issue when using the cards for gate triggering, as they are reading the zero-crossing and the sending a signal at a specific time delay correspondingly.

The same test is done for the two remaining cards and triacs, with identical results.

Appendix F

Description of Circuit Board Operation and Source Code used in Microcontroller

The principle operation of the Remote Hydrolight-produced circuit board used in laboratory testing in this thesis is given in figure F.1. This circuit is also given in figure 9.5 in Chapter 9.

One phase of 230 V and the neutral are connected as inputs to the board, giving a 3 V signal as input to the microcontroller after passing through a voltage divider. The phase and the neutral also acts as power supply to the board itself, through a 230 V/7.4 V transformer denoted TR1. The P1.7 output of the microcontroller gives the calculated gate signal based on the source code programmed, and this is transported to the external connected triac (T1) and dump load (R1).

The source code for programming the processor on the circuit board provides trigger signals for the triac gate. The code given under sets a fixed time delay for a circuit board only using phase 1 in a 3 phase card. The code is provided by Anders Austegaard.

The original code for the ELC used by Remote Hydrolight is given at Remote Hydrolight webpage [2].

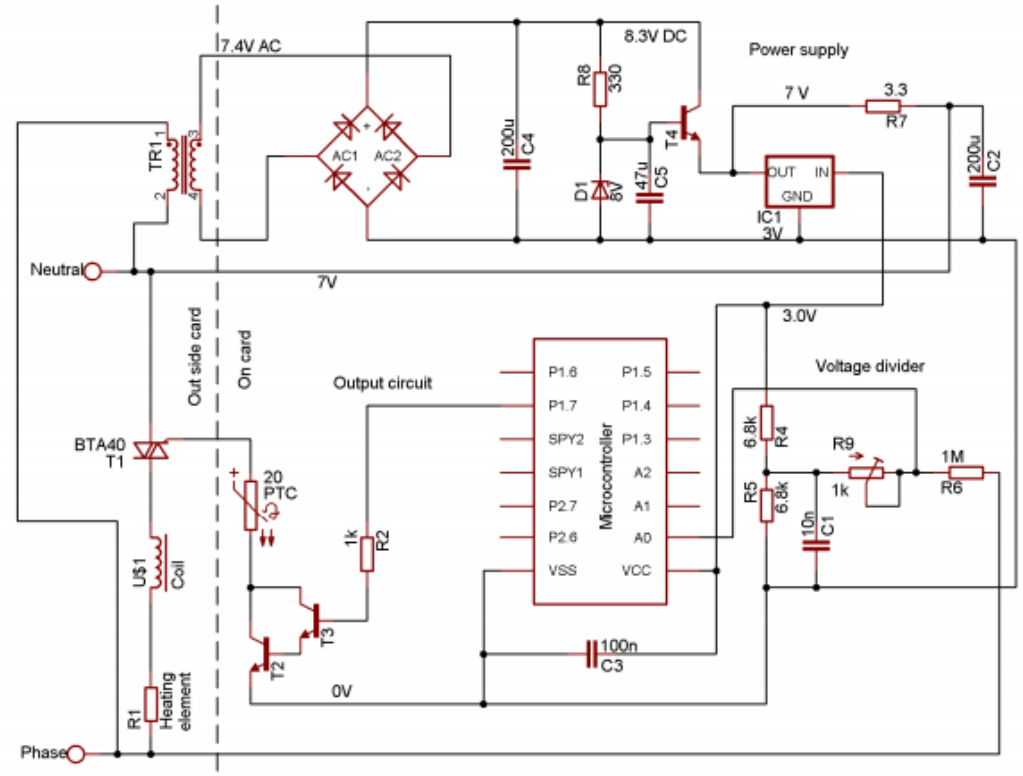

FIGURE F.1: Principle operation of the ELC circuit board

Three phase circuit board using one phase. Source [2] p. 13

```
#include <msp430x20x2.h>
//Uses only phase 1 in 3 phase card
//Fixed time delay:
#define tMinOffTRIAC 800
#define rSet 1400
// = (t-tMinOffTriac)/3
//t = Time triac is off in us
#define tMinHalfPeriod 6000
//Minium time gfor half period
//Should be longer than t + 300

//Single phase ELC with 3 phase card: Uses nly phase 1:
//#define InpVolt
//#define sim
#define wWatchdog

//Ports
// Processor on card turned wrong way:
// Old                    New Poer
// 0x01: A0: Input voltage     0x01: A0
// 0x02: P1.1: Not connected
// 0x04: P1.2: Not connected
// 0x08: P1.3: Not connected
// 0x10: P1.4: Not connected
// 0x20: P1.5: LED Low  -      0x20: P1.5
// 0x40: P1.6: LED Normal      0x80: P2.7
// 0x80: P1.7: LED High        0x40: P2.6
// 0x40: P2.6: Triac           0x80: P1.7
// 0x80: P2.7: LED: Triac      0x40: P1.6


//----------turning on and off TRIACS----------
#define tOnTRIAC 300
#define rMax 4016
#define tOffTRIAC_Off (3*rMax + tMinOffTRIAC -100)
//Nessesary to work at low frequence

signed int tOffTRIAC = 3000;  //How long the triacs should be off
#define P_TRIAC 0x80
//S const unsigned char P_TRIAC[3] = {0x80,0x08, 0x10};
//S #define P_TRIAC_ALL 0x98  //Sum of all tiracs
#define LED_TRIAC 0x40
unsigned int tStartTRIAC;  //Time when triac starts
unsigned char AllowTRIAC; //Is zero in area when TRIAC not should be turned on

//-----Reading of voltage----------
//S unsigned int uread[3];
//S char PhaseNoInput = 0;
```

```
//----------STructure in AllPeriods
//Have one structire for each phase, Shown to give least space
//Also saves 1 variable since the pointer of that variable is not nessesary

//*****************************************************************************

//---------LimitInt-----------------------------
void LimitInt(int *x, int min, int max)
{ if (*x > max)
    *x=max;
  else if ( *x < min)
    *x = min;
}

//----------GetVolt-----------------------------------------
#ifdef InpVolt
#define tWaveORV 2000
#define tPer 21840 //=2^16/3
#define tPer2 (tPer/2)

int GetVolt()
{ unsigned int uOut, tt;
  signed char sign0;

   tt = TAR - tWaveORV;
    while (tt > tPer)
      tt = tt - tPer;
    if (tt < tPer2)
      sign0 = 1;
    else if ( tt < tPer)
    { sign0 = -1;
      tt -= tPer2;
    }
    else
    { sign0 = 1;
      tt -= tPer;
    }
    __disable_interrupt();  //Interupt here can give stack error
    uOut =  512 + (sign0 * ((long)tt * (long)(tPer2-tt)) >> 16);  // /65536 gives max value 381
    __enable_interrupt();  //Interrupt here can give stack error

 return uOut;
#ifdef sim
  TAR+=211;
#endif
}
#endif
```

```
//--------Interrupt TimerA0: TRIAC ON-----------------------------------

#pragma vector = TIMERA0_VECTOR
__interrupt void TimerA0(void)
{unsigned int tt;
   tt = TAR;
   if ( tOffTRIAC < tOffTRIAC_Off)
   { if ( AllowTRIAC )
     {  P1OUT |= (P_TRIAC + LED_TRIAC);
        TACCR0 = tt + 30000;
        TACCR1 = tt + tOnTRIAC;
     }
   }
}

//--------Interrupt TimerA1: TRIAC OFF----------------------------
#pragma vector = TIMERA1_VECTOR
__interrupt void TimerA1(void)
{//Turn triacs off
  TAIV; //REset inerupt. If not called this routine will continue calling itselves
  P1OUT &= ~P_TRIAC;  //Turn of all triacs
}

//------------StartPerod-----------------------------------
void StartPeriod(unsigned int tZeroCrossing)
{unsigned int tt;
 __disable_interrupt();  //do not want triacs to start when one calcualtes starting time
 tt =  tZeroCrossing + tOffTRIAC;
 if ( (int)(tt - TAR - tOnTRIAC) < 0 )
   tt = TAR + tOnTRIAC;
 tStartTRIAC = tt;
 TACCR0 = tStartTRIAC;
 //Find next TRIAC, ps: If old TACCR0 = TAR during this routine it utn on after with triac iTRIACOn

 //SetTACCR: Set the next interupt
 //This routine is always called with interupt not enabled
 //THen it can happend itnerupt have happened after interupt is disabled
 //but before it is enabled. In that case interupt is done here
 __enable_interrupt();  //If TACCR0 =
 P1OUT &= ~LED_TRIAC;
}

#define WantedVolt 4464
#define ddperMax 50
#define dpUnlin 1000
#define tPerMax 23250
#define PerMax ((tPerMax-20000)*8)
```

```
#define tPerMin 17500
#define PerMin ((tPErMin-20000)*8)


signed int per0 = 0, perWant = 2000*8;  //Start at 45 Hz
signed int ddper0 = 0, dPerWD = 0, ri=2000, iLoop=0;

//---------DoReg-------------------------------------------------------------
void DoReg(unsigned int tPeriod, signed int u2)
{signed int du2, per, ddper, f2, f3, du22, rp, r;
 char unLin;

   du2 = u2 - WantedVolt; //Average voltage 230 V

 //....Check period.....................................
    if (tPeriod > 12000  && tPeriod < 30000)  //Often period is < 6000  when no signal
      per = tPeriod - 20000  - (perWant>>3);
    else
      per = per0;
    LimitInt(&per, -3000, 3000 ); //Limit per so one not can get overflow

 //Sometimes tPeriod oscilate with period= 2 sycles. (Increase and then reduce in next)
 //Change in r can gives a large differense in tPeriod withouth changing rotation speed
 //See RoutineTOStopOsilating.xls for example
 //At to big difference in per will one not axept the difference but use the old value
 //However when two steps have too big difference, will one acept the second step
    ddper = per - per0;
    if ( (ddper > ddperMax && ddper0 < ddperMax) || ( ddper < -ddperMax && ddper0 > -
ddperMax))
      per = per0;
    per0 = per;
    ddper0 = ddper;

 //.........Watchdog.....................


 // dPerWD = (dPerWD* 3 + per ) >> 2;
 dPerWD += (per - dPerWD) >> 2;
 #ifdef wWatchdog
    if (iLoop > 25)
      if (dPerWD < -2000)
        WDTCTL = WDTCNTCL;   //Generates a reset mode when frequense goes high. PS -1500 gave
often reset
    WDTCTL = WDTPW + WDTCNTCL;   //clear watchdog counter
 #endif

 //...........Regulating.....................
      f2 = (tPerMin - (int)tPeriod) >>3;
```

```
    f3 = (tPerMax - (int)tPeriod) >>3;

    du22= du2;
    if ( f2 > du22 ) //Max(du22, f2)
    {  du22 = f2;
    }
    if ( f3 < du22) //Min(du22, f3)
    {  du22 = f3;
    }

    rp = dPerWD;

    if (per > dpUnlin)
    {   rp += 2*(per - dpUnlin);
        unLin=1;
    } else if (per < -dpUnlin)
    {   rp += 2*(per + dpUnlin);
        unLin=1;
    }else
    {   ri -= du22 >> 5;
        unLin=0;
    }

    if (unLin==1)
      ri -= du22 >> 2;     //why not du22 ???

    LimitInt( &ri, -500, rMax + 500);
         r = ri + rp;

   r = rSet;  //Fixed value on r
   LimitInt(&r, 1, rMax);
   tOffTRIAC = 3*r + tMinOffTRIAC;

//.....Using voltage.....
   if ( (du22 > 0 && r > 82 )   //To high voltage and not ful load
      || ( du22 < 0 && r < rMax) ) //To low voltage and not no load
   { perWant += rp >> 6;
   }

 //Setting LED

//.....Turning on LEDs.....
     P1OUT &= ~0x20; //Turn off low votage LED
     P2OUT &= ~0xC0;

     if (r > rMax - 50 )
       P1OUT |= 0x20;    //Turn on low voltage LED
     if (r < 50)
```

```
        P2OUT |=0x40;     //Turn on high voltage LED
      if (r > 5 && r < rMax-5)
        P2OUT |= 0x80;
//      if (per > -1000 && per < 1000 && du2 > -400 && du2 < 400)
       //Turn off LED for normal when votlage is outside 10V and frequence is inside 2.5 Hz
       //PS: Must NEVER be turned off when LED1 and LED3 also is turned off, because if all ELD is off,
it means no power to the processor.
      if (u2 < 200)
      {
        P1OUT |= 0x20;    //Turn on high and low if input voltage is zero
        P2OUT |= 0x40;
      }
}


//----------AllPeriods--------------------------------------------------------
void AllPeriods()
{ unsigned int tStartSample, tInPeriod, per, iCount=0, tStartPer=0;
  signed int UInpAbs, UInp;
  signed long uSum=0, UMean;
  unsigned int t0Wave; //Time when the line crosses zero
  signed int UInpR, UInpR_Old;
  unsigned char isNeg;
 // *ptp_end; //Pointer to type tPhase stored in tp that stores all values for a phase
 // const tPhase *ptp_end = &tp[0] + 3;

    //Saves 64 Byte by using unsigned long instead of signed long, mostly in dividion at end of routine

//  ptp_end = ptp+3;
  ADC10CTL0 |= ADC10SC;   //Start sample and conversion for next reading
#ifdef InpVolt
  UInpR = GetVolt() - 512;
#else
  while( ADC10CTL1 & ADC10BUSY );  //Wait to voltage is read if nessesary
  UInpR = ADC10MEM - 512;
#endif
  isNeg = 0;
  AllowTRIAC = 1;
  do  //For every reading of voltages takes 74 us per iteration withouth InpVolt
  {//Storing old values
    while( ADC10CTL1 & ADC10BUSY ); //Wait to voltage is read if nessesary
//     i++;  Usually i reaches 10
    UInpR_Old = UInpR;
    UInpR = ADC10MEM - 512;
    LimitInt( &UInpR, UInpR_Old-40, UInpR_Old+40);
    __disable_interrupt();  //Important to take time at same time as conversion starts
    tStartSample = TAR;
#ifndef InpVolt
```

```
#endif
  ADC10CTL0 |= ADC10SC;  //Start sample and conversion for next reading
  __enable_interrupt();
#ifdef InpVolt
  UInpR = GetVolt() - 512;
#endif
//   if (TAR > (long)tOn0Last + (long)12000)
//     _NOP(); //Debug
  tInPeriod = TAR - t0Wave;
  UInp = ( UInpR + UInpR_Old ) >> 1;
  UInpAbs = (isNeg) ? (- UInp) : UInp;
  //Toi secure that gate is off when in forbidene sone
  uSum += UInpAbs;
  iCount++;
  if ( UInpAbs < 60 && AllowTRIAC && tInPeriod > tMinHalfPeriod ) //Before one reaches zero
  {  AllowTRIAC = 0;  //Does not allow triac to turn on
    P1OUT &= ~P_TRIAC;
  }
  if ((UInpAbs < 0 && tInPeriod > tMinHalfPeriod) || tInPeriod > 25000)  //Ocures 2 rimes in one
period
  { isNeg = !isNeg;
    t0Wave = tStartSample;
#ifdef wWatchdog
      WDTCTL = WDTPW + WDTCNTCL;  //clear watchdog counter
#endif
    if (isNeg == 0 )
    {//One time for each period
      per = tStartSample - tStartPer;
      iCount = iCount >> 4;
      if ( uSum < 0)
        uSum = 1;
      UMean = (unsigned long)uSum / iCount;  //Saves 46 Byte by transfering to unsigend long
//       IncrEven(per, UMean);  //Debug
      if (tInPeriod > 2500 && tInPeriod < 24500)  //Normal behaviour, does not want to do regulation
othrewise
        DoReg(per, UMean);
      iCount = 0;
      uSum = 0;
      tStartPer = tStartSample;
//         PhaseNoInput = 0;
//         if (UMean < 200)  //< 10V:
    }
    StartPeriod(tStartSample);
//     __enable_interrupt(); Called in STartPEriod unnessesary one time more
      //Check uSum: Measured to -384 at no conection, calculated to 6928 at normal operation. Use
limit 1630 to divide
      //Do it after _enable interupt of folowing reason
```

```
      //Sometimes: TACCR0 = TAR before TACCR0 is set in STartPEriod but after interupts is not
enabled
      //THen TIMERA0 is called abouot 2 comands after __enable_interruot and it will be called with
AllowTRIAC = 1
//       PhaseNoInput = (PhaseNoInput | (ptp->uSum < 100 ));
//       ptp->uSum=0;
     AllowTRIAC = 1;  // Allow TRIACs to turn on first now after TAR and t0Wave is set.
   }
  }while(1); //Infinity loop
}

//------------------WaitVoltOk--------------------
void WaitToVoltOk()
{// First wait to voltage has reached an okey level
int i=30000;
  ADC10CTL0 &= ~ENC;
  ADC10CTL1 = INCH_11;  //MEasure 0.5*(Vss + Vcc)
  ADC10CTL0 = SREF_1  //Vr+ = VRef = 1.5V, Vr- = VSS
    + ADC10SHT_3  //64*ADC10CLK
    + REFON //Turn reference voltage on
    + ADC10ON  //ADC10 is on
    + ENC;    //ADC10 is enabled
  do
  { ADC10CTL0 |= ADC10SC;  //STart sample and conversion for next reading
    i--;
    WDTCTL = WDTPW + WDTCNTCL; //Reset conunter
    while (ADC10CTL1 & ADC10BUSY );  //Wait to data is read
  }while (ADC10MEM< 900 && i > 0); // Wait to Vcc is 2.5V = 1024*2.5/3
//  ADC10CTL0 &= ~(ENC + ADC10ON);  //Turn of AD converter
}

//-------------Wait volt stable-----------------------------------
void WaitToVoltStable()
{// Then wait further in 1/halves period at low frequence(20 Hz)
 unsigned int t0, uReadOld,uRead=900, iCount=0;

  t0 = TAR;
  do
  { ADC10CTL0 |= ADC10SC;
    while (ADC10CTL1 & ADC10BUSY); //Wait to data is read
    uReadOld = uRead;
    uRead = ADC10MEM;
    iCount++;
    if (ADC10MEM < 870 && uReadOld < 870)
      t0 = TAR;
  }while( (int)(TAR-t0- 25000) < 0 || iCount > 3000);
//  idbg = iCount + uRead + uReadOld; //Debug
```

```
  ADC10CTL0 &= ~(ENC + ADC10ON); //Turn of AD converter
}

//-------------------------------------------------------------------

int main(void)
{ //Watchdog timer
#ifdef wWatchdog
  WDTCTL = WDTPW //Pasword
       + WDTCNTCL; //Reset conunter
  //Set reset if WDTCNT = 32768, after 32 ms if WDTCNT is not reset
#else
  WDTCTL = WDTPW + WDTHOLD;   //Stop watchdog timer
#endif

#ifndef sim
// if (!(IFG1 & WDTIFG) )
    WaitToVoltOk();
#endif
//Clock
  DCOCTL  = CALDCO_8MHZ;
  BCSCTL1 = CALBC1_8MHZ;  //Use 8 MHz clock frequency
  BCSCTL2 += DIVS_3;     //Divides SMCLK that is input to TImerA with 8
//Timer A
  TACTL =  TASSEL_2     //In put is SMCLK
       + MC_2          //The counter count up to 0FFFFh
       + TACLR ;       //Clear the timer
  TACCTL0 = CCIE;      //Ineterupt enabled on Compare register 0
  TACCTL1 = CCIE;      //Interupt also enabled on compare register 1

  WaitToVoltStable();

  //Port
  P1DIR |= 0xE0;  //Turn P1.5 to P1.7  as output
  P1SEL = 0;
  P2DIR |= 0xC0;  //Turn P2.6 and P2.7 as output
  P2SEL = 0;
  P1OUT = 0xE0; // Turn on port. must do it otherwise it sometimes not start at all
  P1OUT = 0;
  P2OUT = 0xC0; //Turn on port, otherwise it start at all.
  P2OUT = 0;

//Analig to digital converter
  ADC10CTL0 &= ~ENC; //Sometimes startet from interupt must then set ENC=0 before values can
change
  ADC10CTL1 = INCH_0;    //Input channel A0
  ADC10CTL0 = SREF_0         //SREF_0: VR+ = VCC and VR- = VSS
        + ADC10SHT_3       //64 x ADC10CLKs
```

Appendix G

Full-Load Capacitor Bank Testing in Laboratory - Error Search

Test	R [Ω]	C [μF]	f [Hz]	n [rpm]	V_L [V]	I_L [A]	P [kW]	Q [KVar]
1	53	99	45	1385	184	4.2	0.64	1.38
2	53	99	45.5	1400	188	4.5	0.65	1.65
3	53	165	41	1263	171	4.6	0.54	1.35
4	70.5	132	47.9	1470	215	5.1	0.63	1.89
5	81.5	132	50.1	1530	236	5.8	0.6	2.33
6	88	106	50.1	1530	215	4.3	0.5	1.6
7	78	132	48.9	1507	226	5.5	0.62	2.12
8	80	132	49.1	1498	227	5.5	0.6	2.15
9	80	132	48.4	1483	221	5.3	0.58	2.01
10	53	165	-	627	166	-	0.33	0.58

TABLE G.1: Results from the full-load test with driving machine as driving unit

TEST 1: When the speed of the driving unit is slowly increased, the frequency reached 50 Hz before the self-excitation process starts. When the generator self-excite and the voltage in the system builds up, the frequency suddenly drops to 45 Hz. It is not possible to increase the speed of the driving unit. The system stabilises at this frequency, with a voltage of 184 V and a power of 0.64 kW. The speed of the driving unit and the frequency is reduced when the voltage builds up. This is when the power drawn by the load increases.

Another test is run with the same parameters, and the results are the same. The speed is slowly increased until the frequency is 50 Hz, then the voltage suddenly increases from 5V to 180 V, and the frequency "jumps down" to 45 Hz. When the voltage is increasing,

the power drawn by the load also increases. It seems like the load may be to high for either the generator or the driving unit.

There may be several factors that leads to the low frequency in the system. The low frequency is problematic, as a reduced frequency results in lower voltage levels at the magnetizing curve, for the same current values. If the frequency is too low, the point of rated voltage at the curve may correspond to a current which is higher than the rated value of the system. It i desirable to run this system with rated frequency.

TEST 2: The starting of an induction generator is a complex process, and especially when loads are connected. The next test involves the same values of the capacitor bank and the load, but now, the load is switched in after the system has reached rated frequency. The results are approximately the same as in the previous test, so something else needs to be changes to increase the frequency.

TEST 3: When the capacitance is increased, the speed and the frequency of the system is reduced. It is not possible to increase the speed on the driving unit to get the desired frequency in the system. The voltage is lower than in the previous tests, and so is the power.

It seems like the driving unit cannot support the power drawn by the loads connected to the generator. The driving unit is rated for 1kW load, but it seems like the torque upon the driving unit is to high when the voltage builds up in the system, and the speed is reduced. As there is no equivalent driving units with higher ratings for power available, the solution is to decrease the load. The load connected should be in the range of $(1.5 - 2.5)P_{load} = P_{gen,rated}$. The load connected can be in the range between 1kW to 0.6kW, and be within these limits.

TEST 4: The load is reduced to 0.75 kW by increasing the resistance from 53 Ω to 70.5 Ω.

At the same time, the capacitor bank is reduced. It is important to not have a to large capacitor connected, as it can cause a high current in the system. It is better to start at a lower capacitance, and then increase it if needed. This results in a higher voltage and frequency, but it is still below rated values. The maximum speed of the system is now 1470 rpm, so the load needs to be decreased further.

TEST 5: The resistance is increased to 81.5 Ω, which is equal to a load of 0.65 kW.

Rated frequency is now reached in the system, at the rotational speed of 1530 rpm. It seems as the driving unit is strong enough for this load. The voltage in the system is a bit high, so the capacitance needs to be reduced.

TEST 6: The capacitance is reduced from 130 μF to 107 μF, which is the smallest possible decrease in capacitance value with the capacitors available. This reduction is fearly big, and it is expected that they cannot provide enough reactive power for the generator at this load. Therefor, the load is reduced to 0.6 kW. The result from this test is a voltage of 215 V. The capacitance is not providing enough reactive effect.

The next step involves increasing the capacitance to 130 μF again, but increasing the load, so that the system may consume more reactive power, and the voltage may not be to high.

TEST 7: When the load is increased to 0.68 kW, with resistors of 78 Ω, the load is to high for the driving unit. The maximum speed it can provide results in a frequency of 48.9 Hz, and voltage a bit below rated value. The load needs to be slightly decreased.

TEST 8: The resistance is increased to 80 Ω, but the driving unit still cannot provide high enough speed for rated frequency. Another observation that is made, is that the speed slowly decreases while the system is running, resulting in a decrease in frequency.

TEST 9: The test is done with the same parameter values, but now the measurements are done after the system has been running for approximately three minutes. As is can be seen from the table, both frequency and voltage is reduced compared to the previous measurements. It does not seem like the speed is stabilising at a value, the reduction continues.

TEST 10: From these test, it seems like the driving unit is not strong enough to run the generator with loads connected. As both the driving unit and the control board attached has been tested, one more thing needs to be tested before this conclusion can be made. There may be something wrong the equipment used. Both the driving unit and the control board for the unit was changed with an equivalent unit, to check if there is something wrong with them. Resulting in four different setups, all giving the same result. Non of the components are defect. As well, the induction generator needs to be tested, as there may be something wrong with it. Therefor, the system is again tested with a load of 1 kW and a capacitance of 160 μF, and a different induction generator with rated effect of 1kW. The generator used is the one the driving unit is designed for, a 1 kW induction generator. When this is loaded the driving unit cannot drive the system at desired speed.

The conclusion is made that the driving machine is not strong enough to drive the induction generator with load at rated speed. The driving unit needs to be changed.

Appendix H

Fixed Firing Angle Measurements

The ELC connected in Y and Δ configurations are tested for the four different firing angles, and frequency, voltage, current, active and reactive power, power factor and THD are measured at the different measurement points. Table H.1 gives the results for the Y connected ELC, while table H.2 gives the results for the Δ connected ELC.

α [degrees]	18			
System Part	Generator	ELC	Cap Bank	Village Load
f [Hz]	51.27	51.17	51.23	
V_L [V]	400	396	398	
I_L [A]	3.2	1.4	2.9	
P [kW]	0.95	0.95	-0.04	
Q [kVar]	1.96	0.12	2.00	
S [kVA]	2.18	0.96	2.00	
pf	0.43	0.99	-0.02	
THD,V [%]	1.5			
THD,I [%]	4.7	10.7	7.0	

α [degrees]	81			
System Part	Generator	ELC	Cap Bank	Village Load
f [Hz]	51.12	51.07	51.11	51.05
V_L [V]	368	367	368	367
I_L [A]	2.5	1.0	2.7	0.5
P [kW]	0.76	0.45	-0.03	0.32
Q [kVar]	1.44	0.41	1.70	0.03
S [kVA]	1.63	0.61	1.70	0.33
pf	0.47	0.74	-0.02	1.00
THD,V [%]	1.5			
THD,I [%]	17.1	54.8	8.9	2.0

α [degrees]	90			
System Part	Generator	ELC	Cap Bank	Village Load
f [Hz]	51.11	51.11	50.18*	51.10
V_L [V]	369	369	349*	368
I_L [A]	2.5	0.9	2.5*	0.6
P [kW]	0.75	0.38	-0.02	0.42
Q [kVar]	1.45	0.42	1.50	0
S [kVA]	1.63	0.56	1.50	0.42
pf	0.46	0.67	-0.01	1
THD,V [%]	1.8			
THD,I [%]	18.5	62.8	10.2	1.7

α [degrees]	135			
System Part	Generator	ELC	Cap Bank	Village Load
f [Hz]	51.03	50.96	51.21	-
V_L [V]	388	386	390	-
I_L [A]	2.9	0.4	2.8	-
P [kW]	0.89	0.07	-0.03	-
Q [kVar]	1.78	0.24	1.93	-
S [kVA]	1.98	0.25	1.93	-
pf	0.45	0.29	-0.02	-
THD,V [%]	2.1			-
THD,I [%]	7.3	129.5	10.5	-

TABLE H.1: Results from Induction Generator and ELC Y connected with different Firing Angles

α [degrees]	18			
System Part	Generator	ELC	Cap Bank	Village Load
f [Hz]	50.48	50.68	5.68	
V_L [V]	230.5	231.5	231.6	
I_L [A]	5.9	2.5	5.5	
P [kW]	0.97	0.99	-0.02	
Q [kVar]	2.16	0.00	2.21	
S [kVA]	2.36	0.99	2.21	
pf	1.00	0.87	-0.01	
THD,V [%]	1.4			
THD,I [%]	6.0	5.7	6.4	
α [degrees]	81			
System Part	Generator	ELC	Cap Bank	Village Load
f [Hz]	50.26	50.26	50.27	50.25
V_L [V]	215.5	215.5	216	215
I_L [A]	4.9	1.6	5.1	0.9
P [kW]	0.84	0.51	-0.02	0.34
Q [kVar]	1.64	0.31	1.91	0.01
S [kVA]	1.84	0.59	1.91	0.34
pf	0.46	0.85	-0.01	1.00
THD,V [%]	2.6	2.7		
THD,I [%]	7.7	27.6	14.1	2.9
α [degrees]	90			
System Part	Generator	ELC	Cap Bank	Village Load
f [Hz]	50.43	50.25	50.40	50.31
V_L [V]	217	214.7	216.7	215.3
I_L [A]	5.0	1.4	5.2	1.1
P [kW]	0.85	0.41	-0.02	0.43
Q [kVar]	1.66	0.31	1.94	0.00
S [kVA]	1.86	0.52	1.94	0.43
pf	0.46	0.80	-0.01	1.00
THD,V [%]	2.4			
THD,I [%]	7.6	31.4	13.3	2.7
α [degrees]	135			
System Part	Generator	ELC	Cap Bank	Village Load
f [Hz]	50.11	50.14	50.17	50.11
V_L [V]	222.4	223.3	223.7	221.8
I_L [A]	5.5	0.6	5.3	2.2
P [kW]	0.93	0.08	-0.02	0.85
Q [kVar]	1.89	0.21	2.04	0.03
S [kVA]	2.10	0.20	2.04	0.85
pf	0.44	0.38	-0.01	1.00
THD,V [%]	2.1			
THD,I [%]	4.5	90.5	10.5	2.0

TABLE H.2: Results from Induction Generator and ELC Y connected with different Firing Angles

Bibliography

[1] A Andersson and E. Bye. Self-excited induction generator with electronic load control. *Project Thesis, NTNU*, 12 2015.

[2] Anders Austegaard. Electronic load control elc from remote hydrolight for synchronous generator. 2012.

[3] N. Smith. *Motor as Generators for Micro-Hydro Power*. Intermediate Technology Development Group. Intermediate Technology Publications Ltd, 1994. ISBN 1853392863.

[4] P. Maher. Kenya case study. *Micro Hydro Centre, The Nottingham Trent University (www.picohydro.org.uk)*, 02 2002.

[5] Olje og energidepartementet. Forskrift om leveringskvalitet i kraftsystemet. 12 2004.

[6] W. E Reid. Power quality issues-standards and guidelines. *IEEE*, 1996.

[7] Mohan, N., Undeland, T. and Robbins, W. *Power Electronics: Converters, Applications and Design*. John Wiley and Sons, Inc, 1 edition, 2003.

[8] E. Marra and J. A Pomilio. Self-excited induction generator controlled by a vs-pwm bidirectional converter for rural applications. *IEEE*, 08 1999.

[9] C. Sankaran. Effects of harmonics on power systems. *Electrical Construction and Maintenance*, 10 1991.

[10] Franca P.M. Lyra C. Pissarra C. Mendes, M. and C. Cavellucci. Capacitor placement in large-sized radial distribution networks. *IEEE*, 07 2005.

[11] S. Paul and Jewell. W. Optimal capacitor placement and sizes for power loss reduction using combined power loss index-loss sensitivity factor and genetic algorithm. *IEEE*, 2012.

[12] Xu W. Nassif, A.B. and W. Freitas. An investigation on the selection of filter topologies for passive filter applications. *IEEE*, 07 2009.

[13] Simes, M. G. and Farret, F. A. *Alternative Energy System.* CRC Press, 2 edition, 2008.

[14] Chapman, S. J. *Electrical Machinery Fundamentals.* McGraw-Hill, 4 edition, 2005.

[15] Chapman, S. J. *Electrical Machinery Fundamentals.* McGraw-Hill, 5 edition, 2012.

[16] J. Bjrnstedt. *Island Operation with Induction Generators.* PhD thesis, Department of Measurement Technology and Industrial Electrical Engineering, Faculty of Engineering, Lund University, 2009.

[17] PSCAD Cookbook Induction Machines. Technical report, 6 2013.

[18] N. H Malik and A. A. Mazi. Capacitance requirements for isolated self excited induction generators. *IEEE*, 03 1987.

[19] A. K. Al Jabri and A. I. Alolah. Capacitance requirements for isolated self excited induction generators. *IEEE*, 05 1990.

[20] A. K. Al Jabri and A. I. Alolah. An experimental investigation of self-excitation in capacitor excited induction generators. *Elsevier, Electric Power Systems Research 53 (2000) page 5965*, 06 2000.

[21] T Toftegaag. Lecture elk-12 - grid connection of wind farms - reactive power, voltage control, etc. University Lecture, 9 2015.

[22] McPherson, G. and Laramore, R. D. *An Introduction to Electrical Machines and Transformers.* John Wiley and Sons, 2 edition, 1990.

[23] W. R. Finley. Troubleshooting induction motors. *IEEE*, 10.

[24] E. C. Bansal. Three-phase self-excited induction generators: An overview. *IEEE*, 06 2005.

[25] Murthy S.S. Singh, B and R. Jose. A practical load controller for stand alone small hydro systems using self excited induction generator. *IEEE*, 1998.

[26] Shridhar L. Murthy S. S. Singh B. Jha, C. and B. P. Singh. Selection of capacitors for the self regulated short shunt self-excitet generator. *IEEE*, 3 1995.

[27] M. H. Haque. Characteristics of shunt, short-shunt and long shunt single-phase induction generators. *IEEE*, 06 2009.

[28] T.F. Chan. Analysis of self-excited induction generators using an iterative method. *IEEE*, 09 1995.

[29] Singh M. Singh, B. and A. K. Tandon. Transient performance of series-compensated three-phase self-excited induction generator feeding dynamic load. *IEEE*, 08 2010.

[30] Khan R. Khan, F. and A. Iqbal. Performance analysis of shunt, short shunt and long shunt self excitet induction generator. *IEEE*, 2012.

[31] Hingorani, N. G. and Gyugyi, L. *Understanding FACTS: Concepts and technology of flexible AC transmission systems.* IEEE Press, 1 edition, 2000.

[32] Kundur, P. *Power System Stability and Control.* McGraw-Hill, Inc., 1 edition, 1994.

[33] Bhattarai R. Adhikari, R. and I. Tamrakar. Improved electronic load controller for three phase isolated micro-hydro generator. *Fifth International Conference on Power and Energy Systems, Kathmandu, Nepal*, 2013.

[34] Braga A. V. Silva V. F. Viana A. N. C. Bortoni E. C. Sanchez W. D. C. Rezek, A. J. J. and P. F Ribeiro. Isolated induction generator in rural brazilian area: Field performance test. *Elsevier Renewable Energy*, 11 2014.

[35] Simes L. H. Vicente J. M. E. Rodrigues J. C. G. Bernardes D. F. Rezek A. J. J. Braga A. V. Marques, G. R. and V. F. Silva. Frequency control of induction generator in standalone operation using bynary logic. *Second Intl. Conf. on Advances in Mechanical and Automation Engineering (MAE), Rome, Italy*, 05 2015.

[36] D. Henderson. An advanced electronic load governor for control of micro hydro-electric generation. *IEEE*, 09 1998.

[37] Singh B. Gupta S. Kulkarni A. amd Sivarajan R. Murthy, S.S. "water, water.. anywhere" field experience on a novel pico hydro system to supply power to remote locations. *IEEE*, 08 2006.

[38] Singh S. P. Mahato, S. N. and M. P. Sharma. Transient performance of a three-phase self-excited induction generator supplying single phase load with electronic load controller. *IEEE*, 2010.

[39] Porkumaran K. Kathirvel, C. and S. Jaganathan. Design and implementation of improved electronic load controller for self-excited induction generator for rural electrification. *The Scientific World Journal*, 2015.

[40] Murthy S.S. Goel M. Singh, B and A.K. Tandon. A steady state analysis on voltage and frequency control of self-excited induction generator in micro-hydro system. *IEEE*, 2006.

[41] R. Bonert and S. Rajakaruna. Self-excited induction generator with excellent voltage and frequency control. *IEEE*, 1998.

[42] R. Bonert and G. Hoops. Stand alone induction generator with terminal impedance controller and no turbine controls. *IEEE*, 1990.

[43] C. P. Ion and C. Marinescu. Autonomous micro hydro power plant with induction generator. *Elsevier; Renewable Energy, Volume 36, Issue 8*, 08 2011.

[44] Sobota P. Slivka M. Rusnok, S. and P. Svoboda. Assessment transients during starting of induction motor in matlab simulink and verification by measurement. *Advanced Research in Scientific Areas 2012*, 2012.

[45] Allaith H. N. AL-Mawsawi, S. A. and Q. S. Dhiya. An accurate formula for the firing angle of the phase angle control in terms of the duty cycle of the integral cycle control. *Journal of Automation and Systems Engineering - 61*, 2012.

[46] alldatasheet.com. Bta140 datasheet.